STUDY OF SURFACE CHEMISTRY STRATEGIES TO ENHANCE THE ELECTROCHEMICAL DETECTION OF PROTEINS AND DNA MARKERS

Josep Lluís Acero Sánchez

UNIVERSITAT
ROVIRA i VIRGILI

Study of surface chemistry strategies to enhance the electrochemical detection of proteins and DNA markers

---

Josep Lluís Acero Sánchez

DOCTORAL THESIS

2016

UNIVERSITAT ROVIRA I VIRGILI
STUDY OF SURFACE CHEMISTRY STRATEGIES TO ENHANCE THE ELECTROCHEMICAL DETECTION OF PROTEINS AND DNA MARKERS
Josep Lluís Acero Sánchez

Josep Lluís Acero Sánchez

STUDY OF SURFACE CHEMISTRY STRATEGIES TO ENHANCE THE ELECTROCHEMICAL DETECTION OF PROTEINS AND DNA MARKERS

DOCTORAL THESIS

Directed by Ciara K. O'Sullivan

Chemical Engineering Department

UNIVERSITAT ROVIRA i VIRGILI

Tarragona

2016

UNIVERSITAT ROVIRA i VIRGILI

Department of Chemical Engineering
Universitat Rovira i Virgili
Av. Països Catalans 26
43007 Tarragona, Spain
Tel: 977 55 96 58
Fax: 977 55 96 67

I STATE that the present study, entitled “Study of surface chemistry strategies to enhance the electrochemical detection of proteins and DNA markers”, presented by Josep Lluís Acero Sánchez for the award of the degree of Doctor, has been carried out under my supervision at the Department of Chemical Engineering of this university.

Tarragona, November 22nd of 2016

Doctoral Thesis Supervisor

Dr. Ciara K. O’Sullivan

Acknowledgements

Diuen que més important que la meta és el camí, i la veritat és que és ben cert. Tot i així, he d'admetre que el camí del doctorat no ha estat fàcil, però he après moltes coses noves i m'ha permès créixer a nivell professional i personal. El més important de tot és que durant aquest camí, no solament del doctorat sinó de més de deu anys involucrat al món de la recerca, he tingut l'oportunitat de creuar-me amb gent meravellosa, interessant i intel·ligent i que d'alguna manera m'han inspirat i ajudat a tirar endavant. Han estat tants i durant tant de temps, que se'm fa difícil poder nombrar-los a tots sense oblidar-me'n injustament d' algú, així que a tots ells els hi voldria donar les gràcies, ja que sense ells no hagués arribat fins al lloc on sóc ara.

M'agradaria donar les gràcies especialment a la Ciara per confiar en mi i donar-me l'oportunitat de fer el doctorat sota la seva supervisió. Gràcies per la seva preocupació, dedicació, implicació i esforç sense límits per intentar que totes les coses surtin sempre bé.

Moltes gràcies als meus pares, a la meva germana i al seu nuvi, per estar al meu costat durant aquest tres anys i sempre. A la meva dona Mary, la persona més especial, pel seu amor infinit, per creure en mi, comprensió i suport incondicional durant aquest temps. Aquesta tesi també et pertany a tu! Als meus petits, Marc i Pau, per regalar-me el seu somriure cada dia. Sense saber-ho, heu estat més important del que us penseu. Vosaltres em recordeu cada dia quines són les coses importants a la vida.

Table of contents

Abstract

Biosensors are analytical devices based on the specific interaction between a biological sensing element and its target molecule in combination with a transducer for signal processing. They have been exploited in many practical applications in several research fields, ranging from medical diagnostics to environmental analysis, and have great potential for commercialization. However, despite these great expectations, there are only a few examples of commercial biosensors, with the market mainly being driven by glucose sensors which accounts for approximately 85 % of the world biosensor market. This slow penetration into the market could be attributed to the elevated development and production costs and some important technological hurdles, such as sensitivity, reproducibility, real sample matrix effects, stability and quality assurance. In this work, we report on an easy strategy to reduce manufacturing costs by simplifying the surface immobilisation method of receptor proteins to a single step. This approach was achieved by the chemical introduction of disulfide groups into the protein structure and was applied to both antibodies and antigens for the optical and electrochemical detection of ischemic stroke and celiac disease related proteins respectively. Several potential advantages, such as miniaturisation, integration, multiplexing analysis, as well as the use of low cost disposable chips, should be exploited for the biosensors to impact on the market and migrate from sophisticated laboratories to the point-of-care. Working in that direction, we also report on a procedure for the multiplexed amplification and detection of seven genetic markers for breast cancer with a single tumour cell sensitivity using a low-density electrode microarray manufactured on standard low-cost printed circuit board (PCB) substrates. This approach provides a novel strategy for the genetic profiling of tumour cells via integrated “amplification-to-detection”.

1 Introduction

1.1 Summary

This chapter presents a brief overview of the field of biosensors, from their origins to their current status, highlighting the key achievements and some of the more exciting trends and challenges in the field. Biosensors are then illustrated in more detail, describing the main characteristics and the different types, focusing more particularly on electrochemical immunosensors and genosensors. Surface chemistry methodologies for immobilisation of biological receptors on transducer surfaces are reviewed, as well as the fabrication techniques for the production of low-density electrode arrays as well as different nucleic acid amplification methods. Finally the objectives of my thesis are outlined.

1.2 Past, present and future of biosensors

Biosensors are analytical devices used for the detection of molecules based on the specific interaction between a biological sensing element and its target molecule in combination with a transducer for signal processing. The biorecognition element responds to the target compound and the transducer converts the biological response to a measurable signal, which can be detected electrochemically, optically, acoustically, mechanically, calorimetrically, or electronically, and then correlated with the analyte concentration. The research field in biosensors started in 1962 with the pioneering work on enzyme electrodes by Clark and Lyons [1], who invented the first glucose biosensor that established the basis of the glucose sensor used daily by millions of diabetics. This biosensor consisted on a thin layer of glucose oxidase (GOx) on an oxygen electrode. The amount of glucose in the sample was determined by measuring the amperometric signal from the reduction of oxygen. In 1973, Guilbault et al. demonstrated that, the hydrogen peroxide produced can also be electrochemically oxidized to determine the glucose concentration [2]. Two years later, in 1975, Yellow Springs Instruments launched the first successful commercial biosensor, which was based on the hydrogen peroxide approach [3], however it was mainly used in clinical laboratories due to its high cost. During the 1970s and 1980s, the works of Schläpfer et al., Cass et al. and Di Gleria et al. based on artificial redox mediators, demonstrated that ferricyanide [4] and ferricinium [5, 6] ions could be efficient electron acceptors for GOx. Moreover, the low detection potential of these mediators (about +0.3 V versus Ag/AgCl reference electrode), suppressed electroactive interfering species such as uric and ascorbic acids. This attractive approach formed the basis for successful commercialisation of a pen-size glucose biosensor for home use by MediSense Inc. (now owned by Abbott) in 1987.

Since then, the field of biosensors has experienced an exponential growth with more than 4500 publications in 2015 according Scopus® from Elsevier B. V. (Figure 1.1). Since 2000, the increase in publications was more accentuated due to the explosion of nanotechnology, which brought new nanomaterials with enhanced chemical, physical and electronic properties for the preparation of the sensors, with the publications concerning immunosensors and DNA sensors exhibiting excellent growth. Genosensors are garnering more attention than immunosensors, probably due to the inherent characteristics of the nucleic acids as compared to traditional antibodies or enzymes, such as the high stability in non-physiological conditions, ease of production through chemical synthesis, ease of modification with reporter molecules, small size and high efficiency of the target recognition event via DNA hybridisation.

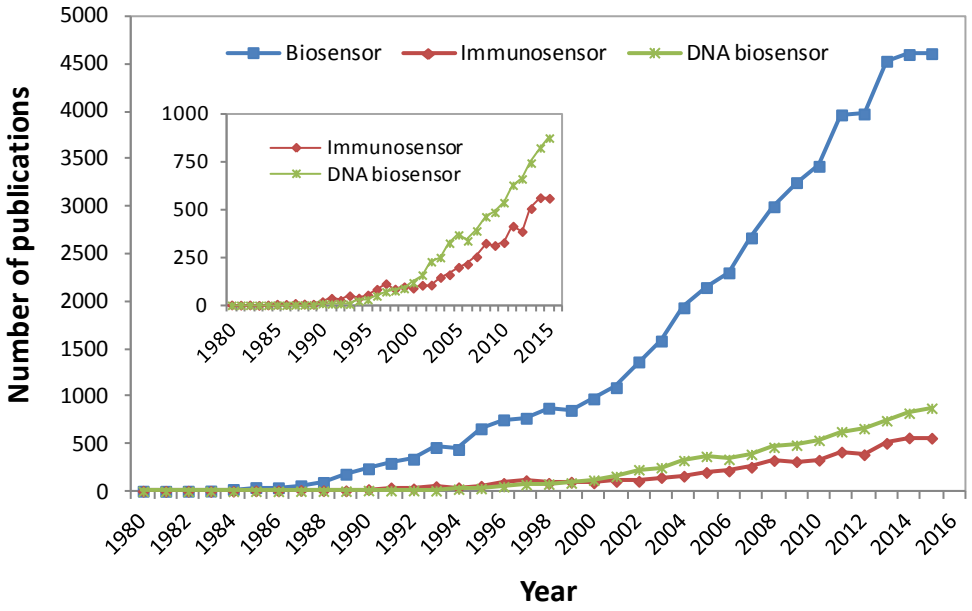

Figure 1.1. Graph of a search of the terms "biosensor", "immunosensor" and "DNA biosensor" during the period 1980 to 2015, using Scopus® from Elsevier B. V. Inset: Close-up graph of the annual publications for immunosenors and DNA biosensors.

Biosensor research has rapidly expanded from chemistry, biochemistry and genetics to other subject areas (Figure 1.2) and have shown many practical applications from several research fields, including medical diagnostics, food quality assurance, environmental monitoring, industrial process control to biological warfare agent detection [7]. The field is mainly dominated by electrochemical and optical transducers, which found their market niche principally in medical diagnostics and R&D, respectively. The other transduction strategies have not had the same success to date. However, despite the great expectations, there are just

a few examples of commercial biosensors, the market mainly being driven by the glucose sensors for people with diabetes, representing approximately 85 % of the world market, and to a smaller extent by the pregnancy test strips based on lateral flow formats [8]. This slow penetration into the market could be attributed to the elevated development and production costs and some important technological hurdles, such as sensitivity, reproducibility, matrix effects in real samples, stability and quality assurance [9]. Several potential advantages, such as miniaturisation, integration, multiplexing analysis, as well as the use of low cost disposable chips, should be exploited for the biosensors to impact on the market and migrate from sophisticated laboratories to the point-of-care. This will result in the development of new point-of-care devices (POCDs) which will play an important role in healthcare and more specifically in personalised medicine, the most significant trend likely to impact on biosensors. Working in that direction Bayer had the idea to integrate blood glucose testing into the world of videogames. The Bayer's DIDGET™ is the first and only blood glucose meter that connects directly to Nintendo DS and DS Lite and allows children to make sugar testing fun. It helps children to manage their diabetes by rewarding them for consistent testing habits with points to unlock new game levels and options.

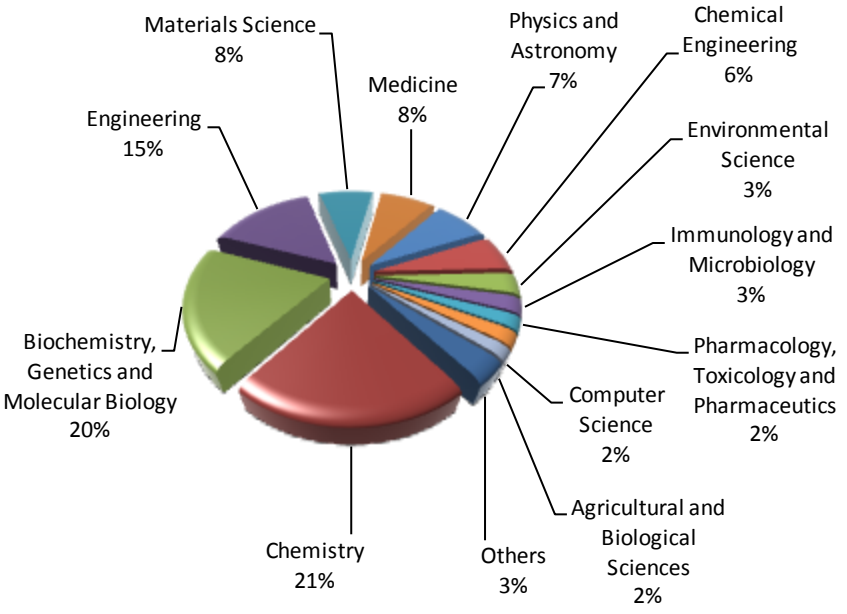

Figure 1.2. Graph of publications organized by subject area based on a search of the term "biosensor" during the period 1980 to 2015, using Scopus® from Elsevier B. V.

Recent advances in several fields of science have led to the discovery of new molecular receptors, which provide more robust, versatile and widely applicable sensors, and new nanomaterials, which facilitates the highly sensitive and efficient transduction of the recognition event. Concerning the biorecognition element, new alternatives to antibodies such as aptamers, affibodies, peptides and molecularly imprinted polymers have emerged as viable ways to construct affinity biosensors. These new receptor molecules can be designed against toxic analytes and other targets that are difficult to raise antibodies to. Aptamers were discovered almost simultaneously in 1990 by Larry Gold and Jack Szostak using the process of systematic evolution by exponential enrichment (SELEX) to produce novel binding partners. They are artificial specific single-stranded (ss) DNA or RNA oligonucleotides with the ability to bind to non-nucleic acid target molecules, such as peptides, proteins, drugs, organic and inorganic molecules or even whole cells, with high affinity and specificity [10]. Aptamers are also referred to as “chemical antibodies” since they interact with their targets via folding into specific three-dimensional (3D) structures, in a process similar to that of an antigen-antibody reaction [11]. Many works can be found in the literature describing the use of aptamers as receptor molecules in sensors for the detection of highly diverse targets [12]. Affibodies are non-immunoglobulin proteins used in imaging, diagnostics and therapeutics, which can also be used as biological receptors in sensors. They are considered single-domain proteins and engineered protein scaffolds, which possess the molecular recognition properties known in antibodies, with improved characteristics, such as small size (6.5 KDa), high binding affinity (sub-nanomolar level) and specificity and high stability [13, 14]. Affibodies have already been used as an alternative to antibodies in biosensors for the detection of cancer markers [15]. Molecularly-imprinted polymers (MIPs) are gaining quite some interest as fully synthetic receptors since they are able to provide the desired sensitivity and selectivity with improved stability and reproducibility [16]. The basic idea was originally elucidated by Günter Wolf and Klaus Mosbach in the 1970s and their synthesis was based on the self-assembly of functional monomers around a target molecule acting as a template, which can be a small molecule, peptide or whole protein, followed by polymerisation and subsequent removal of the analyte. This created polymer structures with “molecular memory”, having specific binding sites for the target analyte, as if it was a “plastic antibody” [17]. The use of MIPs as molecular receptors a have already been demonstrated for the detection of marker proteins for cardiac, cancer and Alzheimer's disease [18].

Nanotechnology has had a great impact on the biosensor research since the beginning of the last decade, basically in two major areas. One of this areas is in the nanofabrication of

biosensing interfaces, where the discovery of self-assembled monolayers (SAMs) opened up a new world of possibilities for immobilising receptors on a variety of transducer surfaces [19–23]. This technology rapidly expanded when in 1983 Nuzzo and Allara showed that SAMs of alkanethiolates on gold could be prepared from dilute solutions of dialkyl disulfides [24]. Many molecular systems are able to undergo the process of self-assembly, which generally consist in a long carbon chain with two functional groups, one at each end of the molecule. One group acts as an anchor to spontaneously chemisorb at the surface and the other one is used to link the biorecognition element via chemical coupling. The attractive of this approach lays on its simplicity, flexibility, the capability to control the packing density of the immobilised receptors and the possibility to mimic naturally occurring molecular recognition processes [25]. The other major area is the application of new nanomaterials, such as nanoparticles, nanotubes, nanowires, nanoporous materials or hybrid nanostructures. Such materials are reported to have good electronic properties enhancing the electron-transfer reaction between the electroactive molecule and the transducer surface. Moreover, the use of high surface area nanomaterials promotes the immobilisation of the receptor molecules which results in biosensors with greater sensitivity and shorter responses times [26, 27].

Despite the tremendous success of glucose sensors, the emergence of new semi-synthetic and synthetic receptors coupled with recent advances in material science and the explosion of nanotechnology should guarantee a promising future for the field of biosensors.

1.3 Biosensors: definition and classification

A chemical sensor is a device that transforms chemical information, ranging from the concentration of a specific sample component to total composition analysis, into an analytically useful signal. Biosensors are a specific type of chemical sensor in which the recognition system utilizes a biochemical mechanism [28]. The most accepted definition was described by the International Union of Pure and Applied Chemistry (IUPAC) as a self-contained integrated device, which is capable of providing specific quantitative or semi-quantitative analytical information using a biological recognition element (biochemical receptor) which is retained in direct spatial contact with a transduction element [29]. Basically a biosensor consists of three main parts, a biological recognition element, a transducer and a signal processing system. The bioreceptor is generally immobilized at the transducer surface and is able to detect the specific target analyte. These biocomponents are mainly composed of antibodies, nucleic acids, enzymes and cells. The transducer converts the biochemical changes produced from the reaction between the analyte and bioreceptor (such as the production of a

new chemical, release of heat, flow of electrons and changes in pH or mass) into an electrical signal, which is proportional to the analyte concentration. Finally, this electrical signal is amplified and sent to a microelectronics and data processor system [30].

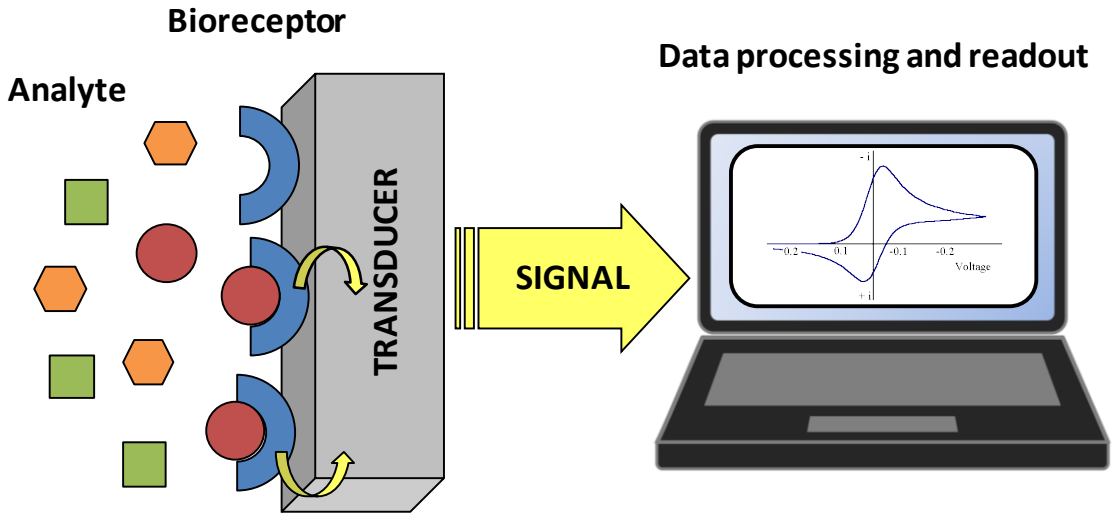

Figure 1.3. Main components in a biosensor

1.3.1 Classification

Several classifications can be found in the literature [3, 29, 30]. Generally, biosensors can be classified either by the type of biological signalling mechanism (catalytic or affinity) or by the type of signal transduction used (electrochemical, optical, piezoelectric and calorimetric). Furthermore, the biosensors can be classified either by the sensing element attached to the transducer (enzymes, antibodies, nucleic acids, cells, tissues, etc) or by their discovery order. In the latter case they can be divided in first generation biosensors, which involves direct detection using natural mediators (e.g. enzymes) for electron transfer; the second generation uses artificial redox mediators like ferrocene, ferricyanide and quinones for electron transfer and lastly, the third generation uses redox enzymes that are immobilised on the electrode surface to allow the direct electron transfer between the enzyme and the transducer.

According to the biological specificity-conferring mechanism, they can be arranged in two classes: catalytic or affinity biosensors. In the former case, the sensors are based on a reaction catalysed by macromolecules, which are present in their original biological environment, have been isolated previously or have been manufactured. Thus, a continuous consumption of

substrate is achieved by the immobilized biocatalyst incorporated into the sensor [29]. The three types of biocatalyst commonly used are: enzymes, cells and tissues. The high specificity of the interaction between the enzyme and its substrate and the usually high turnover rates of the enzymes are the basis of the sensitive and specific enzyme-based biosensor devices. Glucose oxidase (GOD) and horseradish peroxidase (HRP) are the most used enzymes based biosensors reported in literature [31]. In the case of the affinity biosensors, the recognition element forms a complex with the analyte which is based on equilibrium reactions that can be monitored by the integrated detector [29]. These sensors generally use antibodies or antigens and nucleic acids as receptor molecules, however, in the recent years, new semi-synthetic or synthetic receptors, such as aptamers, affibodies and molecularly imprinted polymers (MIPs) have emerged as promising alternatives.

1.3.2 Immunosensors

Immunosensors are based on the highly specific interactions between an antibody and an antigen, one of them being immobilised at the transducer surface. An antibody (Ab), also known as immunoglobulin (Ig), is a large Y-shape protein consisting of two heavy chains and two light chains which form a functionally bivalent monomer that is produced by B cells receptor used by the immune system to identify and neutralize foreign objects (antigens) such as bacteria and viruses [32]. There are five classes of Igs: IgG, IgM, IgA, IgD and IgE, which can be distinguished by the type of heavy chain found in the molecule, which defines the function of the antibody. Generally they exist as monomers (IgG, IgD and IgE), however some antibodies may form dimeric (IgA) and pentameric (IgM) structures. Because of their abundance in human serum and excellent specificity toward antigens, IgG is the main antibody used in immunological research and clinical diagnostics [33].

IgG antibodies are large molecules with a molecular weight of 150 kDa approximately. They consist of two types of polypeptide chains: one, of approximately 50 kDa, is known as the heavy or H chain, and the other, of 25 kDa, is named the light or L chain (Figure 1.4). Each IgG molecule consists of two heavy chains and two light chains. The two heavy chains are linked to each other by disulfide bonds and each heavy chain is linked to a light chain by a disulfide bond. In any immunoglobulin molecule, the two heavy chains and the two light chains are identical, giving an antibody molecule two identical antigen-binding sites, and thus the ability to bind simultaneously to two identical antigenic molecules [34]. The amino-terminal variable (V domains) of the heavy and light chains (V_H and V_L, respectively) together make up the V region of the antibody and confer on it the ability to bind specific antigens. The constant

domains (C domains) of the heavy and light chains (C_H and C_L, respectively) form the C region. The various heavy-chain C domains are numbered from the amino-terminal end to the carboxy terminus, for example CH_1, CH_2 and CH_3. The two identical fragments that contain the antigen-binding site are called Fab fragments (Fragment antigen binding). These fragments contain the complete light chains paired with the V_H and C_H1 domains of the heavy chains. Antibodies posses another fragment with no antigen-binding activity but was originally observed to crystallize, and for this reason was named the Fc fragment (Fragment crystallizable), which corresponds to the paired C_H2 and C_H3 domains [34].

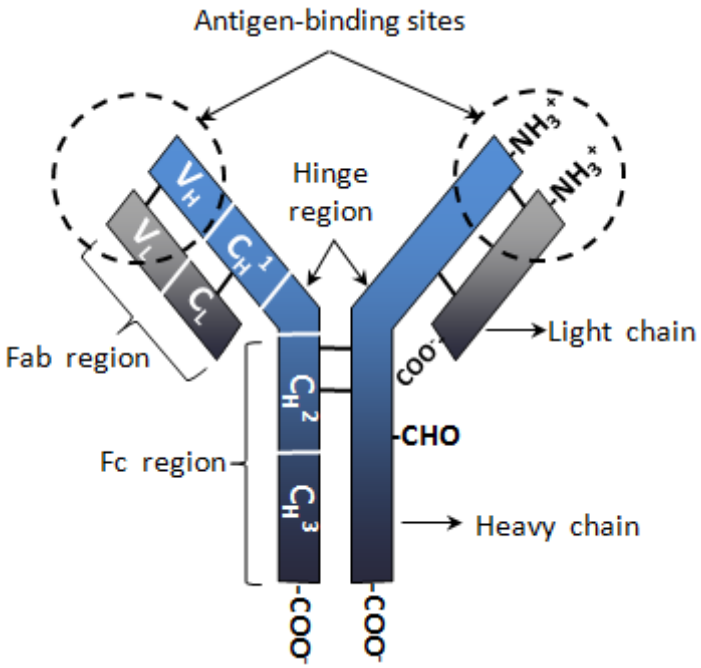

Figure 1.4. Schematic representation of an antibody molecule.

Nowadays, immunosensors play an important role in areas such as clinical chemistry, food quality, and environmental monitoring [35, 36]. Immunosensors are becoming important tools for the detection of the early stages of cancer, since traditional methods are poor in sensitivity and time consuming [37–39]. Electrochemical and optical are the two transduction methods most used in immunosensors, however the former type is gaining more attraction since enables a fast, sensitive, simple and economical detection. Enzyme labels incorporated to the antibodies or antigens, such as horseradish peroxidase (HRP) and alkaline phosphatase (AP) are used to increase the sensitivity of the sensor. The affinity between antibodies and antigens

is very strong but of non-covalent nature, which allows the regeneration and reusability of the immunosensor. The regeneration can be carried out by using a basic solution (NaOH/NaCl) or more commonly by use of glycine/HCl buffer solution (pH 2 - 3) via exposure for a few minutes, and then washing with distilled water or buffer several times to desorb the bound analyte [32].

1.3.3 DNA biosensors

Since the discovery of the deoxyribonucleic acid (DNA) by Fiedrich Miescher in 1869 [40], the field on DNA research has attracted enormous attention, since this molecule stores the hereditary information for the development and functioning of all known living organisms and many viruses. In 1953, Watson, Crick, Wilkins and Franklin proposed the double helix structure of the DNA [41, 42], marking one of the most important scientific discoveries. Another important event that revolutionized the field took place in 1983, when Kary Mullis developed the polymerase chain reaction (PCR) [43]. This method allowed the exponential amplification of a low number of DNA copies from samples in a rapid, sensitive and cost-effective manner. This technique use a polymerase enzyme, deoxyribose nucleoside triphosphates (dNTPs) and two primers, which determine the sequence of the gene that will be amplified. These achievements, among many others, resulted in the launch of the human genome project in 1990. This project aimed to sequence the whole human genome, which was completed in 2003, opening a new era for unveiling and understanding the information contained in genes.

DNA-based sensors (also called genosensors) rely on the recognition of the complementary strand of single stranded (ss) DNA to form a stable hydrogen bond between two nucleic acids to form double stranded (ds) DNA. To achieve this, a ssDNA containing a base sequence complementary to the DNA target is immobilised at the surface of the transducer. The most widely used biomolecule for such sensors is DNA, however other DNA-derived probes are also used, such as peptide nucleic acids (PNAs), dendrimers and molecular beacons [44].

A DNA molecule consists of two long polynucleotide chains (also called strands) composed of four types of nucleotide subunits. Each of these subunits is composed of three main elements: a five-carbon sugar to which are attached one or more phosphate groups and a nitrogen-containing base. In the case of the nucleotides in DNA, the sugar is deoxyribose attached to a single phosphate group, and the nitrogenous base can be either adenine (A), cytosine (C), guanine (G), or thymine (T). These same symbols (A, C, G, and T) are also commonly used to denote the four different nucleotides, that is, the bases with their attached

sugar and phosphate groups. The nucleotides are covalently linked together in a chain through the sugars and phosphates, which thus form a "backbone" of alternating sugar-phosphate-sugar-phosphate (Figure 1.5). The way in which the nucleotide subunits are lined together gives a DNA strand a chemical polarity, with two distinguishable ends, one with a 3'hydroxyl and the other with a 5'phosphate. This polarity in a strand is indicated by referring to one end as the 3' end and the other as the 5' end. A DNA molecule is composed of two DNA strands forming the so-called double helix, which is held together by hydrogen bonds between the paired bases of the different strands in a process called Watson-Crick base-paring. A always pairs with T forming two hydrogen bonds, whereas C pairs with G forming three hydrogen bonds. This base-pairing can only occur if the two polynucleotide chains that contain them are antiparallel to each other [45].

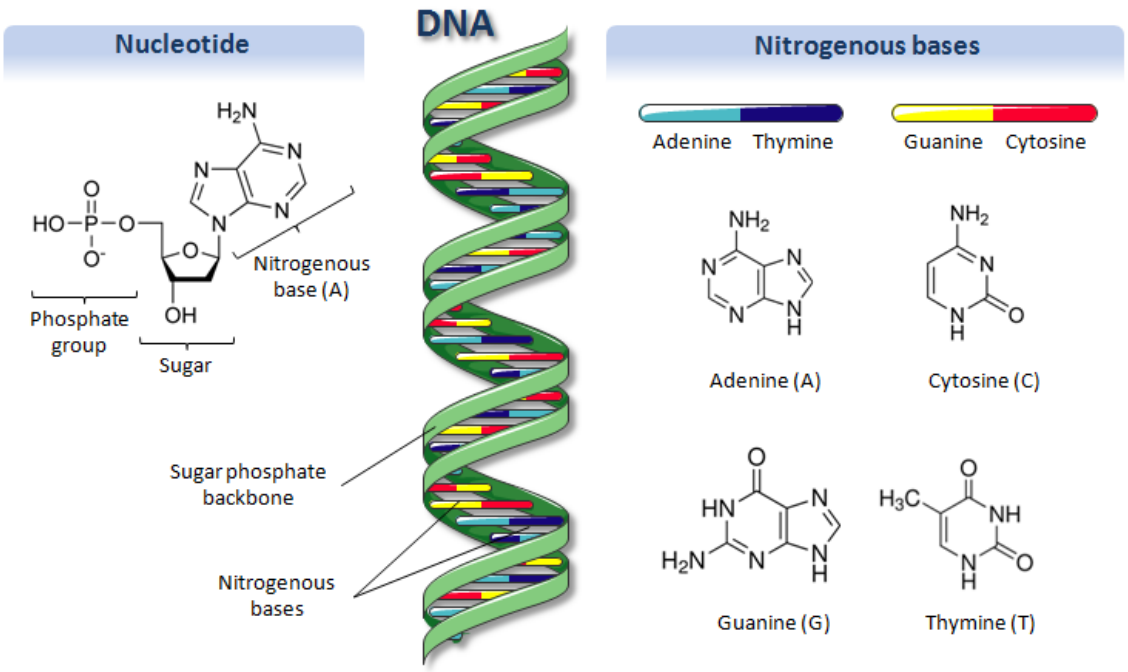

Figure 1.5. Schematic representation of a nucleotide, a double stranded DNA molecule and the four types of nitrogenous bases.

DNA detection technologies exploit this DNA base-pairing through hybridisation assays. Conventional nucleic acid hybridization methods, like Southern blotting, are usually lengthy and labour-intensive. DNA microarrays, which make use of this sequence-specific DNA hybridization, generally suffer from the large size of biological samples, their complex

treatment and high cost, which impedes their application for point-of-care diagnostics. However, DNA biosensors have shown the potential to overcome these inconveniences, allowing easier, faster and cheaper results than in traditional hybridisation based assays, whilst maintaining high sensitivity and specificity of detection [46]. Moreover, DNA sensors can also be integrated in generic lab-on-a-chip platforms for DNA isolation, purification, amplification and detection of genes associated with diseases with the possibility of automation. Such integrated and automated devices are expected to play an important role in POC diagnostics, especially in personalized medicine.

Genosensors are of great importance in the field of molecular diagnostics and have found applications in many fields, such as DNA diagnostics, gene analysis, fast detection of biological warfare agents, and forensic applications. Detection of genetic mutations at the molecular level opens up the possibility of performing reliable diagnostics even before any symptom of a disease appears [44]. As in the case of immunosensors, both electrochemical and optical are the two transduction technologies more frequently used. Detection of DNA hybridisation can also be carried out directly (label-free) or indirectly with the use of labels. The second approach generally shows a higher sensitivity, however is more difficult to implement in POCDs. Labels such as radioisotopes, enzymes, nanoparticles, fluorophores, redox species and quantum dots are often used to monitor the recognition event. Due to the physical nature of the bond between the capture molecule and the target, these sensors offer the possibility to be reused by simply removing the target and leaving the capture probe at the transducer surface. This can be achieved by denaturing the DNA with the use of the suitable solutions or buffers as previously explained.

1.3.4 Electrochemical biosensors

Electrochemical biosensors are the most widely used type of biosensors with applications in several areas and especially in the field of clinical diagnostics, offering a real alternative to the conventional laboratory methods due to their high sensitivity, speed, low cost, small sample volume, simple instrumentation, potential for multitarget analysis and possibility for miniaturisation and integration in point of care devices, [47, 48].

This type of sensor uses an electrode as the transduction element. Generally, electrochemical sensing requires three electrodes: a working electrode, a reference electrode and a counter or auxiliary electrode. The working electrode acts as the transduction element of the biochemical event, while the counter electrode establishes a connection to the

electrolytic solution so that a current can be applied to the working electrode. The reference electrode is commonly made of silver or silver chloride (Ag/AgCl) and is responsible for maintaining a known and stable potential at the working electrode. The working electrodes should be both conductive and chemically stable and they are mainly made of gold, platinum, carbon (e.g. graphite) and silicon compounds are commonly used, depending on the analyte [49]. Electrochemical sensors are based on the measurement of an electrical signal resulting from the biorecognition process, which is proportional to the analyte concentration. Depending on the nature of these electrochemical changes, these sensors can be divided in four categories: amperometric, potentiometric, impedance and conductometric.

Electrochemical sensing can also facilitate direct label-free transduction of the biorecognition process via the use of electrochemical impedance spectroscopy or, in the particular case of genosensors, also by electrochemical reduction of DNA. Although label-free detection simplifies the assay and reduces time and costs of analysis, the level of sensitivity achieved is lower when compared to labelled-detection systems [50]. Thus the majority of electrochemical systems rely on labelled-detection technologies which typically require the introduction of electroactive species in one of the recognition partners or in the solution being analysed, or alternatively the addition of secondary labelled species. Among the most used labels are enzymes such as peroxidase, glucose oxidase, alkaline phosphatase, catalase or luciferase, redox mediators such as ferrocene, $Fe(CN)_6^{3-/4-}$, $Ru(bpy)_3^{3+/2+}$, $Os(bpy)_3^{3+/2+}$ and methylene blue (MB) as well as nanomaterials such as gold nanoparticles [51]. In genosensors, another indirect detection technology involve the use of DNA-intercalating or groove-binding redox indicators, which have a higher affinity for the resulting hybridised DNA duplex as compared to the single-stranded probe. Frequently used indicators involve organic dyes like Hoechst 33258, and methylene blue, organic drug small molecules such as daunomycin, doxorubicin and anthraquinone, and metal-cation compounds like $Co(phen)_3^{3+}$, $[Ru(NH_3)_6]^{3+}$ [52].

Amperometric detection is based on the measurement of current resulting from the oxidation or reduction of an electroactive species in a biochemical process. If the current is measured at a constant potential it is known as amperometry, whereas if the current is measured at variable potentials it is referred to voltammetry. Depending on the way the potential varies, there are also many types of voltammetry, including polarography, linear sweep, differential staircase, normal pulse, reverse pulse, differential pulse [53]. Amperometric sensing typically involves a three-electrode system, which is used to apply a

specific potential between the working and the reference electrode, which produces the oxidation or reduction of the electroactive species at the working electrode. This causes a transfer of electrons which results in a measurable current that is directly proportional to the concentration of the electroactive species. This detection system requires the use of electrochemically active labels (directly or as product of an enzymatic reaction). The most commonly used labels in amperometric biosensors are enzymes, since they provide great signal amplification and also there is a large number of enzyme-conjugated species commercially available. Despite the disadvantage of the labelled-based detection, amperometric devices offer a sensitivity superior to potentiometric devices [30, 53].

Potentiometric biosensors are based on the measurement of the potential difference between the working electrode and reference electrode when zero or negligible current flows through them [48]. Basically, they provide information about the ion activity in an electrochemical process. The working electrode may be an ion selective electrode (ISE) based on thin film or permselective membranes. The ISE converts the biorecognition event into a potential response to provide analytical information. This potential signal is governed by the Nernst equation, which establishes the relationship between the logarithm of the concentration of the substance being measured and the potential difference [54]. ISEs can detect ions such as F^-, I^-, CN^-, Na^+, K^+, Ca^{2+},H^+, NH^{4-}, or gas (CO_2, NH_3) in complex biological matrices. ISEs are mainly used in clinical chemistry for the measurement of relevant electrolytes in physiological fluids and also in analytical chemistry and biochemical/biophysical research, where measurements of ion concentration in an aqueous solution are required [55].

Conductimetric devices rely on the measurement of the electrical conductivity in a solution at constant voltage, produced by biochemical reactions which specifically generate or consume ions. Conductivity varies with changes in the concentration of the ionic species. Enzymes are typically used in these biosensors, since they produce a change in the ionic strength, and thus the conductivity, of a solution as a result of an enzymatic reaction. Some of the advantages of this type of sensor are the low cost and simplicity, since no reference electrodes are needed. However, only a few clinical applications have been reported using these devices. The main reasons are the variable ionic background of clinical samples and the necessity to measure relatively small conductivity changes in media of high ionic strength [49].

As mentioned previously, another electrochemical technique that holds the potential of becoming a powerful tool for clinical diagnostics is electrochemical impedance spectroscopy (EIS). The impedance of a system is generally determined by applying a voltage perturbation

with a small amplitude to an electrochemical cell and measuring the current response [56]. The main advantages of EIS are its high sensitivity and the possibility to perform a label-free or reagentless detection, which makes the technique suitable for real time monitoring. The measurements should be performed under well controlled conditions, otherwise the system may suffer from a lack of reproducibility. In faradaic impedance the measurements are performed in the presence of redox specie, such as iron ferrocyanide, which undergoes oxidation and reduction at the surface of the electrode at a certain potential applied during the measurement. As the analyte binds, the surface availability for redox reaction decreases while impedance increases [57]. Traditionally EIS has been used for the determination of corrosion mechanisms and for the characterisation of charge transport across membranes and membrane/solution interfaces. In recent years, the technique has become very popular for biosensing, especially for the monitoring of biorecognition events at the transducer surface. EIS have been widely used for the detection of proteins, antibodies, antigens, nucleic acids, whole cells and microorganisms [57].

1.3.5 Immobilisation of the recognition element

An ideal biosensor results from the integration of a biological recognition element onto a transducer surface, in such a way that the native specificity of the bioelement is not altered and the recognition event is efficiently transferred to the transducer. The development of techniques for immobilization of the biomaterials plays an important role in biosensor research. The immobilization process not only ensures the intimate contact of the biological entities with the transducer but also aids in the stabilization of the biological system, enhancing its operational and storage stability. Numerous immobilization strategies have been developed to address some of the major issues in biosensor manufacturing, such as the robustness of the link between the bioelement and the transducer surface, the amount of active bioelement immobilized, and the complexity of the immobilization process. The selection of the coupling method depends on both the surface material and the bioreceptors. This section is focused on immobilization techniques for antibodies and DNA. The methods can be classified in three groups: physical, chemical and bioaffinity immobilization [44, 58]. These methods can form two- or three-dimensional (2D or 3D respectively) molecular architectures. The 2D architectures can be achieved by the direct attachment of the ligand to the surface by physisorption or chemisorption, the attachment to a SAM forming a covalent bond, or the coupling to capturing molecules by bioaffinity interactions previously immobilized on the surface. In 3D systems, the ligand can be immobilized by physical or chemical entrapment on a gel or membrane (Figure 1.6). The 3D architectures generally increase the loading capacity

and do not disturb the potential functional sites of the protein; moreover, the aqueous environment of the gel reduces protein denaturation. However, the gel structure can represent a barrier to diffusion and the molecular recognition events may require longer incubation times.

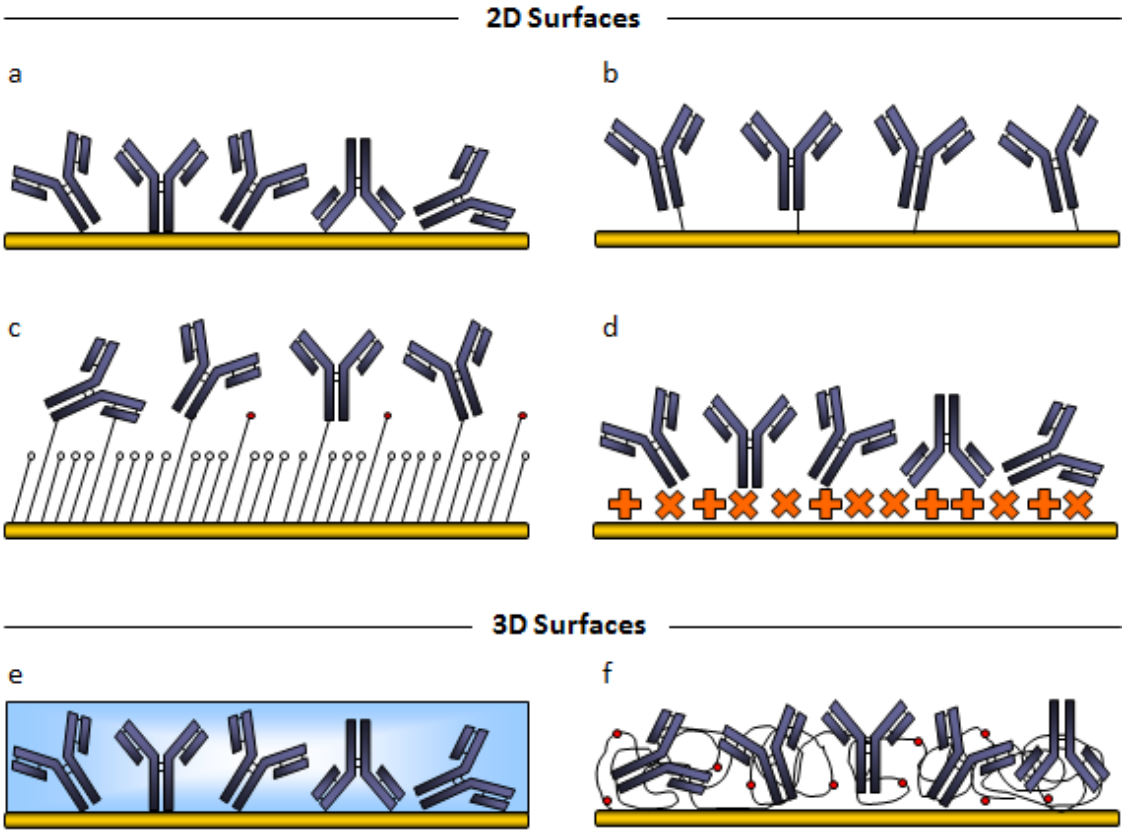

Figure 1.6. Schematic representation of different antibody immobilisation approaches: a) physisorption of unmodified Abs, b) chemisorption of chemically modified Abs, c) covalent immobilisation through a SAM, d) bioaffinity-based immobilisation, e) physical entrapment and f) covalent immobilisation on a matrix containing reactive groups.

To achieve an efficient immobilization the substrate surface should be free of contaminants. The physical method of exposure to ultraviolet-ozone (UV-O_3) is generally effective for removing organic contaminants from surfaces. Another widely used chemical method is based on Piranha solution, which is composed of a 3:1 mixture of H_2SO_4:H_2O_2. This solution is highly oxidative and removes metals, organic and inorganic contamination. Alternatively, a cleaning based on KOH: H_2O_2 solution can also be used with similar results to those obtained by Piranha solution. Electrochemical methods can also be applied for surface cleaning, i.e. cyclic voltammetry between two defined potentials in the presence of H_2SO_4 or

HCl. However, these methods are generally more time-consuming and less compatible with mass-manufacture.

1.3.5.1 Physical methods

Physical immobilization methods basically include adsorption and entrapment. Direct adsorption of biomolecules onto solid supports is the simplest method since the bioelement is used in its native state, offering the advantage of being particularly easy and rapid. This can be achieved by immersing the solid support in a solution containing the biomolecules for a defined amount of time. The bioreceptors are adsorbed on the surface by physical interactions, which are generally weak, sensitive to changes in pH, temperature or salt concentration and offer a poor control over the orientation of the biomolecules. The non-covalent nature of these interactions (hydrogen bonding, electrostatic and hydrophobic interactions and van der Waals forces), typically results in biosensors that suffer from poor analytical performance due to lower operational and storage stability [59]. However, several successful examples of the immobilization by adsorption can be found in the literature for both antibodies [60, 61] and DNA [62, 63]. Another interesting approach is the physical entrapment of biomolecules in gel or membrane coated surfaces [64, 65]. This technique has been reported to improve the stability of the biomolecules due to the hydrophilic nature of the gel, however as mentioned already, the entrapment materials add a diffusional barrier that results in a slower mass transfer [66].

1.3.5.2 Chemical methods

Chemical immobilization methods result in the formation of covalent bonds between the ligand and the surface and basically include chemisorption and covalent attachment on functionalized surfaces. Chemisorption consists of the direct immobilization of ligands on the surface through covalent bonds, generally using thiol-metal interactions. The strong affinity of the thiol groups for noble metal surfaces allows the formation of covalent bonds between the sulphur and gold atoms [67].

$$\text{Biomolecule-SH} + \text{Au} \longrightarrow \text{Biomolecule-S-Au} + e^- + H^+$$

This can be achieved via the introduction of sulphur-containing molecules into the bioelement structure prior to its chemisorption onto gold. In this thesis, this approach was applied to both antibodies and antigens for the optical and electrochemical detection of ischemic stroke and celiac disease related proteins, as described in chapters 2 and 3 respectively. Generally, thiol groups are easily incorporated into the DNA molecule through

the 5' or 3' end. Plethora of biosensors have been developed using thiol-modified DNA probes [68–71]. In the same manner, sulphur-containing molecules can be introduced into the antibody structure. Antibodies have several functional groups suitable for modification including lysine ε-amine, N-terminal α-amine groups, and C-terminal aspartic acid and glutamic acid residues. Primary amine groups are known to have a high nucleophilic behaviour at basic pH. In the presence of an active ester, the free electron pair of the amine group can easily attack the electrophilic carboxylic carbon of the ester. Introduction of disulphides by this synthetic route can be performed by reacting terminal primary amines and lysine residues of IgG with a disulphide-containing active ester, giving rise to a covalent attachment between disulphide groups and IgG [72] (Figure 1.7). Terminal carboxylic acids and glutamic acid residues are also available for modification. At acidic pH, carboxylic acids can react with carbodiimide derivates in the presence of N-hydroxysuccinimide and form an active ester, whilst at basic pH, primary amines can easily attack the electrophile carbon of the ester [72] (Figure 1.8).

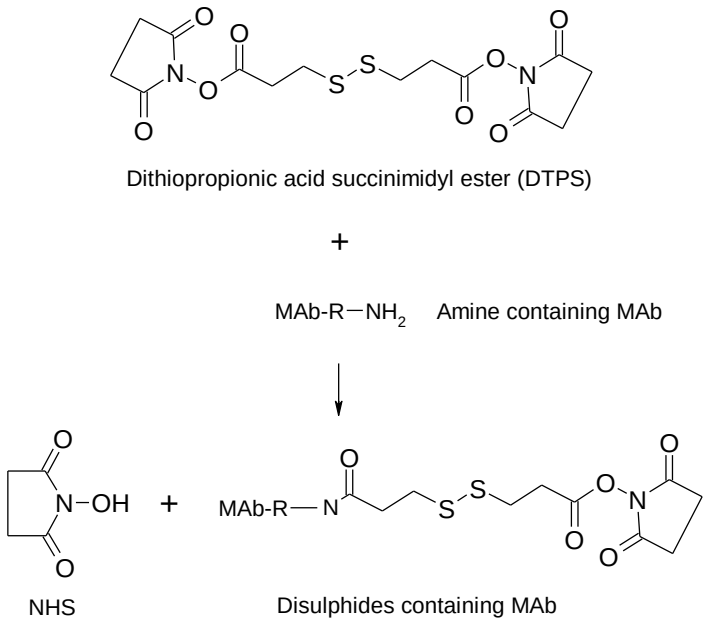

Figure 1.7. Reaction scheme of the introduction of disulphides via $-NH_2$ residues.

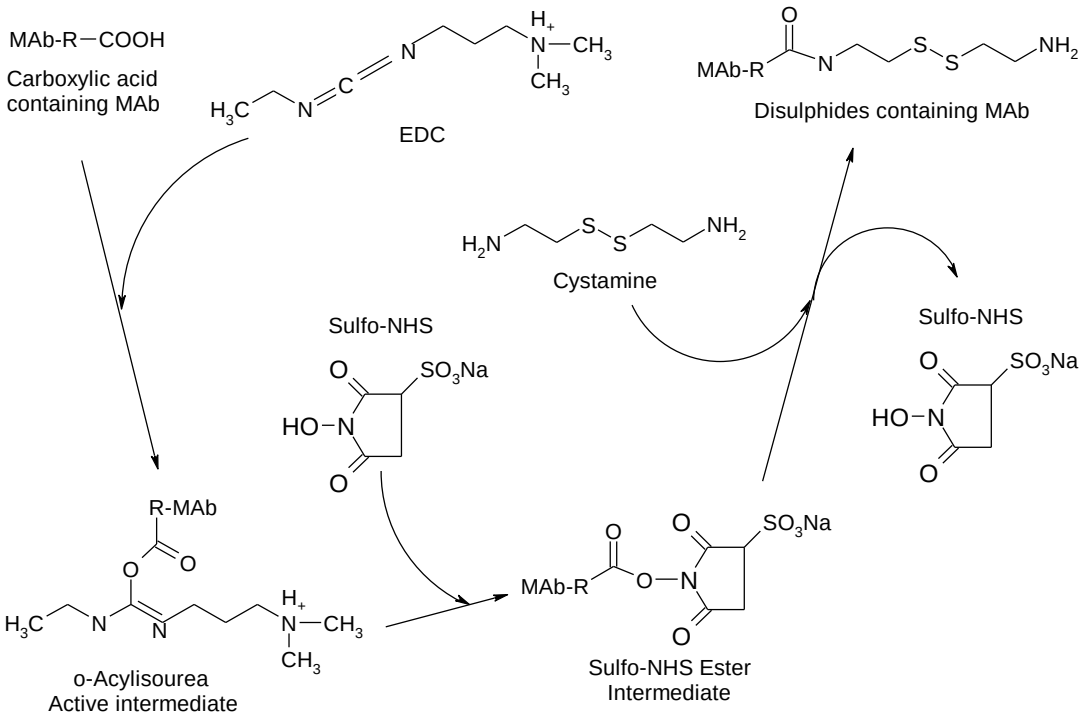

Figure 1.8. Reaction scheme of the introduction of disulphides via –COOH residues.

Chemical conjugation reactions with antibody molecules are generally more successful at preserving activity if the functional groups utilized are present in limiting quantities and only at discrete sites on the molecule. Such "site-directed conjugation" schemes make use of cross-linking reagents that can specifically react with residues that are only in certain positions on the immunoglobulin surface, usually chosen to be well removed from the antigen binding sites. Two site-directed chemical reactions are especially useful in this regard. The disulphide in the hinge region that holds the heavy chains together can be selectively cleaved with the reductant 2-mercaptoethylamine to create two half-antibody molecules, each containing an antigen binding site [72]. The second method of site-directed conjugation is based on the modification of antibodies via their carbohydrates. This method takes advantage of the carbohydrate chains, which are located in the C_H^2 domain within the Fc region. Mild oxidation of the polysaccharide sugar residues with sodium periodate generates aldehyde groups, which then can be used for coupling to another molecule [72]. By proper selection of the conjugation reaction and knowledge of antibody structure, the immunoglobulin molecules can be oriented so that its bivalent binding potential for antigen remains available.

The introduction of disulphide groups into IgG structures was achieved by oxidizing the polysaccharide residues to aldehydes that react with primary amine groups of cystamine via

the formation of Schiff bases (Figure 1.9). Alcohols groups of carbohydrates can be partially oxidised in aldehydes under the oxidative power of periodate ($IO4^-$), in an acidic medium. These aldehydes then easily react with primary amines and form Schiff bases. The unstable imines formed have to be reduced (reductive amination), under the action of borohydride, to stable secondary amines. The precise location of carbohydrates on the constant region of antibodies is particularly interesting to achieve an optimal oriented immobilization [58].

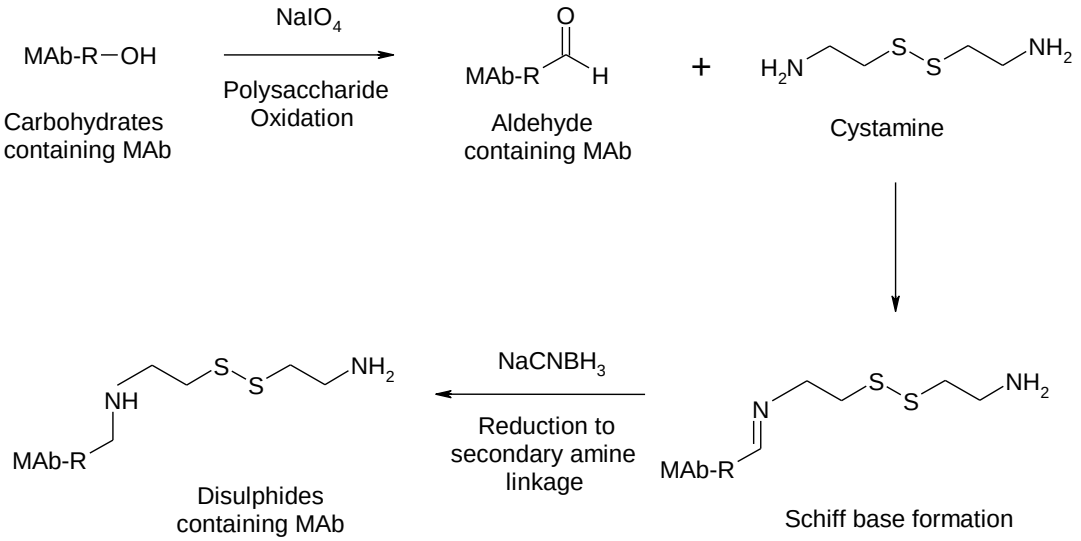

Figure 1.9. Reaction scheme of the introduction of disulphides via carbohydrates.

Another interesting approach of chemical immobilization is the covalent attachment of biomolecules on surfaces functionalized with SAMs. Self-assembly is the spontaneous formation of complex structures of molecules that are held together by non-covalent intermolecular interactions. A self-assembled monolayer is a single layer of ordered molecules that are formed spontaneously at the solid-liquid interface by chemisorption between the solid substrate and the head group of the molecule [23]. Typical molecules used in SAM formation consist of three parts: a head group for coupling with the surface, an end group for the chemical cross-linking with the biomolecule and a chain or backbone, which holds together the two terminal groups and is important for stabilization and order. There are a number of head groups that bind to specific metals, metal oxides, and semiconductors. Several types of biological receptors, including proteins, enzymes, antibodies and their receptors, and even nucleotides for DNA recognition, can be coupled to SAM-modified surfaces [73].

SAMs on surfaces are generally prepared by immersion of the clean substrate into a solution containing an appropriate amphiphile. Several molecular systems are able to undergo the process of self-assembly [74]: long chain carboxylic acids ($C_nH_{2n+1}COOH$) at metal oxide substrates, organosilane species ($RSiX_3$, R_2SiX_2 or R_3SiX, where R is an alkyl chain and X a chloro or alkoxy group) at hydroxylated substrates, such as glass, silicon and aluminium oxide; and organosulfur-based species at noble metal surfaces. Sulphur-containing compounds, such as alkanethiols, dialkyl disulfides and dialkyl sulfides, have a strong affinity for noble metal surfaces. The most used class of SAMs is derived from the adsorption of alkanethiols on gold, silver, copper, palladium, platinum and mercury [75]. The process of formation of self-assembled structures on surfaces can be modeled using the Langmuir equation:

$$\frac{d\theta}{dt} = k\,(1 - \theta) \qquad (1)$$

where θ is the coverage of the surface, and k is the rate constant [76]. The model indicates that the SAM formation rate is proportional to the uncovered surface. Kinetic studies have shown that the process of the self-assembly of alkanethiols compounds onto gold occurs in two steps: an initial step in which the sulphur-containing compound is rapidly chemisorbed in several minutes onto the metal substrate resulting in 80 – 90 % SAM formation, and a second slower step in which the alkyl chains rearrange themselves due to inter-chain van der Waals and electrostatic interactions to produce an extended close packed molecular layer. This molecular reorganization can proceed for up to 12 – 16 hours [77]. The alkyl chains have been found to be tilted from the perpendicular to the gold surface an angle between 26 and 28° [78]. Gold substrates have been widely used for SAM formation as gold is an inert element which has a low toxicity to biological systems and therefore a high biocompatibility. Additionally, thin gold films are very easy to pattern through lithography and chemical etching. Other commonly used metals are silver, copper and palladium [79].

The use of SAMs for creating single molecular films of biological ligands offers multiple advantages, such as, a) the ease of preparation of the self-assembled structures, b) the possibility of modifying the surface properties by simply changing the end group, c) SAMs permit reliable control over the packing density and lateral spacing of the bioelement, d) the ability to mimic naturally occurring molecular recognition processes, e) since SAMs are in intimate contact with the support surface, the recognition event can be more efficiently transferred to the transducer, and f) can be used as as building blocks in more complex structures, e.g., for coupling additional layers to a surface [78, 80]. Moreover, SAMs do not

only allow the coupling of biomolecules, but also serve as nonfouling material to prevent the nonspecific adsorption of molecules to the surface. This can be achieved using highly hydrated molecular systems such as poly (ethylene glycol) (PEG)-based SAMs, which have been demonstrated for their superlow-fouling ability to resist nonspecific protein adsorption and cell adhesion [81]. The use of SAMs in the construction of biosensors is one of the preferred immobilization strategies with multiple examples in the literature [21, 82–85]. One of the most commonly used covalent reactions to couple the biomolecules to the SAM-modified surface is based on the use of 1-ethyl-3-(3-dimethylaminopropyl)cabodiimide (EDC) with or without N-hydroxysuccinimide (NHS). In this one-step reaction, the EDC activates the carboxylic groups present in either the biomolecules or the SAM, which can then react with the primary amines from the functionalized surface or the ligand.

1.3.5.3 Bioaffinity immobilization

Bioaffinity immobilization is another non-covalent method for anchoring biomolecules on surfaces and is based on reversible interactions between the bioreceptor and an intermediate affinity molecule attached to the surface. Compared to the classical non-covalent immobilization strategy (i.e physical adsorption), this technique can provide a higher control over the antibody orientation. In the case of the antibodies, bioaffinity immobilisation methods basically rely on the use of protein A and G, avidin-biotin interactions and affinity tags, whereas in the case of the DNA, these methods are generally reduced to the use of the avidin-biotin system.

Antibodies can be immobilized via an intermediate protein directly attached to the surface, such as protein A and G, which have five and two binding domains specific to the Fc region of antibodies, respectively. This technique predominantly gives a tail-on orientation, resulting in the full availability of the two antigen-binding sites. Several studies have demonstrated an improvement of biosensor performance by orienting the antibodies using protein A or G [86–88]. Alternative immobilization strategy that provides orientation is based on the fusion of a polyhistidine (His_6) affinity-tag on the C- or N-terminus of the antibody [89–91]. The His_6 tag shows a high affinity ($K = 10^7\ M^{-1}$) to Ni^{2+}, Co^{2+} and Cu^{2+} surfaces. The chelating agent nitrilotriacetic acid (NTA) has a strong affinity for bivalent metal ions such as Ni^{2+} which have six coordination sites. Four of these are chelated to NTA, leaving two sites free to coordinate other groups. Several amino acids, including His, have a moderate affinity to Ni^{2+}-NTA complexes [58]. This has been exploited for the of immobilization His-tagged proteins to biosensor surfaces previously modified with NTA [92, 93].

The use of avidin (or streptavidin)-biotin interactions has been widely used to immobilize enzymes, antibodies and DNA. This specific interaction is one of the strongest non-covalent interactions known in biology with an association constant (Ka) of 10^{15} M^{-1} [44]. Both avidin and strepavidin are tetrameric proteins that have four identical binding sites for biotin. Avidin (66 KDa) is a highly cationic glycoprotein with an isoelectric point of about 10.5, while streptavidin (52.8 KDa) is a non-glycosylated protein with a near-neutral isoelectric point. Avidin has been reported to exhibit higher non-specific binding than spreptavidin. This is attributed to its positively charged residues and its oligosaccharide component, which can react non-specifically with negatively charged cell surfaces and nucleic acids, causing background issues [94]. Generally the bioreceptors are conjugated to biotin molecules and subsequently immobilized on streptavidin-modified surfaces. In the case of the DNA, the biotin is typically introduced to the 5' or 3' end by chemical cross-linking, leaving the entire DNA molecule available for hybridization with its complementary target [95–97]. Antibodies can be immobilized in an oriented or random mode depending of the biotinylation procedure used. Oriented methods are based on the site-specific introduction of biotin molecules via the hinge region, C-terminus and sugar moieties and they have been reported to increase the binding signal [98–100].

1.4 Fabrication of low-density electrode arrays

Advances in microfabrication have led to the replacement of traditional "beaker-type" electrochemical cells and bulky electrodes with small and cost-effective easy-to-use sensing devices. This has also driven great advances in the development of miniaturized electrochemical sensors and sensor arrays, which can now be integrated in complex fluidic microsystems, the so-called lab-on-a-chip devices. Electrochemical biosensors consist of a system of electrodes made up of metals which need to be patterned on top of a substrate. Most of these sensors have been fabricated on silicon or glass substrates using standard photolithography techniques and thin or thick film technology. The three basic microfabrication techniques for these biosensors are identical with those used in integrated-circuit (IC) fabrication: deposition, patterning and etching (Figure 1.10). Initially a thin layer is deposited on a substrate, followed by the deposition of a light-sensitive photoresist layer. Subsequently, this layer is patterned by photolithography using the desired mask. The pattern is then transferred from the photoresist layer to the substrate by an etching process. Finally, the remaining photoresist is removed, resulting in a specific configuration of the reference, counter and working electrodes deposited onto the substrate.

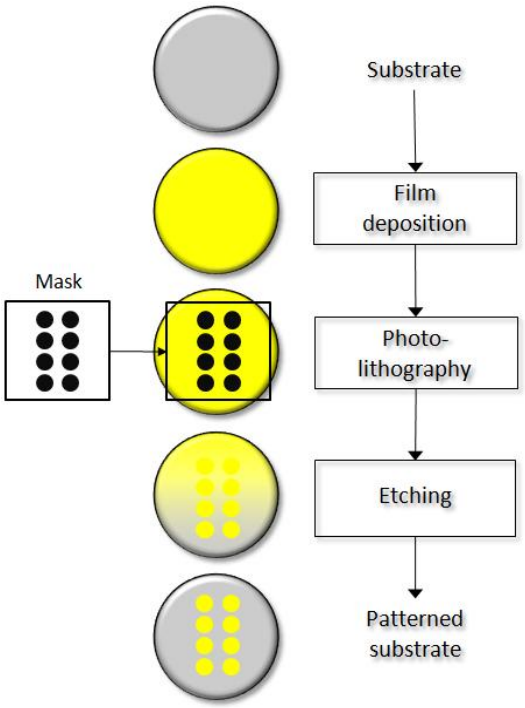

Figure 1.10. Flow diagram of an integrated circuit (IC)-based fabrication process using the three basic microfabrication techniques: film deposition, photolithography and etching.

Metallic layers are used as electrode material and are generally deposited using two thin-film deposition methods, chemical vapour deposition (CVD) and physical vapour deposition (PVD), such us sputtering and evaporating. Film thicknesses achieved by these processes are of tens of nanometres to up to a few micrometers. A great variety of metals can be deposited, including gold, silver, platinum, palladium, copper or alloys [101]. In the photolithographic process, a pattern is transferred to a certain substrate using a mask with the desired pattern. A photoresist layer is spin-coated onto the material to be patterned and subsequently exposed to UV light through the mask using a mask aligner. Depending on the type of photoresist used, positive or negative, the exposed or the unexposed photoresist areas are removed during the resist development process. The remaining photoresist acts as a protective layer during the etching process, which transfers the pattern onto the underlying material. This thin-film photolithographic process is widely used and employs atomic or molecular deposition which results in good quality electrodes with sub-micrometers resolution and highly reproducible. However, this process has a high associated cost.

A widely used technique in industry for the production of electrode arrays is screen-printing. This process is based on thick film technologies and unlikely photolithography, does

not require a complicated flow process and its operation is simple and inexpensive. Paste material is printed onto a matrix directly through a mask-net with a designed pattern resulting in thicknesses of a few to hundreds micrometers [102]. Electrodes are usually made by screen-printing patterns of conductors and insulators by a special printer. The desired patterns are defined by precision screens that are made of stainless-steel wire. Paste materials include carbon nanotubes (CNTs), platinum, silver, gold, carbon, graphite and dielectrics [103]. Each ink is applied individually with the corresponding screen pattern to create the final electrode configuration. This technology is relatively inexpensive and suitable for portable and single use electrode systems, such as disposable screen-printed enzyme strips, widely used by diabetic patients for self-monitoring of their blood glucose levels [104]. The major drawback of this process is the limited resolution after photolithography [103].

Another metal micro-patterning technique for the low-cost mass production of electrochemical sensor arrays is based on standard printed circuit board (PCB) technology. This technique offers several metallic surface finishes, such as gold, copper and silver, compatible with a variety of surface chemistries for the immobilization of biomolecules. PCBs, also called “printed wiring boards” or “printed wiring cards”, are widely used in electronics industry for the manufacturing of integrated circuits. Before the arrival of the PCB, electronic circuits were produced through a tedious process of point-to-point wiring, which was prone to failures at wire junctions and short circuits when wire insulation began to age and crack. PCBs are basically composed of copper sheets laminated onto a non-conductive substrate. The most commonly used substrate is the FR-4 (Flame Resistant 4), a woven fiberglass cloth impregnated with an epoxy resin, with a thin layer of copper foil laminated on one side (single sided PCB) or both sides (double sided PCB) [105]. The two layers can be electrically connected with the use of vias. The copper sheets, usually of 35 μm thickness, can be photopatterned with the desired mask and etched, resulting in features with dimensions as low as 50 μm. The exposed copper layer can subsequently be coated with thin layers of gold, silver or nickel either via electrolytic, electroless or immersion metal deposition techniques. Electrolytic plating is achieved by passing an electric current through a solution (electrolyte) containing dissolved metal ions allowing the metal to deposit on the conductive surface of the PCB. Electroless deposition uses chemical reducing agents to supply the electrons needed for metal deposition on the copper layer. This process generally results in harder and more brittle deposits than electroplating. Immersion plating is based on a galvanic displacement reaction, which causes exchange of metal atoms on the surface with those in the solution.

The most commonly used surface finish types are Imm Ag (Immersion Silver), Imm Sn (Immersion Tin), ENIG (Electroless Nickel/Immersion Gold), ENEG (Electroless Nickel / Electroless Gold) and electrolytic Ni /Au (Electrolytic Nickel / Gold). An intermediate layer of nickel of approximately 1 to 4 μm is generally plated in between the copper and gold layer to prevent the solid-state diffusion of the copper atoms into the gold atoms of the surface. Both electroless and immersion plating of gold generally results in a heterogeneous surface of gold contaminated by the underlying layers (i.e. nickel), which makes these processes inadequate for the fabrication of electrode arrays. In contrast, electrolytic Ni /Au plating results in a homogenous layer of 99.9 % purity of gold of approximately 1 to 3 μm thick, compatible with electrochemistry and surface modification chemistries and therefore suitable for biosensing applications [106, 107].

1.5 Nucleic acid amplification techniques

The first nucleic acid amplification technique was the polymerase chain reaction (PCR). Since its discovery in 1983, it has had a tremendous impact in several fields, such as research, clinical medicine, gene cloning, agriculture, and more specifically in relation to this thesis, in the field of DNA biosensors. The technique allowed the rapid generation of multiple copies from a sample containing just a few target copies, which provides a great improvement on the assay sensitivity. Progress of research has resulted in the development of alternative amplification methods with a higher speed, lower cost and improved portability, mostly focused on isothermal processes and multiplexing ability. The most commonly used isothermal techniques are recombinase polymerase amplification (RPA), loop mediated isothermal amplification (LAMP), nucleic acid sequence based amplification (NASBA), strand displacement amplification (SDA) and rolling circle amplification (RCA). These techniques obviate the use a thermal cycler since the reaction occurs at a constant temperature, however only NASBA and RCA facilitate multiplexing [108]. Alternative multiplexing techniques include universal multiplex PCR (UM-PCR), isoPCR and ligase chain reaction (LCR), however these techniques require the use of several primers sets to amplify the desired regions of the genome [109–111]. The presence of multiple primers may lead to cross hybridization with each other and the possibility of mis-priming with other templates as well as leading to differences in amplification efficiency. The introduction of the multiplex ligation-dependent probe amplification (MLPA) provided an elegant solution avoiding the need for several primers. MLPA is a multiplex-PCR based technique with the ability to amplify up to 50 nucleic acid sequences with a resolution down to the single nucleotide level with a single primer pair [112].

MLPA is based on the hybridisation of probes to target DNA, followed by ligation and quantitative PCR amplification of the ligated products. Each probe generally consists of two oligonucleotides, the left hybridisation oligonucleotide (LHO) and the right hybridisation oligonucleotide (RHO). The LHO is usually the shorter of the two probes (typically 45–70 nt) and is chemically synthesized. It is composed of a unique annealing sequence and a universal PCR forward primer common to all probes. The RHO can be up to 440 nt and are generally produced using M13 cloning vectors, although it can also be chemically synthesised. RHOs are composed of stuffer sequences of different lengths in between a target-specific sequence and a universal reverse primer. Initially, the DNA target is denatured and incubated with a mixture of specific probes. The hybridizing sequences of the LHO and RHO are directly adjacent, permitting the two oligonucleotides to be ligated when both are hybridized to their target sequence. Ligated probes are then PCR amplified resulting in products of between 130 and 480bp in length, each one of a unique size, which can be separated by size using capillary electrophoresis. Probes that are not ligated contain only one primer sequence and cannot be amplified.

Currently there are more than 300 probe sets commercially available with applications in several fields, such us prenatal and postnatal testing (Down syndrome, metal retardation, microdeletions, etc.), cancer diagnosis (breast, stomach and colon cancer, cutaneous melanoma, etc.) and neurogenetic testing (Alzheimer and Parkinson diseases, epilepsy, etc.) among others. Most of these MLPA kits have been developed by MRC-Holland and the semi-quantitative detection of probe amplification products is generally carried out by capillary electrophoresis, since the amplified products vary in length. An alternative electrochemical quantification technique based on a barcode approach is described in Chapter 4 of this thesis. Basically, this approach consists of the replacement of the stuffer sequences of the RHO of each probe set by unique DNA sequences (i.e. barcodes), which are used as a recognition sites by complementary capture probes immobilised at the surface of the electrochemical transducer. This approach was successfully used for the amplification and detection of gene markers related to breast cancer [107].

MLPA offers several advantages over other multiplex PCR techniques, such as the use of a single PCR primer pair for amplification, which eliminates the differences in primer annealing efficiency. Another advantage is that the protocol is simple with a limited number of steps and PCR conditions for all MLPA applications are identical. Finally, the steps in the MLPA process, probe hybridization, ligation of probes, and PCR amplification of ligated products, go to

completion. This makes MLPA less sensitive to differences in PCR conditions, such as changes in reaction times, reaction temperatures, DNA concentration, and several other parameters [113].

Advances in the MLPA technique have resulted in the development of reverse transcriptase MLPA (RT-MLPA) [114]. This method can be used for mRNA profiling as an alternative to real-time PCR and micro-arrays, due to its simplicity, lower cost and moreover, there is no need to perform a sample labelling reaction. In this method, firstly the RNA in converted to cDNA using a reverse transcriptase enzyme and a special RT primer mix, which contains one RT primer for each of the MLPA probes. The conversion into cDNA is a mandatory step, since the probes that are used in the subsequent MLPA reaction are complementary to the cDNA, not to the mRNA. Moreover, the ligase-65 enzyme used in MLPA, cannot ligate DNA probes that are hybridized to RNA sequences. This method then proceeds as the traditional MLPA technique. The RT-MLPA technique combined with the electrochemical detection based on the barcode approach was used for mRNA profiling of single cancer cells (Figure 1.11), as described in chapter 5.

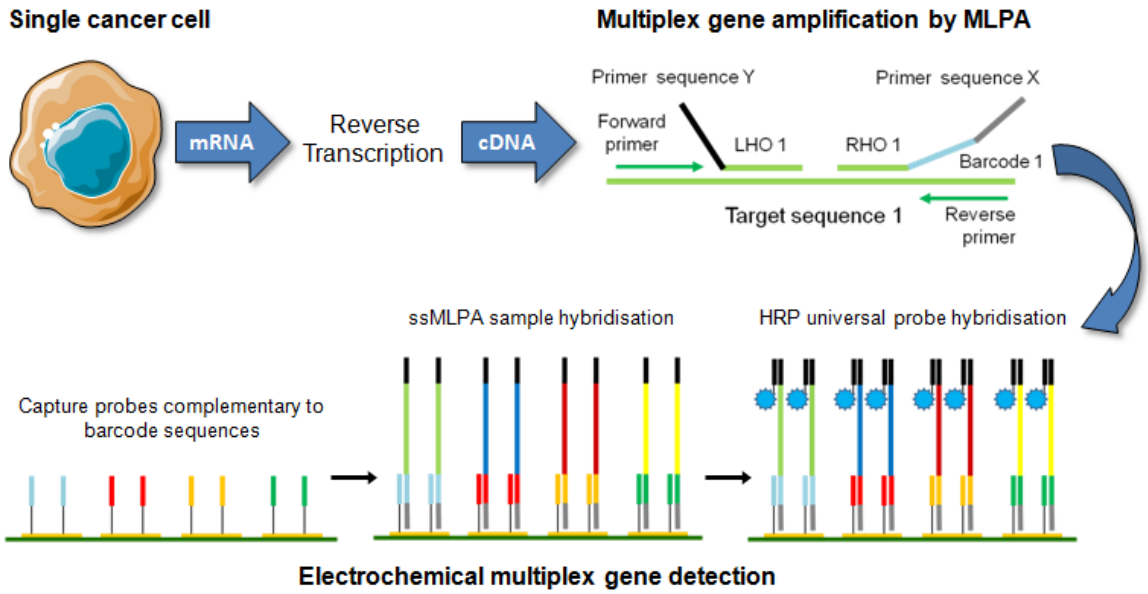

Figure 1.11. Schematic representation of the simultaneous barcode-based electrochemical detection of multiple breast cancer related mRNA markers from a single tumour cell using RT-MLPA.

1.6 Thesis objectives

The general objective of this doctoral thesis is the development of cost-effective electrochemical detection platforms for the quantification of protein and DNA biomarkers related to human diseases.

The first part of my thesis is focused on the development of electrochemical immunosensors for the detection of neuron specific enolase and anti-tissue transglutamise antibodies, an ischemic stroke and celiac disease markers respectively. To achieve this goal the following specific objectives were defined:

- To develop different strategies for covalent self-assembly of both antibodies and antigens onto bare gold substrates by introducing disulphide groups in the protein structure.
- To assess the developed surface chemistries using surface plasmon resonance and apply the optimal chemistry to electrochemical biosensors.
- To compare the developed approach with other covalent immobilisation methods for proteins such as, cross-linking to self-assembled monolayers or to a carboxylated dextran matrix.
- To evaluate the suitability of the optimal surface chemistry for real sample analysis.

The second part of my thesis aimed at the development of a genosensor for the multiplex detection of genetic markers for breast cancer with single cell sensitivity. The following sub-objectives were carried out to accomplish this task:

- To develop surface chemistries for the covalent attachment of DNA at the transducer surface.
- To develop a method for the multiplex amplification and electrochemical detection of seven genetic markers for breast cancer with single cell sensitivity.
- To design, manufacture and assess low-cost electrode arrays.

Overall, the main contribution of this thesis to the field of biosensors is that it provides a simple method for the covalent attachment of proteins directly on the transducer surface limiting the immobilisation to a single step. Additionally, it also presents a flexible and cost-effective strategy for the multiplex amplification and detection of DNA from tumour cells with a potential applicability for genetic profiling.

1.7 References

1. Clark LC, Lyons C (1962) Electrode systems for continuous monitoring in cardiovascular surgery. Ann N Y Acad Sci 102:29–45. doi: 10.1111/j.1749-6632.1962.tb13623.x
2. Guilbault GG, Lubrano GJ (1973) An enzyme electrode for the amperometric determination of glucose. Anal Chim Acta 64:439–455. doi: 10.1016/S0003-2670(01)82476-4
3. Arora N (2013) Recent Advances in Biosensors Technology: A Review. Octa J Biosci Octa J Biosci Octa J Biosci 1:147–150.
4. Schläpfer P, Mindt W, Racine PH (1974) Electrochemical measurement of glucose using various electron acceptors. Clin Chim Acta 57:283–289. doi: 10.1016/0009-8981(74)90408-2
5. Cass AEG, Davis G, Francis GD, Hill HAO, Aston WJ, Higgins IJ, Plotkin E V., Scott LDL, Turner APF (1984) Ferrocene-mediated enzyme electrode for amperometric determination of glucose. Anal Chem 56:667–671. doi: 10.1021/ac00268a018
6. Di Gleria K, Hill HAO, McNeil CJ, Green MJ (1986) Homogeneous ferrocene-mediated amperometric immunoassay. Anal Chem 58:1203–1205.
7. Lee TM-H (2008) Over-the-Counter Biosensors: Past, Present, and Future. Sensors 8:5535–5559. doi: 10.3390/s8095535
8. Turner APF (2013) Biosensors: sense and sensibility. Chem Soc Rev 42:3184. doi: 10.1039/c3cs35528d
9. Mongra AC (2012) Commercial Biosensors: An outlook. J Acad Indus Res 1:310–312.
10. Mairal T, Cengiz Özalp V, Lozano Sánchez P, Mir M, Katakis I, O CK (2008) Aptamers: molecular tools for analytical applications. Anal Bioanal Chem 390:989–1007. doi: 10.1007/s00216-007-1346-4
11. Sun H, Zhu X, Lu PY, Rosato RR, Tan W, Zu Y (2014) Oligonucleotide Aptamers: New Tools for Targeted Cancer Therapy. Mol Ther Nucleic Acids 3:e182. doi: 10.1038/mtna.2014.32
12. Santosh B, Yadava PK (2014) Nucleic acid aptamers: research tools in disease diagnostics and therapeutics. Biomed Res Int 2014:540451. doi: 10.1155/2014/540451
13. Justino CIL, Duarte AC, Rocha-Santos TAP (2015) Analytical applications of affibodies. TrAC Trends Anal Chem 65:73–82. doi: 10.1016/j.trac.2014.10.014
14. Löfblom J, Feldwisch J, Tolmachev V, Carlsson J, Ståhl S, Frejd FY (2010) Affibody molecules: Engineered proteins for therapeutic, diagnostic and biotechnological applications. FEBS Lett 584:2670–2680. doi: 10.1016/j.febslet.2010.04.014
15. Harris MD, Tombelli S, Marazza G, Turner APF (2012) Affibodies as an alternative to antibodies in biosensors for cancer markers. In: Biosens. Med. Appl. pp 217–232
16. Uzun L, Turner APF (2016) Molecularly-imprinted polymer sensors: realising their potential. Biosens Bioelectron 76:131–144. doi: 10.1016/j.bios.2015.07.013
17. Haupt K, Mosbach K (2000) Molecularly imprinted polymers and their use in biomimetic sensors. Chem Rev 100:2495–504.
18. Erdőssy J, Horváth V, Yarman A, Scheller FW, Gyurcsányi RE (2016) Electrosynthesized molecularly imprinted polymers for protein recognition. TrAC Trends Anal Chem 79:179–190. doi: 10.1016/j.trac.2015.12.018
19. Asav E, Akyilmaz E (2010) Preparation and optimization of a bienzymic biosensor based on self-assembled monolayer modified gold electrode for alcohol and glucose detection. Biosens Bioelectron 25:1014–1018. doi: 10.1016/j.bios.2009.09.019
20. Zhang QD, March G, Noel V, Piro B, Reisberg S, Tran LD, Hai LV, Abadia E, Nielsen PE, Sola C, Pham MC (2012) Label-free and reagentless electrochemical detection of PCR fragments using self-assembled quinone derivative monolayer: Application to Mycobacterium tuberculosis. Biosens Bioelectron 32:163–168. doi: 10.1016/j.bios.2011.11.048

21. Yang H, Zhou H, Hao H, Gong Q, Nie K (2016) Detection of Escherichia coli with a label-free impedimetric biosensor based on lectin functionalized mixed self-assembled monolayer. Sensors Actuators B Chem 229:297–304. doi: 10.1016/j.snb.2015.08.034
22. Zhang G-J, Huang MJ, Ang JJ, Liu ET, Desai KV (2011) Self-assembled monolayer-assisted silicon nanowire biosensor for detection of protein–DNA interactions in nuclear extracts from breast cancer cell. Biosens Bioelectron 26:3233–3239. doi: 10.1016/j.bios.2010.12.032
23. Chaki NK, Vijayamohanan K (2002) Self-assembled monolayers as a tunable platform for biosensor applications. Biosens Bioelectron 17:1–12. doi: 10.1016/S0956-5663(01)00277-9
24. Nuzzo RG, Allara DL (1983) Adsorption of bifunctional organic disulfides on gold surfaces. J Am Chem Soc 105:4481–4483. doi: 10.1021/ja00351a063
25. Ferretti S, Paynter S, Russell DA, Sapsford KE, Richardson DJ (2000) Self-assembled monolayers: a versatile tool for the formulation of bio-surfaces. TrAC Trends Anal Chem 19:530–540. doi: 10.1016/S0165-9936(00)00032-7
26. Jianrong C, Yuqing M, Nongyue H, Xiaohua W, Sijiao L (2004) Nanotechnology and biosensors. Biotechnol Adv 22:505–518. doi: 10.1016/j.biotechadv.2004.03.004
27. Zhang X, Guo Q, Cui D (2009) Recent Advances in Nanotechnology Applied to Biosensors. Sensors 9:1033–1053. doi: 10.3390/s90201033
28. Cammann K (1977) Bio-sensors based on ion-selective electrodes. Anal Chem 287:1–9. doi: 10.1007/BF00539519
29. Thévenot DR, Toth K, Durst R a., Wilson GS (1999) Electrochemical biosensors: Recommended definitions and classification. Pure Appl Chem 71:2333–2348. doi: 10.1016/S0956-5663(01)00115-4
30. Perumal V, Hashim U (2014) Advances in biosensors: Principle, architecture and applications. J Appl Biomed 12:1–15. doi: 10.1016/j.jab.2013.02.001
31. Leca-Bouvier BD, Blum LJ (2010) Enzyme for Biosensing Applications. In: Recognit. Recept. Biosens. Springer New York, New York, NY, pp 177–220
32. Ramírez NB, Salgado a. M, Valdman B (2009) The evolution and developments of immunosensors for health and environmental monitoring: Problems and perspectives. Brazilian J Chem Eng 26:227–249. doi: 10.1590/S0104-66322009000200001
33. Kaneko Y, Nimmerjahn F, Ravetch J V (2006) Anti-inflammatory activity of immunoglobulin G resulting from Fc sialylation. Science (80-) 313:670–3. doi: 10.1126/science.1129594
34. Charles A Janeway J, Travers P, Walport M, Shlomchik MJ (2001) The structure of a typical antibody molecule.
35. Braiek M, Rokbani K, Chrouda A, Mrabet B, Bakhrouf A, Maaref A, Jaffrezic-Renault N (2012) An Electrochemical Immunosensor for Detection of Staphylococcus aureus Bacteria Based on Immobilization of Antibodies on Self-Assembled Monolayers-Functionalized Gold Electrode. Biosensors 2:417–426. doi: 10.3390/bios2040417
36. Holford TRJ, Davis F, Higson SPJ (2012) Recent trends in antibody based sensors. Biosens Bioelectron 34:12–24. doi: 10.1016/j.bios.2011.10.023
37. Hong W, Lee S, Cho Y (2016) Dual-responsive immunosensor that combines colorimetric recognition and electrochemical response for ultrasensitive detection of cancer biomarkers. Biosens Bioelectron 86:920–926. doi: 10.1016/j.bios.2016.07.014
38. Chuang C-H, Du Y-C, Wu T-F, Chen C-H, Lee D-H, Chen S-M, Huang T-C, Wu H-P, Shaikh MO (2016) Immunosensor for the ultrasensitive and quantitative detection of bladder cancer in point of care testing. Biosens Bioelectron 84:126–132. doi: 10.1016/j.bios.2015.12.103
39. Duangkaew P, Tapaneeyakorn S, Apiwat C, Dharakul T, Laiwejpithaya S, Kanatharana P, Laocharoensuk R (2015) Ultrasensitive electrochemical immunosensor based on dual signal amplification process for p16INK4a cervical cancer detection in clinical samples.

Biosens Bioelectron 74:673–679. doi: 10.1016/j.bios.2015.07.004
40. Dahm R (2005) Friedrich Miescher and the discovery of DNA. Dev Biol 278:274–288. doi: 10.1016/j.ydbio.2004.11.028
41. Watson JD, Crick FHC (1953) Genetical Implications of the structure of Deoxyribonucleic Acid. Nat 171:964–967.
42. Watson JD, Crick FHC (1953) A Structure for Deoxyribose Nucleic Acid. Nature 171:737–738.
43. Mullis KB, Faloona FA (1987) Specific synthesis of DNA in vitro via a polymerase-catalyzed chain reaction. Methods Enzymol 155:335–350. doi: 10.1016/0076-6879(87)55023-6
44. Sassolas A, Leca-Bouvier BD, Blum LJ (2008) DNA biosensors and microarrays. Chem Rev 108:109–139. doi: 10.1021/cr0684467
45. Alberts B, Johnson A, Lewis J, Raff M, Roberts K, Walter P (2002) The Structure and Function of DNA.
46. Teles FRR, Fonseca LP (2008) Trends in DNA biosensors. Talanta 77:606–623. doi: 10.1016/j.talanta.2008.07.024
47. Wang J (2006) Electrochemical biosensors: Towards point-of-care cancer diagnostics. Biosens Bioelectron 21:1887–1892. doi: 10.1016/j.bios.2005.10.027
48. Burcu Bahadır E, Kemal Sezgintürk M (2015) Applications of electrochemical immunosensors for early clinical diagnostics. Talanta 132:162–174. doi: 10.1016/j.talanta.2014.08.063
49. GS S, CV A, Mathew BB (2014) Biosensors: A Modern Day Achievement. J Instrum Technol 2:26–39. doi: 10.12691/JIT-2-1-5
50. Cagnin S, Caraballo M, Guiducci C, Martini P, Ross M, SantaAna M, Danley D, West T, Lanfranchi G (2009) Overview of Electrochemical DNA Biosensors: New Approaches to Detect the Expression of Life. Sensors 9:3122–3148. doi: 10.3390/s90403122
51. Sadik OA, Aluoch AO, Zhou A (2009) Status of biomolecular recognition using electrochemical techniques. Biosens Bioelectron 24:2749–65. doi: 10.1016/j.bios.2008.10.003
52. Liu CC (2012) Electrochemical based biosensors. Biosensors 2:269–272. doi: 10.3390/bios2030269
53. Grieshaber D, Mackenzie R, Vörös J, Reimhult E (2008) Electrochemical Biosensors - Sensor Principles and Architectures. Sensors 8:1400–1458. doi: 10.3390/s8031400
54. You Wang HXJZGL (2008) Electrochemical Sensors for Clinic Analysis. Sensors (Basel) 8:2043.
55. Bard a, Faulkner L (2002) Allen J. Bard and Larry R. Faulkner, Electrochemical Methods: Fundamentals and Applications, New York: Wiley, 2001. Russ J Electrochem 38:1505–1506. doi: 10.1023/A:1021637209564
56. Lisdat F, Schäfer D (2008) The use of electrochemical impedance spectroscopy for biosensing. Anal Bioanal Chem 391:1555–1567. doi: 10.1007/s00216-008-1970-7
57. Bogomolova A, Komarova E, Reber K, Gerasimov T, Yavuz O, Bhatt S, Aldissi M (2009) Challenges of Electrochemical Impedance Spectroscopy in Protein Biosensing. Anal Chem 81:3944–3949. doi: 10.1021/ac9002358
58. Trilling AK, Beekwilder J, Zuilhof H (2013) Antibody orientation on biosensor surfaces: a minireview. Analyst 138:1619–27. doi: 10.1039/c2an36787d
59. Suárez G, Jackson RJ, Spoors J a., McNeil CJ (2007) Chemical introduction of disulfide groups on glycoproteins: A direct protein anchoring scenario. Anal Chem 79:1961–1969. doi: 10.1021/ac0613030
60. Figueroa J, Magaña S, Lim D V., Schlaf R (2012) Antibody immobilization using pneumatic spray: Comparison with the avidin–biotin bridge immobilization method. J Immunol Methods 386:1–9. doi: 10.1016/j.jim.2012.08.007
61. Zhao X, Pan F, Garcia-Gancedo L, Flewitt AJ, Ashley GM, Luo J, Lu JR (2012) Interfacial

recognition of human prostate-specific antigen by immobilized monoclonal antibody: effects of solution conditions and surface chemistry. J R Soc Interface 9:2457–67. doi: 10.1098/rsif.2012.0148

62. Xu C, Cai H, Xu Q, He P, Fang Y (2001) Characterization of single-stranded DNA on chitosan-modified electrode and its application to the sequence-specific DNA detection. Fresenius J Anal Chem 369:428–32.
63. Zhou XC, Huang LQ, Li SF (2001) Microgravimetric DNA sensor based on quartz crystal microbalance: comparison of oligonucleotide immobilization methods and the application in genetic diagnosis. Biosens Bioelectron 16:85–95.
64. Thomas G, El-Giar EM, Locascio LE, Tarlov MJ (2006) Hydrogel-immobilized antibodies for microfluidic immunoassays: hydrogel immunoassay. Methods Mol Biol 321:83–95. doi: 10.1385/1-59259-997-4:83
65. Xiong X, Wu C, Zhou C, Zhu G, Chen Z, Tan W (2013) Responsive DNA-based hydrogels and their applications. Macromol Rapid Commun 34:1271–83. doi: 10.1002/marc.201300411
66. D'Souza SF (2001) Immobilization and Stabilization of Biomaterials for Biosensor Applications. Appl Biochem Biotechnol 96:225–238. doi: 10.1385/ABAB:96:1-3:225
67. Pensa E, Cortés E, Corthey G, Carro P, Vericat C, Fonticelli MH, Benítez G, Rubert AA, Salvarezza RC (2012) The Chemistry of the Sulfur–Gold Interface: In Search of a Unified Model. Acc Chem Res 45:1183–1192. doi: 10.1021/ar200260p
68. Chen M, Hou C, Huo D, Bao J, Fa H, Shen C (2016) An electrochemical DNA biosensor based on nitrogen-doped graphene/Au nanoparticles for human multidrug resistance gene detection. Biosens Bioelectron 85:684–691. doi: 10.1016/j.bios.2016.05.051
69. Izadi Z, Sheikh-Zeinoddin M, Ensafi AA, Soleimanian-Zad S (2016) Fabrication of an electrochemical DNA-based biosensor for Bacillus cereus detection in milk and infant formula. Biosens Bioelectron 80:582–589. doi: 10.1016/j.bios.2016.02.032
70. Wang B, Jing R, Qi H, Gao Q, Zhang C (2016) Label-free electrochemical impedance peptide-based biosensor for the detection of cardiac troponin I incorporating gold nanoparticles modified carbon electrode. J Electroanal Chem. doi: 10.1016/j.jelechem.2016.08.005
71. Huang S, Lu S, Huang C, Sheng J, Zhang L, Su W, Xiao Q (2016) An electrochemical biosensor based on single-stranded DNA modified gold electrode for acrylamide determination. Sensors Actuators B Chem 224:22–30. doi: 10.1016/j.snb.2015.10.008
72. Hermanson GT (2013) Bioconjugate Techniques. Bioconjugate Tech. doi: 10.1016/B978-0-12-382239-0.00026-1
73. Wink T, van Zuilen SJ, Bult A, van Bennekom WP (1997) Self-assembled Monolayers for Biosensors. Analyst 122:43R–50R. doi: 10.1039/a606964i
74. Ulman A (1996) Formation and Structure of Self-Assembled Monolayers. Chem Rev 96:1533–1554. doi: 10.1021/cr9502357
75. Love JC, Estroff LA, Kriebel JK, Nuzzo RG, Whitesides GM (2005) Self-Assembled Monolayers of Thiolates on Metals as a Form of Nanotechnology. Chem Rev 105:1103–1170. doi: 10.1021/cr0300789
76. Schwartz DK (2001) Mechanisms and kinetics of self-assembled monolayer formation. Annu Rev Phys Chem 52:107–137. doi: 10.1146/annurev.physchem.52.1.107
77. Bain CD, Troughton EB, Tao YT, Evall J, Whitesides GM, Nuzzo RG (1989) Formation of monolayer films by the spontaneous assembly of organic thiols from solution onto gold. J Am Chem Soc 111:321–335. doi: 10.1021/ja00183a049
78. Ferretti S, Paynter S, Russell DA, Sapsford KE, Richardson DJ (2000) Self-assembled monolayers: a versatile tool for the formulation of bio-surfaces. TrAC Trends Anal Chem 19:530–540. doi: 10.1016/S0165-9936(00)00032-7
79. Zhou Y, Chiu CW, Liang H (2012) Interfacial structures and properties of organic materials for biosensors: An overview. Sensors (Switzerland) 12:15036–15062. doi:

10.3390/s121115036

80. Schreiber F (2000) Structure and growth of self-assembling monolayers. Prog Surf Sci 65:151–256. doi: 10.1016/S0079-6816(00)00024-1
81. Chen S, Li L, Zhao C, Zheng J (2010) Surface hydration: Principles and applications toward low-fouling/nonfouling biomaterials. Polymer (Guildf) 51:5283–5293. doi: 10.1016/j.polymer.2010.08.022
82. Ren W, Zhou LY, Zhang Y, Li NB, Luo HQ (2016) A reusable and label-free supersandwich biosensor for sensitive DNA detection by immobilizing target-triggered DNA concatamers on ternary self-assembled monolayer. Sensors Actuators B Chem 223:24–29. doi: 10.1016/j.snb.2015.09.050
83. Mukdasai S, Langsi V, Pravda M, Srijaranai S, Glennon JD (2016) A highly sensitive electrochemical determination of norepinephrine using l-cysteine self-assembled monolayers over gold nanoparticles/multi-walled carbon nanotubes electrode in the presence of sodium dodecyl sulfate. Sensors Actuators B Chem 236:126–135. doi: 10.1016/j.snb.2016.05.086
84. Alonso JM, Bielen AAM, Olthuis W, Kengen SWM, Zuilhof H, Franssen MCR (2016) Self-assembled monolayers of 1-alkenes on oxidized platinum surfaces as platforms for immobilized enzymes for biosensing. Appl Surf Sci 383:283–293. doi: 10.1016/j.apsusc.2016.05.006
85. Yeh C-H, Kumar V, Moyano DR, Wen S-H, Parashar V, Hsiao S-H, Srivastava A, Saxena PS, Huang K-P, Chang C-C, Chiu P-W (2016) High-performance and high-sensitivity applications of graphene transistors with self-assembled monolayers. Biosens Bioelectron 77:1008–1015. doi: 10.1016/j.bios.2015.10.078
86. de Juan-Franco E, Caruz A, Pedrajas JR, Lechuga LM (2013) Site-directed antibody immobilization using a protein A-gold binding domain fusion protein for enhanced SPR immunosensing. Analyst 138:2023–31. doi: 10.1039/c3an36498d
87. Lee JE, Seo JH, Kim CS, Kwon Y, Ha JH, Choi SS, Cha HJ (2013) A comparative study on antibody immobilization strategies onto solid surface. Korean J Chem Eng 30:1934–1938. doi: 10.1007/s11814-013-0117-5
88. Seo J, Lee S, Poulter CD (2013) Regioselective covalent immobilization of recombinant antibody-binding proteins A, G, and L for construction of antibody arrays. J Am Chem Soc 135:8973–80. doi: 10.1021/ja402447g
89. Cherkouk C, Rebohle L, Lenk J, Keller A, Ou X, Laube M, Neuber C, Haase-Kohn C, Skorupa W, Pietzsch J (2016) Controlled immobilization of His-tagged proteins for protein-ligand interaction experiments using Ni2+-NTA layer on glass surfaces. Clin Hemorheol Microcirc 61:523–539. doi: 10.3233/CH-151950
90. Ericsson EM, Enander K, Bui L, Lundström I, Konradsson P, Liedberg B (2013) Site-Specific and Covalent Attachment of His-Tagged Proteins by Chelation Assisted Photoimmobilization: A Strategy for Microarraying of Protein Ligands. Langmuir 29:11687–11694. doi: 10.1021/la4011778
91. Baio JE, Cheng F, Ratner DM, Stayton PS, Castner DG (2011) Probing orientation of immobilized humanized anti-lysozyme variable fragment by time-of-flight secondary-ion mass spectrometry. J Biomed Mater Res - Part A 97 A:1–7. doi: 10.1002/jbm.a.33025
92. Kimple AJ, Muller RE, Siderovski DP, Willard FS (2010) A capture coupling method for the covalent immobilization of hexahistidine tagged proteins for surface plasmon resonance. Methods Mol Biol 627:91–100. doi: 10.1007/978-1-60761-670-2_5
93. Raina M, Sharma R, Deacon SE, Tiede C, Tomlinson D, Davies AG, McPherson MJ, Wälti C (2015) Antibody mimetic receptor proteins for label-free biosensors. Analyst 140:803–810. doi: 10.1039/C4AN01418A
94. Thermo Fisher Scientific Inc. (2003) Avidin-Biotin Binding. In: Thermo Sci. Avidin-Biotin Tech. Handb. pp 24–25

95. Bonel L, Vidal JC, Duato P, Castillo JR (2011) An electrochemical competitive biosensor for ochratoxin A based on a DNA biotinylated aptamer. Biosens Bioelectron 26:3254–3259. doi: 10.1016/j.bios.2010.12.036
96. YESIL M, DONMEZ S, ARSLAN F (2016) Development of an electrochemical DNA biosensor for detection of specific Mycobacterium tuberculosis sequence based on poly(L-glutamic acid) modified electrode. J Chem Sci 1–7. doi: 10.1007/s12039-016-1159-0
97. Zhang B, Dallo S, Peterson R, Hussain S, Weitao T, Ye JY (2011) Detection of anthrax lef with DNA-based photonic crystal sensors. J Biomed Opt 16:127006. doi: 10.1117/1.3662460
98. Cho I-H, Paek E-H, Lee H, Kang JY, Kim TS, Paek S-H (2007) Site-directed biotinylation of antibodies for controlled immobilization on solid surfaces. Anal Biochem 365:14–23. doi: 10.1016/j.ab.2007.02.028
99. Babos F, Szarka E, Nagy G, Majer Z, Sármay G, Magyar A, Hudecz F (2013) Role of N- or C-terminal biotinylation in autoantibody recognition of citrullin containing filaggrin epitope peptides in rheumatoid arthritis. Bioconjug Chem 24:817–27. doi: 10.1021/bc400073z
100. Franco EJ, Hofstetter H, Hofstetter O (2006) A comparative evaluation of random and site-specific immobilization techniques for the preparation of antibody-based chiral stationary phases. J Sep Sci 29:1458–69. doi: 10.1002/JSSC.200600062
101. Hierlemann A, Brand O, Hagleitner C, Baltes H (2003) Microfabrication techniques for chemical/biosensors. Proc IEEE 91:839–863. doi: 10.1109/JPROC.2003.813583
102. Wang Y, Xu H, Zhang J, Li G (2008) Electrochemical sensors for clinic analysis. Sensors 8:2043–2081. doi: 10.3390/s8042043
103. Huang X-J, O'Mahony AM, Compton RG (2009) Microelectrode Arrays for Electrochemistry: Approaches to Fabrication. Small 5:776–788. doi: 10.1002/smll.200801593
104. Hayat A, Marty JL (2014) Disposable screen printed electrochemical sensors: Tools for environmental monitoring. Sensors (Switzerland) 14:10432–10453. doi: 10.3390/s140610432
105. Varteresian J (2002) Fabricating printed circuit boards. Newnes, Amsterdam [etc.] :
106. Salvo P, Henry OYF, Dhaenens K, Acero Sanchez JL, Gielen a, Werne Solnestam B, Lundeberg J, O'Sullivan CK, Vanfleteren J (2014) Fabrication and functionalization of PCB gold electrodes suitable for DNA-based electrochemical sensing. Biomed Mater Eng 24:1705–1714. doi: 10.3233/bme-140982
107. Acero Sánchez JL, Henry OYF, Joda H, Werne Solnestam B, Kvastad L, Johansson E, Akan P, Lundeberg J, Lladach N, Ramakrishnan D, Riley I, O'Sullivan CK (2016) Multiplex PCB-based electrochemical detection of cancer biomarkers using MLPA-barcode approach. Biosens Bioelectron. doi: 10.1016/j.bios.2016.04.018
108. Fakruddin M, Mannan KS Bin, Chowdhury A, Mazumdar RM, Hossain MN, Islam S, Chowdhury MA (2013) Nucleic acid amplification: Alternative methods of polymerase chain reaction. J Pharm Bioallied Sci 5:245–52. doi: 10.4103/0975-7406.120066
109. Wen D, Zhang C (2012) Universal Multiplex PCR: a novel method of simultaneous amplification of multiple DNA fragments. Plant Methods 8:32. doi: 10.1186/1746-4811-8-32
110. Jean J, D'Souza DH, Jaykus L-A (2004) Multiplex nucleic acid sequence-based amplification for simultaneous detection of several enteric viruses in model ready-to-eat foods. Appl Environ Microbiol 70:6603–10. doi: 10.1128/AEM.70.11.6603-6610.2004
111. Søe MJ, Rohde M, Mikkelsen J, Warthoe P (2013) IsoPCR: An Analytically Sensitive, Nested, Multiplex Nucleic Acid Amplification Method. Clin. Chem. 59:
112. Schouten JP, Schouten JP, McElgunn CJ, McElgunn CJ, Waaijer R, Waaijer R,

Zwijnenburg D, Zwijnenburg D, Diepvens F, Diepvens F, Pals G, Pals G (2002) Relative quantification of 40 nucleic acid sequences by multiplex ligation-dependent probe amplification. Nucleic Acids Res 30:e57. doi: 10.1093/nar/gnf056

113. Sepers EM, Schouten JP (2010) Chapter 13 – Multiplex Ligation-Dependent Probe Amplification (MLPA) and Methylation-Specific (MS)-MLPA: Multiplex Detection of DNA/mRNA Copy Number and Methylation Changes. In: Mol. Diagnostics. pp 183–198
114. Eldering E, Spek CA, Aberson HL, Grummels A, Derks IA, de Vos AF, McElgunn CJ, Schouten JP (2003) Expression profiling via novel multiplex assay allows rapid assessment of gene regulation in defined signalling pathways. Nucleic Acids Res 31:e153.

2 Site-directed introduction of disulphide groups on antibodies for highly sensitive immunosensors

Site-directed introduction of disulphide groups on antibodies for highly sensitive immunosensors

Josep Ll. Acero Sánchez[1], Alex Fragoso[1], Hamdi Joda[2], Guillaume Suárez[3], Calum J. McNeil[3], Ciara K. O'Sullivan[1,4]

[1] Nanobiotechnology & Bioanalysis Group, Departament d'Enginyeria Química, Universitat Rovira i Virgili, Avinguda Països Catalans 26, 43007 Tarragona, Spain
[2] Department of Chemistry, University at Albany, 1400 Washington Ave, Albany NY 12222, United States
[3] Institute of Cellular Medicine, Newcastle University, Newcastle-upon-Tyne NE2 4HH, UK
[4] Institució Catalana de Recerca i Estudis Avançats (ICREA), Passeig Lluís Companys 23, 08010 Barcelona, Spain

2.1 Abstract

The interface between the sample and the transducer surface is critical to the performance of a biosensor. In this work we compared different strategies for covalent self-assembly of antibodies onto bare gold substrates by introducing disulfide groups into the immunoglobulin structure, which acted as anchor molecules able to chemisorb spontaneously onto clean gold surfaces. The disulphide moieties were chemically introduced to the antibody via the primary amines, carboxylic acids and carbohydrates present in its structure. The site-directed modification via the carbohydrate chains exhibited the best performance in terms of analyte response using a model system for the detection of the stroke marker Neuron Specific Enolase. SPR measurements clearly showed the potential for creating biologically active densely packed self-assembled monolayers (SAMs) in a one step protocol compared to both mixed SAMs of alkanethiol compounds and commercial immobilization layers. The ability of the carbohydrate strategy to construct an electrochemical immunosensor was investigated using electrochemical impedance spectroscopy (EIS) and differential pulse voltammetry (DPV) transduction.

2.2 Introduction

Immunosensors have been developed for a plethora of applications, including medical diagnostics and environmental analysis and have great potential for commercialization, but still face a challenge in achieving a simple, robust and inexpensive surface functionalisation method compatible with mass-manufacturing techniques. Generally, functionalisation

processes require the biochemical modification of either the sensor surface or the antibody or both, and this usually involves several steps that in some cases are time consuming, costly and difficult to implement in large-scale production process.

The immobilization of antibodies on solid support transducers is a critical issue for the sensor performance, as the affinity, orientation and stability of the antibodies are affected by the immobilization strategy selected [1]. A variety of surface chemistry methods have been reported with those introducing orientation and maintaining native antibody conformation being of greatest relevance [2, 3]. Specific orientation should expose free antigen-binding regions of the antibody following surface anchoring, resulting in increased analyte binding and improved sensitivity. Passive adsorption of biomolecules on solid substrates has been widely explored [4] due to its simplicity, but results in unstable adsorption with no control of orientation, and often results in protein unfolding [5, 6]. Alternatively, the use of self-assembled monolayers (SAMs), with two terminal functional groups, one enabling binding to the sensor surface, and the other allows coupling of the biocomponent, has been widely used [7-11], due to the high diversity of functionalized SAMs and chemical cross-linkers available, and provides a strong and stable attachment. Nevertheless, it needs a previous functionalisation of the surface and the molecules attached to the SAMs can be randomly oriented [12]. To minimize random orientation and uniformly orientate the antibodies on the surface, several strategies have been developed, including the use of receptors that bind the Fc portion of the antibody (e.g. proteins A, G, L, anti-Fc), which improves sensitivity [1, 13-15], but also requires an initial surface modification. Immobilization via antibody fragments through sulfhydryl groups also improves the sensitivity [16-19] but may form a very compact layer, giving rise to significant steric hindrance effects [20] and the potential loss of biological activity of the antibody fragments [21]. Oxidized oligosaccharide moieties of the antibodies coupled to amine or hydrazine modified solid supports, have also been provided to providing great sensitivity [22-24], but again require a surface pre-functionalisation step.

A single immobilization step can be achieved via the introduction of sulfur-containing molecules into the bioelement structure prior to its chemisorption onto gold [23, 25] (Scheme 2.1). Antibody molecules possess a number of functional groups suitable for modification including lysine ε–amine, N-terminal α-amine groups, and C-terminal aspartic acid and glutamic acid residues. Chemical conjugation reactions with antibody molecules are generally more successful at preserving activity if the functional groups utilized are present in limiting quantities and only at discrete sites on the molecule. In one approach, the disulphide in the

hinge region of the antibody that holds the heavy chains together can be selectively cleaved with a reducing agent such as 2-mercaptoethylamine to create two half-antibody molecules, each containing an antigen binding site [26]. An alternate method is based on the modification of antibodies via their carbohydrates, which are located in the C_H^2 domain within the Fc region. Mild oxidation of the polysaccharide sugar residues with sodium periodate generates aldehyde groups, which can then be used for coupling to another molecule [26]. By proper selection of the conjugation reaction and knowledge of antibody structure, antibodies can be oriented so that their bivalent binding potential for antigen remains available.

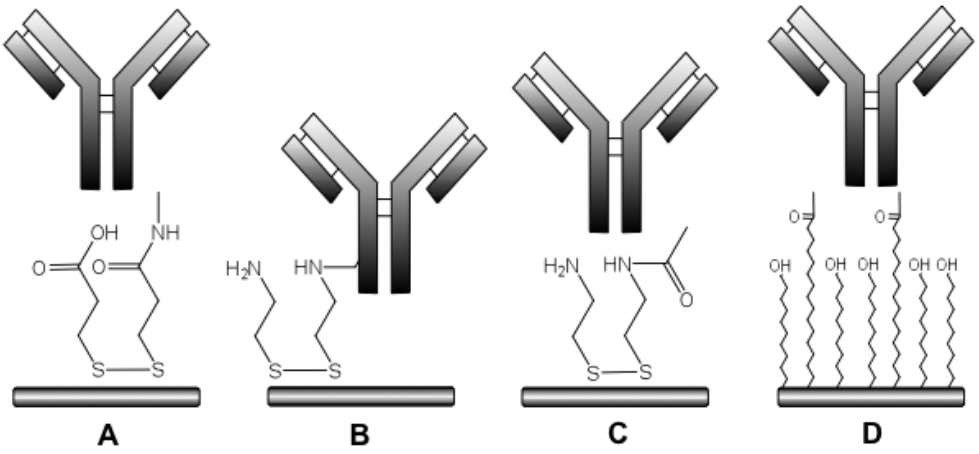

Scheme 2.1. Functionalization strategies of bare gold substrates via direct bio-SAM using disulphide-containing antibody chemically modified via their primary amines (A), carbohydrates (B) and carboxylic acids (C) and via classic SAM (D) using unmodified antibodies attached on a long-chain of alkanethiols previously self-assembled onto a bare gold substrate.

In this work, we developed a simple one-step surface functionalisation method based on the covalent coupling of antibodies by chemical introduction of sulfur-derivative molecules into the antibody structure prior to its adsorption onto gold via the primary amines, carboxylic acids and carbohydrates present in its structure. Additionally, a classic SAM approach was also evaluated using unmodified antibodies attached to a long-chain of alkanethiols previously self-assembled onto a bare gold substrate. The model antibody-antigen system applied to carry out this work consisted of two monoclonal antibodies, a capture anti-NSE21 antibody and a reporter anti-NSE17 antibody, against neuron specific enolase (NSE), a dimeric isoenzyme of the glycolytic enzyme enolase and derives from neuronal cytoplasm and neuroendocrine cells

[27]. Several studies have demonstrated significantly lower NSE concentrations in serum in healthy subjects, with levels lower than 12.5 ng/ml, than in patients with acute ischemic stroke [28], and has thus been identified as a possible biological marker for the diagnosis of ischemic stroke [29] and used in an electrochemical sensor, achieving a detection limit of 0.18 ng/ml [30]. A Biacore® 3000 surface plasmon resonance (SPR) system was employed to characterize the different immobilization techniques and monitor the antibody-antigen interactions, and the optimal antibody modification applied in an immunosensor, achieving a clinically relevant detection limit of 4.6 ng/ml.

2.3 Experimental

2.3.1 Chemicals and materials

Neuron specific enolase (NSE), anti-NSE21 monoclonal antibody (MAb) and anti-PSA66 (Prostate Specifc Antigen) MAb were kindly supplied by Fuijirebio Diagnostics (Gothenburg, Sweden). Human CEA (Carcino Embryonic Antigen) was purchased from SCIPAC (Sittingbourne, UK). Both anti-PSA66 MAb and human CEA were employed for non-specific binding studies as non-specific ligand and as non-specific marker, respectively. Bare gold substrates (SIA-kit), gold substrates mounted in chip (Au chip) dextran-coated gold substrates (CM5 chip) and HEPES buffered saline (HBS) (10 mM 4-(2-hydroxyethyl) piperazine-1-ethanesulfonic acid, 150 mM NaCl, 3.4 mM ethylenediaminetetraacetate, and 0.005% Tween 20 (pH 7.4)) were purchased from Biacore (GE Healthcare, Barcelona). Thiolated polyethylenglycol 1-(mercaptoundec-11-yl)-tetra(etlyleneglycol) (PEG) was supplied by SensoPath Technologies (Bozeman, USA). Cystamine dihydrochloride, 1-Ethyl-3-(3-dimethylamino-propyl) carbodiimide (EDC), N-hydroxysuccinimide (NHS), sulfo-NHS, dithiopropionic acid succinimidyl ester (DTPS), 16-mercapto-1-hexadecanoic acid (16-MHA), 11-mercapto-1-undecanol (11-MUOH), and carbonate-bicarbonate capsules for preparation of carbonate buffer (0.05 M, pH 9.6) were purchased from Sigma (Barcelona, Spain). Ethanol, acetone, dimethyl sulfoxide (DMSO), sodium di-hydrogen phosphate (NaH_2PO_4) and di-sodium hydrogen phosphate (Na_2HPO_4) were obtained from Panreac Química (Barcelona, Spain). Sodium chloride (NaCl), sodium hydroxide (NaOH), potassium chloride (KCl), sodium acetate, acetic acid and sodium periodate were supplied by Scharlau (Barcelona, Spain). Centrifugal filter membranes of 100 molecular weight cut off (MWCO) and 0.2 μm membrane filters were supplied by Whatman GmbH (Dassel, Germany). Deionised water was produced using a Milli-Q RG system (Millipore Ibérica, Madrid, Spain). The concentration of the chemically modified antibodies was determined using a Cary 100 UV-Vis spectrophotometer supplied by Varian (Barcelona, Spain). To evaluate the different

immobilization techniques a Biacore® 3000 Surface Plasmon Resonance (SPR) system was used.

2.3.2 Chemical modification of biocomponents

Disulphide groups were covalently introduced into the structure of both anti-NSE21 and anti-PSA66 via its primary amines, carboxylic acids and carbohydrates, whereas the anti-NSE17 was used in its' unmodified state as second primary antibody for sandwich assay experiments.

Chemical introduction of disulphides in anti-NSE21 antibody using -NH_2 residues. Introduction of disulphides by this synthetic route was performed by reacting terminal primary amines and lysine residues of IgG with a disulphide-containing active ester, giving rise to a covalent attachment between disulphide groups and IgG. Anti-NSE21 (3.6×10^{-9} mol) diluted in 0.5 ml of 0.01 M carbonate buffer pH 9.5 was mixed with 0.07 mg of dithiopropionic acid succinimidyl ester (DTPS) (1.8×10^{-7} mol) prepared in 0.05 ml of DMSO. The mixture was allowed to react in dark conditions for 5 hours at room temperature under vigorous stirring. The excess of DTPS was removed by ultrafiltration (100 kDa Molecular Weight Cut Off (MWCO) membranes) and the modified antibody was recollected in PBS buffer pH 7.4. The concentration of the modified antibody was determined by UV-Vis spectrophotometry at 280 nm using an extinction coefficient of 1.38 ml/mg•cm for 1 mg/ml IgG solutions in a 1-cm path length [31].

Chemical introduction of disulphides in anti-NSE21 antibody using carbohydrates. Polysaccharide residues were oxidized to aldehydes that react with primary amine groups of cystamine via the formation of Schiff bases. Initially, 0.5 mg of anti-NSE21 was diluted in 100 µl of 0.01M acetate buffer pH 5.0, and then a 5 mM solution of sodium periodate was added to the antibody solution. The mixture was left to react in the dark and under stirring conditions for 1 h at room temperature. The oxidized antibody solution was slowly added to 900 µl of a 0.1 M cystamine solution diluted in 0.05 M carbonate buffer (pH 9.5) and left to react for 3 hours at room temperature. In the next step, unstable imines were reduced to amine bonds by dropping 10 mM cyanoborohydride into the solution. Finally, the antibody solution was purified from the large excess of cystamine by filtration using 100 kDa MWCO membranes and, the modified antibody subsequently recollected in PBS buffer pH 7.4.

Chemical introduction of disulphides in anti-NSE21 antibody using –COOH residues. Disulphides were covalently attached to the IgG structure through the terminal carboxylic acids and the glutamic acid residues. Firstly, 0.5 mg of anti-NSE21 antibody (3.6×10^{-9} mol), 7.8

mg of sulfo-NHS (3.6 x 10^{-5} mol) and 6.9 mg of EDC (3.6 x 10^{-5} mol) were mixed and allowed to react for 10 min under stirring conditions at room temperature in 100 μL of 10 mM acetate buffer pH 4.5. Subsequently, this mixture was added to 900 μL of 50 mM HEPES buffer pH 8.5 containing 20 mg of cystamine (9 x 10^{-5} mol). Nucleophilic substitution took place during 2 hours at room temperature under vigorous stirring conditions. Excess reagents and by-products were removed by filtration (100 kDa MWCO membranes) and the antibodies were dissolved in PBS buffer pH 7.4.

2.3.3 Biological functionalization of bare gold substrates

Different biological functionalisation strategies of bare gold substrates were characterized using a Biacore® 3000 SPR system [32]. Surface functionalisation was exploited using two different approaches: (i) Direct bio-SAM using the chemically modified antibodies containing disulphide groups and (ii) Classic SAM using unmodified antibodies attached to a long-chain of alkanethiols previously self-assembled onto a bare gold substrate (Scheme 2.1). Additionally, the efficiency of these two approaches was compared with the performance of both a commercial carboxymethylated dextran surface (CM5 chip) and the immobilization of the unmodified antibody directly on gold substrates.

Direct bio-SAM approach. Bare gold substrates were rinsed with acetone and incubated for 15 min in an UV/O_3 chamber to remove all organic contaminants on gold substrates [33]. Covalent immobilization of chemically modified antibodies containing disulphide groups was achieved by injecting 100 μl of the modified antibody solution (100 μg/ml in PBS buffer pH 7.4), followed by injection of 35 μl of a 1 mM PEG solution in order to block remaining free sites on the surface. A continuous flow of HEPES buffered saline (HBS) (10 mM 4-(2-hydroxyethyl) piperazine-1-ethanesulfonic acid, 150 mM NaCl, 3.4 mM ethylenediaminetetraacetate, and 0.005% v/v Tween 20 (pH 7.4)) at 5 μl/min was maintained during the immobilization step. To test the non-specific adsorption of NSE on the PEG blocking layer, a control experiment was performed by injecting 100 μl of the non-specific PSA66 antibody (100 μg/ml in PBS buffer pH 7.4) previously modified with disulphides via its primary amines, carboxylic acids and carbohydrates as described above. Subsequently, the surface was backfilled by an injection of 35 μl of a 1 mM PEG solution. NSE detection experiments were performed by injecting serial dilutions of NSE (3.1 – 200 ng/ml) prepared in HBS buffer over the antibody-immobilized surface at a flow rate of 20 μl/min. After 6 min of association, the sample solution was replaced by a HBS buffer flow for 7 min, allowing the complex to dissociate. Regeneration of the surface was performed by injecting two pulses of 10 mM

glycine (pH 2.2) between each analyte injection. The recognition experiments were carried out at 25 °C. Specificity of the recognition layer for NSE was tested by injecting two concentrations of human CEA (1 and 10 μg/ml) as a non-specific marker.

In addition to the NSE recognition experiments, sandwich assays were also performed to test the specificity of the NSE binding. These assays consisted of a NSE recognition step by injecting both 100 ng/ml and 200 ng/ml of NSE for 6 min, followed by a 10 μg/ml solution of unmodified NSE17 for a further 6 min. Subsequent to association, the sample solution was replaced by a HBS buffer flow for 7 min at 20 μl/min.

Classic SAM approach. Immediately after cleaning, the gold substrates were immersed in a mixture of 5% 1mM 16-mercapto-1-hexadecanoic acid (16-MHA) and 95% 1mM 11-mercapto-1-undecanol (11-MUOH) in ethanol. Mixed SAMs were prepared in glass recipients cleaned with 2M NaOH for at least 1 h. After 3 h of SAM deposition, the substrates were thoroughly rinsed with ethanol and dried under a stream of nitrogen, producing stable and fully covered SAMs on gold [34]. The mixed SAM used is considered as optimal for obtaining a high degree of antibody immobilization with maximal elimination of non-specific adsorption due to the high content of thiols with OH end groups [35].

Covalent immobilization of unmodified anti-NSE21 monoclonal antibody was accomplished via coupling to their primary amines. A continuous flow of HBS at 5 μl/min was maintained during the immobilization step. The carboxylic groups of the mixed SAM were activated by injection of 50 μl of a 1:1 mixture of 400mM EDC and 100 mM NHS in deionized water. Subsequently, 100 μl of the antibody solution (100 μg/ml in 10 mM acetate buffer pH 5.0) was injected, followed by injection of 35 μl of ethanolamine (1.0 M in deionized water, pH 8.5) in order to block remaining NHS ester active groups, followed by two 10 μl injections of 10 mM glycine (pH 2.2) in order to remove non-specifically bound molecules from the surface. To test the non-specific binding of NSE, a control experiment was performed by injecting 100 μl of unmodified anti-PSA66 solution (100 μg/ml in 10 mM acetate buffer pH 5.0) as control antibody. The experiments were carried out at 25 °C.

Bio-functionalisation of CM5. A commercial carboxymethylated dextran surface (CM5 chip) was used to immobilize the unmodified anti-NSE21. Immobilization was achieved via coupling to their primary amines to the previously activated carboxylic groups of the dextran matrix. Immobilization was performed in the same manner as described above for the classic SAM approach.

Direct immobilization on gold substrates of unmodified anti-NSE21. Immobilization of unmodified anti-NSE21 was carried out by injecting 100 μl of the antibody solution (100 μg/ml in PBS buffer pH 7.4), followed by an injection of 35 μl of a 1 mM thiolated PEG solution.

2.4 Electrochemical instrumentation

Electrochemical measurements were performed on a PC controlled PGSTAT12 Autolab potentiostat (EcoChemie, The Netherlands) with an in-built frequency response analyzer FRA2 module. Electrochemical impedance measurements were performed using a standard three-electrode configuration (reference electrode: Ag/AgCl(sat), counter electrode Pt wire) in 1 mM $Fe(CN)_6^{3-/4-}$ in 0.1 M KCl, as previously described [36].

Electrochemical characterization of SAM formation of anti-NSE21-CHO modified electrodes. For the impedimetric study of SAM formation, clean gold electrodes were functionalized by immersion in a freshly prepared 1 μg/ml solution of disulphide modified anti-NSE21 in PBS for fixed times followed by rinsing with copious amounts of PBS-Tween. After each modification and washing, Faradaic EIS were recorded [36]; the electrodes were then washed with Milli-Q water and argon dried.

Electrochemical immunosensor construction and optimization. The incubation time of the specific recognition of NSE was optimized by immersion of the antibody modified electrode in a 100 ng/mL solution of NSE in PBS at different incubation times (0-60 min) and recording the change in R_{ct} of the faradaic response 1 mM $Fe(CN)_6^{3-/4-}$ in 0.1 M KCl.

Electrochemical Detection of NSE. A SAM of disulphide modified antibody was formed by immersion of a clean electrode on a 1 μg/ml solution of NSE-CHO in PBS for three hours followed by blocking with 1 mM 1-(mercaptoundec-11-yl)-tetra(ethyleneglycol) in PBS for 30 minutes. The electrodes were then exposed to different concentrations of NSE antigen in PBS for 30 min, rinsed with PBS-Tween and further incubated with 10 μg/ml of anti-NSE17-HRP conjugate in PBS for 10 at room temperature. The differential pulse voltammetry (DPV) response was recorded in triplicate in the potential range 0.2 to -0.4 V versus Ag/AgCl using a modulation amplitude of 25 mV), a step potential of 5 mV, and a scan rate of 50 $mV \cdot s^{-1}$) after 5 min of addition of a mixture of hydroquinone (1 mM) and hydrogen peroxide (1 mM) in PBS pH 6.

2.5 Results and discussion

2.5.1 Immobilization efficiency of modified and unmodified antibodies

Immobilization efficiency of the different functionalisation strategies was evaluated by monitoring the coupling level of the antibodies on the gold substrates. For all immobilization strategies, PEG or ethanolamine, depending on the surface, were used to backfill the remaining free sites on the surface and to cap any remaining activated groups. Immobilization levels were measured after the addition of the backfiller or capping agent depending on the experiment (Figure 2.1).

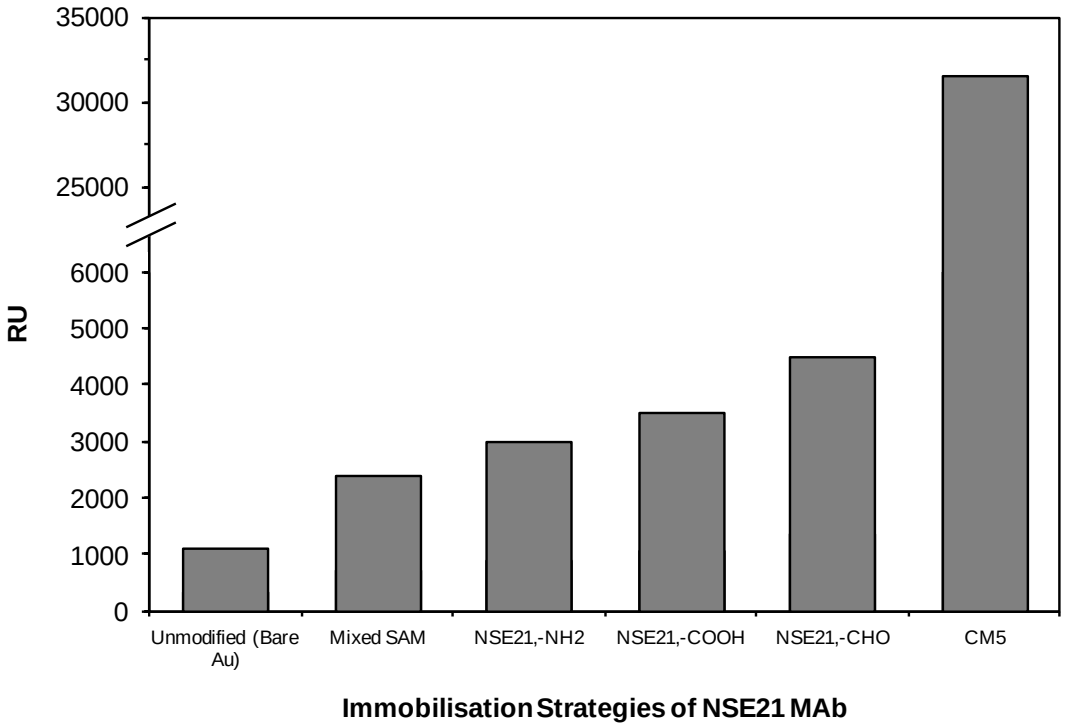

Figure 2.1. SPR signals for immobilization of unmodified NSE21 antibody on bare gold substrate, disulphide-containing antibody chemically modified via their primary amines (-NH_2), carbohydrates (-CHO) and carboxylic acids (-COOH), unmodified antibody via mixed SAM and unmodified antibody on a commercial layer (CM5 chip).

Based on the linear regression of the response and the amount of protein coated on the sensor surface, the theoretical surface concentrations of the antibodies were determined assuming that for matrix surfaces, an SPR signal of 1000 RU corresponds to a 1 ng/mm^2 of

protein [37,38]. For planar surfaces, however, this assumption needs to be corrected by a factor 3, so that 3000 RU equals 1 ng/mm^2 [39, 40]. Additionally, each sensor's maximum antigen binding capacity (Rmax) was also evaluated for each immobilization strategy by using the following relation (1):

$$R_{max} = (Mw_{Analyte}/Mw_{Ligand}) \cdot R_{Ligand} \cdot V_{Ligand} \quad (1)$$

where $Mw_{Analyte}$ and Mw_{Ligand} are the molecular weights of the analyte and ligand respectively, R_{Ligand} is the SPR response due to the ligand immobilization, and V_{Ligand} is the valency of the ligand (amount of binding sites). The valency for IgGs is considered to be equal to 2 (Table 2.1).

Table 2.1. SPR response due to the ligand immobilization (RLigand), surface concentrations of the immobilized species and sensor's maximum antigen binding capacity (Rmax) for each immobilization strategy.

Immobilization Strategy	R_{Ligand} (RU)	Surface conc. (ng/mm^2)	R_{max} (RU)
Unmodified (Bare Au)	1100	0.4	1144
-NH_2	2994	1.0	3114
-CHO	4492	1.5	4672
-COOH	3514	1.2	3655
Mixed SAM	2380	0.8	2475
CM5 chip	31443	31.4	32700

2.5.2 Binding efficiency of the different functionalization strategies

The affinity of the anti-NSE antibody immobilized using different strategies was evaluated by capture assay by injecting serial dilutions of NSE (3.1 – 200 ng/ml) prepared in HBS buffer over the antibody-immobilized surfaces for an association time of 6 min. A zero analyte concentration was also included to obtain measurements for system related bias. SPR signals for NSE recognition levels of gold substrates functionalized with both disulphide-containing and unmodified IgGs are depicted in figures 2.2 and 2.3, respectively. The degree of binding was calculated by measuring the response signal at the end of the dissociation phase in three replicate experiments subtracted by the signal from the control surface (non-specific PSA66 MAb). In the case of the disulphide-containing antibodies (Figure 2.2), only the antibodies

modified via their carbohydrate moiety exhibited a typical sigmoidal response. Very low responses to different NSE concentrations were obtained for the IgGs modified via their amine or carboxylate groups. The carbohydrate chains are attached to the CH_2 domain within the Fc region of the IgGs. This site-directed conjugation orientates the attached molecule away from the antigen binding regions, preventing blockage of these sites and thus preserving activity [26]. Both amine and carboxylate groups within the three-dimensional structure of an antibody is nearly uniform throughout the surface topology [26], and conjugation procedures that utilize these groups randomly cross-link to many parts of the antibody molecule, leading to a random orientation of the antibody within the conjugate structure, often blocking the antigen binding sites, resulting in a decrease in antigen binding activity. The level of non-specific adsorption of CEA on the surfaces containing the modified IgGs was lower than 9 RU and therefore insignificant.

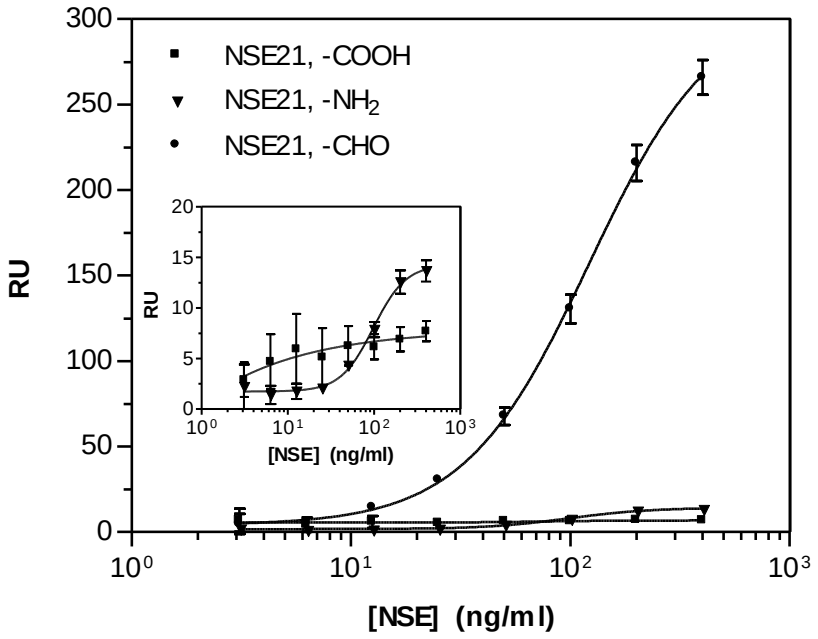

Figure 2.2. SPR signals for NSE binding levels (Capture Assay) of gold substrates functionalized with disulphide-containing anti-NSE21 antibodies modified via their primary amines, carbohydrates and carboxylic acids and immobilized on a bare gold substrate. Inset: NSE binding levels obtained with the anti-NSE21 modified via their primary amines and carboxylic acids. Error bars represent n = 3.

Figure 2.3 illustrates the target response levels for the unmodified anti-NSE21 immobilized on a CM5 chip, a mixed SAM and on a bare gold substrate. NSE was only detected using the CM5 and mixed SAM functionalized surfaces. Target binding levels on these two

immobilization strategies are very similar up to a concentration of 100 ng/ml, and at higher antigen concentrations the mixed SAM surface starts to become saturated, as most of the antibodies have been associated with the target. On the other hand, the response on the CM5 keeps increasing linearly. This indicates the capacity of the CM5 chip to accommodate more antigen molecules, as was expected taking into account the high immobilization level of antibodies obtained for this three-dimensional surface.

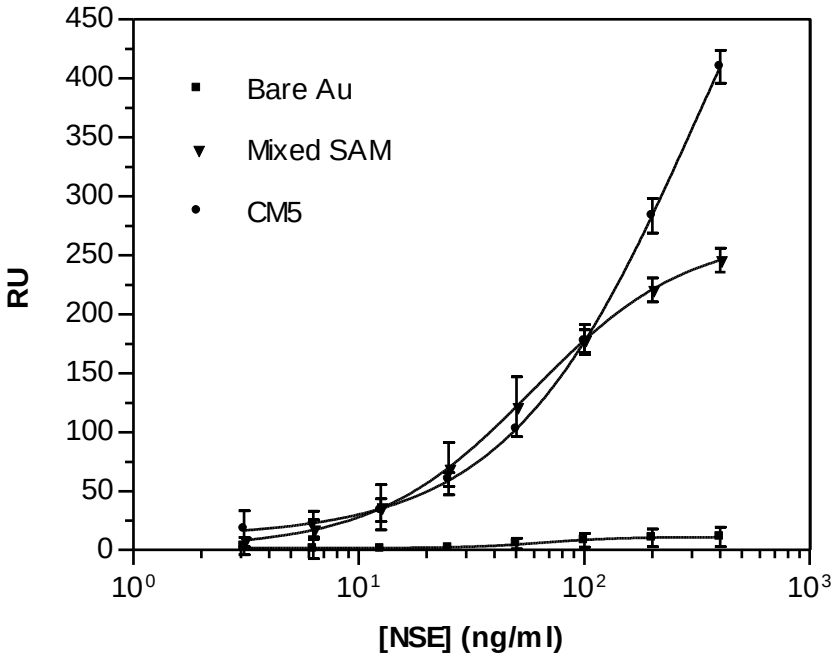

Figure 2.3. SPR signals for NSE binding levels (Capture Assay) of gold substrates functionalized with unmodified anti-NSE21. The unmodified antibodies were immobilized on a CM5 chip, a mixed SAM and on a bare gold substrate. Error bars represent n = 3.

The level of non-specific adsorption of CEA on the surfaces functionalized with unmodified IgGs was lower than 5 RU for the both the CM5 and the surface containing unmodified IgG, whereas for the mixed SAM the levels were lower than 11 RU. NSE detection using antibodies immobilized via the carbohydrate modification, on CM5 or via mixed SAMs were also evaluated by measuring assay critical parameters such as the limit of detection (LOD), the sensitivity, EC50 (concentration of target needed to obtain a 50 % of the maximum signal) and dynamic range. The sensitivity, EC50 and dynamic range was not determined for the CM5 chip because the top plateau was not defined by the experimental data and thus, these parameters would lack accuracy. The LOD was taken as the mean concentration value obtained for three

blanks plus three times the standard deviation of the blank. The low LOD (6.8 ± 2.1 ng/ml) obtained for the –CHO modification compared well with the other two strategies, classic SAM (1.8 ± 0.3 ng/ml) and commercial layer (3.3 ± 1.3 ng/ml) (Table 2.1).

Table 2.2. Assay performance parameters for the detection of NSE using (i) disulphide-containing NSE21 modified via their carbohydrates (-CHO) immobilized on a bare gold substrate and (ii) unmodified NSE21 immobilized on a mixed SAM.

Immobilization Strategy	R^2	EC_{50} (ng/ml)	Sensitivity (RU/(ng/ml))	Dynamic range (ng/ml)	LOD (ng/ml)
-CHO	0.999	171 ± 4	1.32 ± 0.20	17.1 – 603	6.8 ± 2.1
Mixed SAM	0.999	59 ± 2	1.28 ± 0.05	4.8 – 1170	1.8 ± 0.3

SPR was also used to determine the strength of the antibody-antigen binding by calculating the dissociation constant (K_D) using the BIAevaluation® software from Biacore. Experimental kinetic data was fitted to the 1:1 binding model and the goodness of fit was assessed by calculating the chi-square (χ^2). The K_D for the –CHO, CM5 and mixed SAM strategies was of $4.4 \cdot 10^{-11}$ M (χ^2=2.3), $4.8 \cdot 10^{-12}$ M (χ^2=2.2) and $1.9 \cdot 10^{-9}$ M (χ^2=5.1) respectively. Besides the low chi-square values obtained that suggested the good fitting to the ideal 1:1 binding model, differences in the K_D of 1 and 2 orders of magnitude were exhibited among the different strategies. These results clearly indicate that binding kinetics were affected by the immobilization approaches, mass-transfer limitations and surface heterogeneity due to the covalent immobilization procedures. The 3D surface of the CM5 chip is prone to mass transport limitations and therefore the kinetic parameter is underestimated, probably due to (i) the slower transport step of the antigens to the immobilized anti-NSE21 because of the three-dimensional dextran structure and (ii) the high binding capacity of ligands of this chip. Immobilization procedures on both the CM5 and mixed SAM are achieved via coupling primary amines of the antibodies, and this can modify the antigen binding sites, resulting in a decrease in affinity. On the other hand, the - CHO strategy offers a 2D surface, less subjected to mass transfer limitations, where the antibody binding sites have been unaffected by chemical reactions and thus, this surface is more reliable for binding kinetic calculations.

NSE recognition levels did not reach the theoretical maximum antigen binding capacity (Rmax) for any of the immobilization techniques. This revealed that all immobilized ligand

molecules were not fully accessible or functional, or that the NSE concentration assayed was not high enough to interact with all ligand molecules. The stoichiometry of the binding of the NSE to antibody was calculated using the molecular mass values for the anti-NSE MAb (150 kDa) and NSE (78 kDa) and their immobilization degree and response level. To this end, experimental stoichiometries of anti-NSE21 were 0.11, 0.20 and 0.03 for carbohydrate modification, mixed SAM and CM5 chip, respectively.

For the recognition experiments, the flow rate was increased to 20 μl/min to minimize re-binding and to reduce mass transport limitations, allowing rapid diffusion of the analyte from the bulk solution to the surface. Sensor chips were regenerated by selective dissociation of the analyte from the covalently immobilized ligand. Conditions were chosen to achieve complete dissociation of the analyte without affecting the binding characteristics of the ligand. Regeneration of the surfaces was achieved by injecting two pulses of 10 mM glycine (pH 2.2) between each analyte injection [41]. Regeneration efficiencies were higher than the 90 % for all experiments. Sandwich assays were performed to test the specificity of the NSE binding, consisting of a NSE recognition step by injecting 100 ng/ml and 200 ng/ml of NSE, followed by the injection of 10 μg/ml of unmodified NSE17 (Figure 2.4). Binding responses obtained for the addition of the second primary antibody demonstrated the higher presence of analyte molecules bound on the surface prepared using the –CHO modification, mixed SAM and CM5 chip, confirming the results obtained for direct capture of NSE. Both carbohydrate modification and mixed SAM displayed the highest responses for 100 ng/ml of NSE, while for an antigen concentration of 200 ng/ml the best surface was the –CHO modified. Whilst high binding levels were obtained for the direct capture of NSE in a CM5 chip, low binding levels of NSE17 were observed, which can be attributed to a highly packed surface too dense to accommodate the subsequent binding of the second antibody.

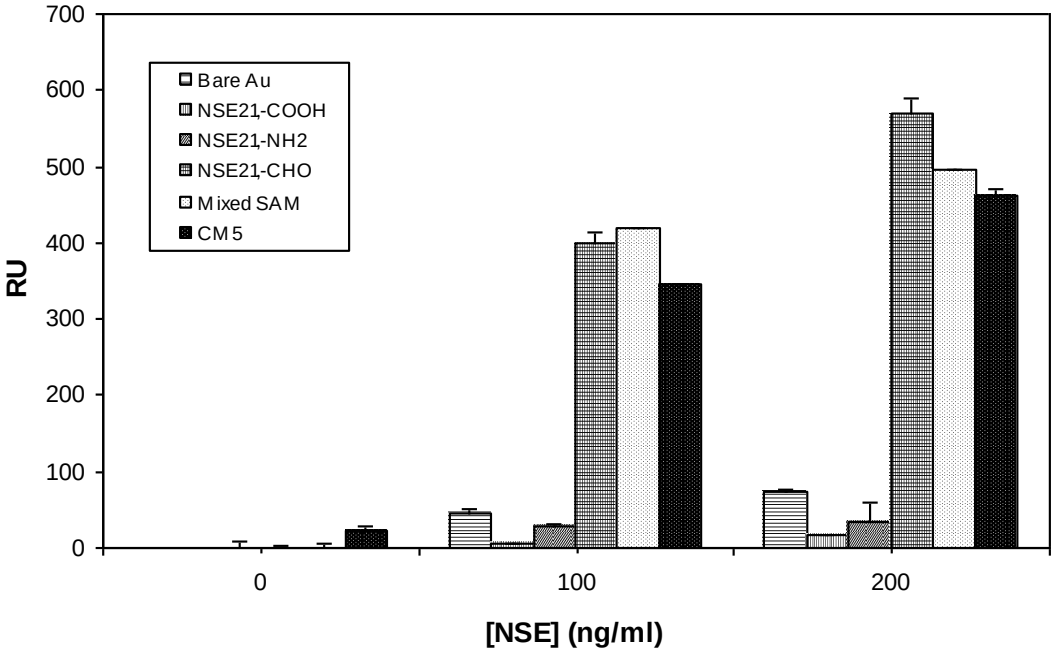

Figure 2.4. SPR signals for anti-NSE17 binding levels (Sandwich Assay) for a gold substrate functionalized with anti-NSE21. Unmodified antibodies were immobilized on a CM5 chip, a mixed SAM and on a bare gold substrate. Disulphide-containing antibodies were modified via their primary amines, carbohydrates and carboxylic acids immobilized on a bare gold substrate. Error bars represent n = 3.

2.5.3 Electrochemical detection of NSE

The immobilization of CHO-modified anti-NSE on gold electrodes was for use as an electrochemical immunosensor was explored. Impedance changes following different antibody immobilization times were monitored. Charge transfer resistance (R_{ct}) values, indicative of the opposition of the interface to the passage of electrical current from an electroactive probe present in solution, were obtained from simulation of the equivalent circuit shown in Scheme 2.2, where C_{dl} is the double layer capacitance and R_s is the solution resistance of the circuit.

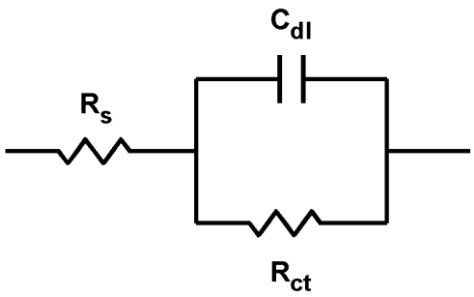

Scheme 2.2. Equivalent circuit used to model the impedance data (Rs: solution resistance, R_{ct}: resistance to charge tranfer, C_{dl}: double layer capacitance).

The R_{ct} values increased steadily with time (Figure 2.5), reaching saturation after 3 hours. This impedance increase does not account for multilayer formation since each point represents the constant impedance value obtained after repeated washings to remove physically adsorbed molecules. The maximum deposition time for NSE-CHO is considerably lower than that observed for the formation of SAMs of alkanethiols, which usually require an overnight exposure of the electrodes to the modifying solution in order to form a compact monolayer, highlighting the advantage of the direct attachment of modified antibodies on surfaces in immunosensor construction. The same procedure was employed in order to optimize the time required for the specific recognition of NSE (Figure 2.5, inset). The impedance response increased up to saturation after 30 minutes of interaction and this time was thus used in the detection experiments. Electrochemical determination of NSE was carried out using anti-NSE17-HRP conjugate as reporter antibody with differential pulse voltammetric detection. Figure 2.6a shows the DPV responses of the immunosensor with increasing concentrations of NSE in the potential range 0.1 to –0.4 V. As can be seen from Figure 2.6b the peak height increased with NSE concentration and showed a linear relationship with the logarithm of the NSE concentration. The limit of detection (4.6 ng/ml) was calculated with a linear relationship between 0-25 ng/ml.

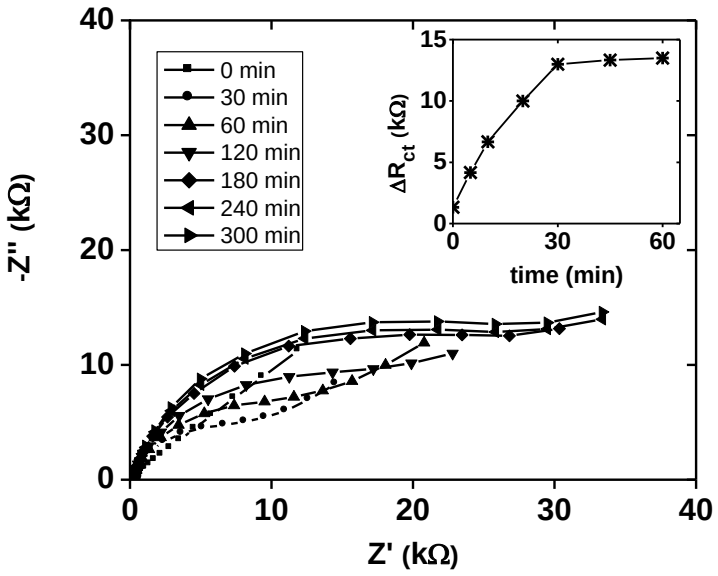

Figure 2.5. Complex impedance plot (in 1 mM $K_3Fe(CN)_6$ solution in PBS pH 7.4) for the formation of a SAM of NSE21-CHO at gold electrodes at different exposure times. Inset: Impedance variations for the specific interaction of NSE with NSE21-CHO modified surface.

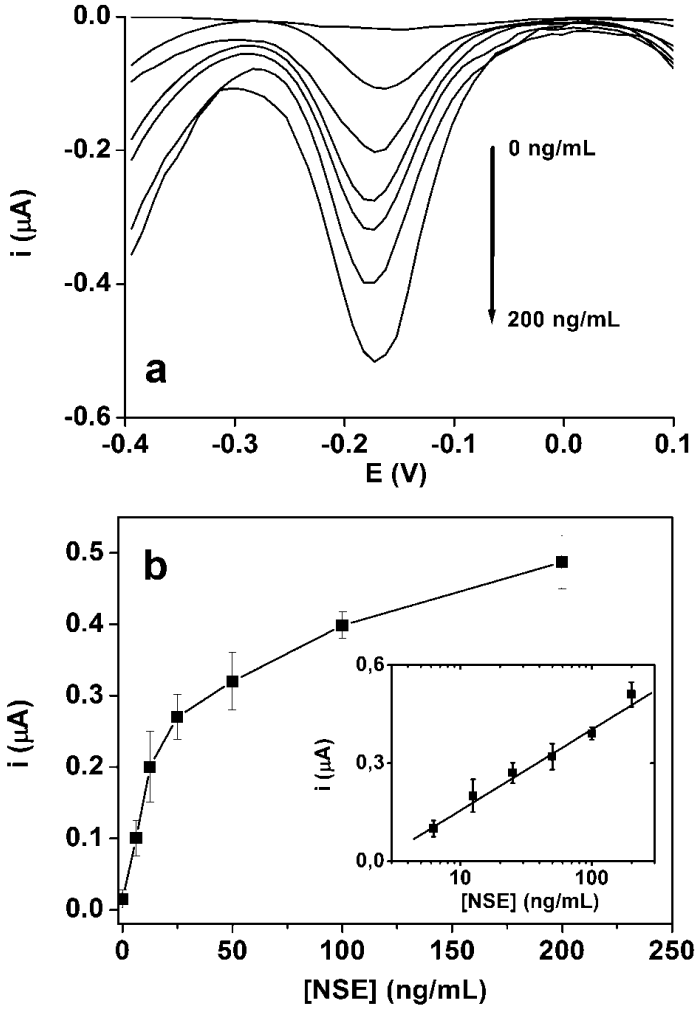

Figure 2.6. a) DPV responses at NSE21-CHO modified immunosensor in PBS (pH 7.4) at different NSE concentrations. b) Dependence of the peak height with NSE concentration. Inset: Logarithmic calibration plot.

2.6 Conclusions

Different strategies have been developed for antibody immobilization, based on the chemical modification of their functional groups with disulphide "anchors" able to spontaneously chemisorb onto gold, with no need for surface pre-functionalisation. Among the three chemical routes investigated, the site-directed conjugation of antibodies via their carbohydrate chains exhibited a good analyte response in both capture and sandwich assays using SPR. Surfaces prepared with this approach also compared well with both the classic two step SAM scenario and the 3D-CM5 chip in terms of analyte response, LOD and sensitivity, suggesting that the immobilization of carbohydrate-modified antibodies driven by chemisorption of their disulphide moieties represents a successful approach for creating

biologically active dense monolayers on gold devices due to an optimisation of orientation of the capture (primary) antibody. The chemical specificity of the reaction toward carbohydrate residues opens up an attractive option for oriented antibody immobilization since their sugar moieties are specifically located on the constant region of the immunoglobulins. Finally, in terms of simplicity, required time, and minimal use of reagents, the use of modified carbohydrate residues presents an extremely effective approach for antibody immobilization with application in electrochemical, optical, and gravimetric immunosensors.

2.7 References

1. Suárez G, Jackson RJ, Spoors JA, McNeil CJ. Chemical introduction of disulphide groups on glycoproteins: A direct protein anchoring scenario. Anal Chem. 2007;79:1961–1969. doi: 10.1021/ac0613030.
2. Baniukevic J, Kirlyte J, Ramanavicius A, Ramanaviciene A. Application of oriented and random antibody immobilization methods in immunosensor design. Sensors Actuators B Chem. 2013;189:217–223. doi: 10.1016/j.snb.2013.03.126.
3. Baniukevic J, Hakki Boyaci I, Goktug Bozkurt A, Tamer U, Ramanavicius A, Ramanaviciene A. Magnetic gold nanoparticles in SERS-based sandwich immunoassay for antigen detection by well oriented antibodies. Biosens Bioelectron. 2013;43:281–288. doi: 10.1016/j.bios.2012.12.014.
4. Vashist SK, Dixit CK, MacCraith BD, O'Kennedy R. Effect of antibody immobilization strategies on the analytical performance of a surface plasmon resonance-based immunoassay. Analyst 2011;136:4431. doi: 10.1039/c1an15325k.
5. Makaraviciute A, Ramanaviciene A. Site-directed antibody immobilization techniques for immunosensors. Biosens Bioelectron. 2013;50:460–71. doi: 10.1016/j.bios.2013.06.060.
6. Trilling AK, Beekwilder J, Zuilhof H. Antibody orientation on biosensor surfaces: a minireview. Analyst 2013;138:1619–27. doi: 10.1039/c2an36787d.
7. Castner DG, Ratner BD. Biomedical surface science: Foundations to frontiers. Surf Sci. 2002;500:28–60. doi: 10.1016/S0039-6028(01)01587-4.
8. Borges J, Campiña JM, Silva AF. Chitosan Biopolymer-F(ab´)2 Immunoconjugate Films for Enhanced Antigen Recognition. J Mater Chem B. 2013;500–511. doi: 10.1039/c2tb00115b.
9. Baniukevic J, Kirlyte J, Ramanavicius A, Ramanaviciene A. Comparison of oriented and random antibody immobilization techniques on the efficiency of immunosensor. Procedia Eng. 2012;47:837–840. doi: 10.1016/j.proeng.2012.09.277.
10. Niu Y, Matos AI, Abrantes LM, Viana AS, Jin G. Antibody oriented immobilization on gold using the reaction between carbon disulphide and amine groups and its application in immunosensing. Langmuir 2012;28:17718–17725. doi: 10.1021/la303032f.
11. Ferreira NS, Sales MGF. Disposable immunosensor using a simple method for oriented antibody immobilization for label-free real-time detection of an oxidative stress biomarker implicated in cancer diseases. Biosens Bioelectron. 2014;53:193–9. doi: 10.1016/j.bios.2013.09.056.
12. Perez JB, Tyagi D, Mo Y, Calvo L, Perez R, Moreno E, Zhu J. Predicting the right spacing between protein immobilization sites on self-assembled monolayers to optimize ligand binding. Anal Biochem. 2015;484:133–135. doi: 10.1016/j.ab.2015.05.005.
13. Luna DMN, Avelino KYPS, Cordeiro MT, Andrade CAS, Oliveira MDL. Electrochemical immunosensor for dengue virus serotypes based on 4-mercaptobenzoic acid modified

gold nanoparticles on self-assembled cysteine monolayers. Sensors Actuators B Chem. 2015;220:565–572. doi: 10.1016/j.snb.2015.05.067.

14. Hazarika P, Behrendt JM, Petersson L, Wingren C, Turner ML. Photopatterning of self assembled monolayers on oxide surfaces for the selective attachment of biomolecules. Biosens Bioelectron. 2014;53:82–9. doi: 10.1016/j.bios.2013.09.001.
15. Kausaite-Minkstimiene A, Ramanaviciene A, Kirlyte J, Ramanavicius A. Comparative study of random and oriented antibody immobilization techniques on the binding capacity of immunosensor. Anal Chem. 2010;82:6401–8. doi: 10.1021/ac100468k.
16. De Juan-Franco E, Caruz A, Pedrajas JR, Lechuga LM. Site-directed antibody immobilization using a protein A-gold binding domain fusion protein for enhanced SPR immunosensing. Analyst 2013;138:2023–31. doi: 10.1039/c3an36498d.
17. Miyao H, Ikeda Y, Shiraishi A, Kawakami Y, Sueda S. Immobilization of immunoglobulin-G-binding domain of Protein A on a gold surface modified with biotin ligase. Anal Biochem. 2015;484:113–121. doi: 10.1016/j.ab.2015.05.010.
18. Tajima N, Takai M, Ishihara K. Significance of antibody orientation unraveled: Well-oriented antibodies recorded high binding affinity. Anal Chem. 2011;83:1969–1976. doi: 10.1021/ac1026786.
19. Crivianu-Gaita V, Thompson M. Immobilization of Fab' fragments onto substrate surfaces: A survey of methods and applications. Biosens Bioelectron. 2015;70:167–180. doi: 10.1016/j.bios.2015.03.032.
20. Trilling AK, Hesselink T, Houwelingen A Van, Cordewener JHG, Jongsma M A, Schoffelen S, Hest JCM Van, Zuilhof H, Beekwilder J. Orientation of llama antibodies strongly increases sensitivity of biosensors. Biosens Bioelectron. 2014;60:130–136. doi: 10.1016/j.bios.2014.04.017.
21. Balevicius Z, Ramanaviciene A, Baleviciute I, Makaraviciute A, Mikoliunaite L, Ramanavicius A. Evaluation of intact- and fragmented-antibody based immunosensors by total internal reflection ellipsometry. Sensors Actuators B Chem. 2011;160:555–562. doi: 10.1016/j.snb.2011.08.029.
22. Nassef HM, Civit L, Fragoso A, O'Sullivan CK. Amperometric immunosensor for detection of celiac disease toxic gliadin based on fab fragments. Anal Chem. 2009;81:5299–5307. doi: 10.1021/ac9005342.
23. Vikholm I. Self-assembly of antibody fragments and polymers onto gold for immunosensing. Sensors Actuators B Chem. 2005;106:311–316. doi: 10.1016/j.snb.2004.07.034.
24. Bonroy K, Frederix F, Reekmans G, Dewolf E, De Palma R, Borghs G, Declerck P, Goddeeris B. Comparison of random and oriented immobilisation of antibody fragments on mixed self-assembled monolayers. J Immunol Methods 2006;312:167–81. doi: 10.1016/j.jim.2006.03.007.
25. Prieto-Simón B, Saint C, Voelcker NH. Electrochemical biosensors featuring oriented antibody immobilization via electrografted and self-assembled hydrazide chemistry. Anal Chem. 2014; 86:1422–9. doi: 10.1021/ac401747j.
26. Sorci M, Dassa B, Liu H, Anand G, Dutta AK, Pietrokovski S, Belfort M, Belfort G. Oriented covalent immobilization of antibodies for measurement of intermolecular binding forces between zipper-like contact surfaces of split inteins. Anal Chem. 2013;85:6080–6088. doi: 10.1021/ac400949t.
27. Ho J-AA, Hsu W-L, Liao W-C, Chiu J-K, Chen M-L, Chang H-C, Li C-C. Ultrasensitive electrochemical detection of biotin using electrically addressable site-oriented antibody immobilization approach via aminophenyl boronic acid. Biosens Bioelectron. 2010;26:1021–7. doi: 10.1016/j.bios.2010.08.048.
28. Hermanson GT. Bioconjugate Techniques. Elsevier; 2013. doi: 10.1016/B978-0-12-382239-0.00026-1.

29. Barone FC, Clark RK, Price WJ, White RF, Feuerstein GZ, Storer BL, Ohlstein EH. Neuron-specific enolase increases in cerebral and systemic circulation following focal ischemia. Brain Res. 1993;623:77–82.
30. Zhong Z, Peng N, Qing Y, Shan J, Li M, Guan W, Dai N, Gu X, Wang D, An electrochemical immunosensor for simultaneous multiplexed detection of neuron-specific enolase and pro-gastrin-releasing peptide using liposomes as enhancer, Electrochim Acta. 2011;56:5624-5629
31. Johnstone A, Thorpe R. Immunochemistry in Practice, 2nd ed. Oxford: Blackwell Scientific; 1988.
32. Jönsson U, Fägerstam L, Ivarsson B, Johnsson B, Karlsson R, Lundh K, Löfås S, Persson B, Roos H, Rönnberg I. Real-time biospecific interaction analysis using surface plasmon resonance and a sensor chip technology. Biotechniques 1991; 11:620–7.
33. Moon DW, Kurokawa A, Ichimura S, Lee HW, Jeon IC. Ultraviolet-ozone jet cleaning process of organic surface contamination layers. J Vac Sci Technol A Vacuum, Surfaces, Film 1999;17:150. doi: 10.1116/1.581565
34. Frederix F, Bonroy K, Reekmans G, Laureyn W, Campitelli A, Abramov MA, Dehaen W, Maes G. Reduced nonspecific adsorption on covalently immobilized protein surfaces using poly(ethylene oxide) containing blocking agents. J Biochem Biophys Methods 2004;58:67–74.
35. Frederix F, Bonroy K, Laureyn W, Reekmans G, Campitelli A, Dehaen W, Maes G. Enhanced Performance of an Affinity Biosensor Interface Based on Mixed Self-Assembled Monolayers of Thiols on Gold. Langmuir 2003;19:4351–4357. doi: 10.1021/la026908f.
36. Fragoso A, Laboria N, Latta D, O'Sullivan CK (2008) Electron permeable self-assembled monolayers of dithiolated aromatic scaffolds on gold for biosensor applications. Anal Chem 80:2556–2563.
37. Biacore Sensor Surface Handbook. Uppsala, 2003.
38. Stenberg E, Persson B, Roos H, Urbaniczky C. Quantitative determination of surface concentration of protein with surface plasmon resonance using radiolabeled proteins. J Colloid Interface Sci. 1991;143:513–526. doi: 10.1016/0021-9797(91)90284-F.
39. Gizeli E, Lowe CR. Biomolecular Sensors. London: Taylor & Francis. 2002.
40. Schasfoort RBM, Tudos AJ. Handbook of surface Plasmon resonance, RSC Pub., Cambridge, UK, 2008.
41. Andersson K, Areskoug D, Hardenborg E. Exploring buffer space for molecular interactions. J Mol Recognit. 1999;12:310–5.

3 Disulphide-modified antigen for detection of coeliac disease associated anti-tissue transglutaminase autoantibodies

Disulphide-modified antigen for detection of coeliac disease associated anti-tissue transglutaminase autoantibodies

Luis Carlos Rosales-Rivera[1], Samuel Dulay[1], Pablo Lozano Sánchez[1], Ioanis Katakis[1], Josep Lluis Acero Sánchez[1], Ciara K. O'Sullivan[1,2]

[1] Departament d'Enginyeria Quimica, Universitat Rovira I Virgili, Avinguda Països Catalans 26, 43007 Tarragona, Spain.
[2] Institució Catalana de Recerca i Estudis Avançats, Passeig Lluís Companys, 23, 08010 Barcelona, Spain

3.1 Abstract

A simple and rapid immunosensor for the determination of the coeliac disease related antibody, anti-tissue transglutaminase, was investigated. The antigenic protein tissue transglutaminase was chemically modified introducing disulphide groups through different moieties of the molecule (amine, carboxylic and hydroxyl groups), and self-assembled on gold surfaces and used for the detection of IgA and IgG autoantibodies. The modified proteins were evaluated using enzyme linked immunosorbent assay and surface plasmon resonance, which showed that only introduction of disulphide groups through amine moieties in the tissue transglutaminase preserved its antigenic properties. The disulphide-modified antigen was co-immobilised via chemisorption with a poly (ethylene glycol) alkanethiol on gold electrodes. The modified electrodes were then exposed to IgA anti-tissue transglutaminase antibodies and subsequently to horse radish peroxidase labelled anti-idiotypic antibodies, achieving a detection limit of 260 ng/mL. Immunosensor performance in the presence of complex matrixes, including clinically relevant serum reference solutions and real patient samples was evaluated. The introduction of disulphides in the antigenic protein enabled a simple and convenient one-step surface immobilisation procedure involving only spontaneous gold-thiol covalent binding. Complete amperometric assay time was 30 minutes.

3.2 Introduction

Immunosensors offer an alternative to classical methods like enzyme-linked immunosorbent assays (ELISA) in point-of-care and portable testing scenarios [1], with characteristics including portability, low cost, miniaturizability and high sensitivity, facilitating their used in a wide range of applications including environmental control, food analysis and clinical diagnostics [2-6]. Integration with other technologies allows continuous operation and

multiplexed analysis [7]. A plethora of immunosensors applied to clinical diagnosis have been reported using both electrochemical [8-11] and optical transduction [12, 13].

Despite of the high number of immunosensors reported, a simple, robust and low-cost surface functionalisation strategy is still unavailable. Different procedures have been used to ensure the immobilisation of immunoreactants to solid supports and to form an immunoaffinity layer, *i.e.*, physical adsorption [14]; polymer entrapment [15], sol-gel entrapment [16], covalent attachment [17], Langmuir–Blodgett deposition [18] or self assembled monolayers (SAM) [19, 20]. One of the main requirements for immobilisation is the maintenance of the biological properties of the immobilised molecule, which in the case of immunoreactants is mainly related to the maintenance of their functionality and protein conformation to ensure the occurrence of antigen-antibody recognition events [21].

A widely reported immobilisation method of biomolecules onto metallic solid supports for biosensor application is the chemisorption of a monolayer of molecular thickness, also known as a self-assembled monolayer (SAM). They can be formed directly by adsorbing a molecule that contains a ligand with affinity towards the surface or by attaching the molecule to an already SAM-modified surface [22]. Modified proteins with thiol/disulphide groups can form ordered SAMs on gold surfaces, reducing the steps and time of immobilisation. Functionalisation of whole molecules or just fragments with thiol/disulphide groups, and subsequent attachment to gold surfaces has been successfully implemented in biosensor devices [23-26].

Coeliac disease (CD) is an autoimmune disorder that is triggered in persons genetically predisposed by ingestion of gluten and related proteins [27,28] and typical symptoms range from malabsorption of nutrients to chronic diarrhea, weight loss, abdominal distension and general malnutrition [29]. The only successful treatment against celiac disease is a gluten free diet [30], with recorded improvements in days or weeks after adherence to a gluten free program [31]. The detection of anti-tissue transglutaminase (tTG) IgA and anti-endomysium antibodies (EMA) IgA are highly sensitive and specific for the detection CD in children and adults >95% [32]. Due to poor sensitivity anti-gliadin antibody (AGA) tests have mainly been discarded, but are sometimes used for children below 18 months [33]. The need for the development of cost-effective CD detection platforms has focused the interest of many researchers. Köger et. al. performed an epitope mapping of tTG with a series of peptides using a label-free parallel method, reflectometric interference spectroscopy (RIfS), adapted to a high throughput screening format which provided an important step towards a fast non-surgical

test for the detection of anti-tTG antibodies [34]. Habtamu et al. developed an immunosensor based on an electrogenerated chemiluminescence readout, using membrane-templated gold nanoelectrode ensembles with a detection limit for anti-tTG of 0.5 ng/ml [35]. Several electrochemical sensors for anti-tTG detection have also been reported using different immobilisation strategies of the tTG antigen. Dulay et al. used self-assembled monolayers of a carboxylic group terminated bipodal alkanethiol to covalently link the tTG on gold electrodes [10]. Glassy carbon electrodes functionalized with gold nanoparticles and subsequently derivatized with a SAM of 11-mercaptoundecanoic acid was used by Giannetto et. al. for the covalent anchoring of the enzyme [36]. Neves et al. developed a sensor using screen printed carbon electrodes nanostructured with a carbon–metal hybrid system. This involved the modification of the electrodes with multiwalled carbon nanotubes in a first step and the electrochemical deposition of gold nanoparticles in a second step [37, 38]. Although the reported sensors performed well in terms of sensitivity, their surface immobilisation strategies of tTG involve several steps which may result in costly and time-consuming approaches, difficult to implement in large scale production process. In this work the introduction of disulphide groups through the carboxylic, carbohydrates and amino moieties of tTG was used to immobilize the antigenic protein for the subsequent detection of anti-tissue transglutaminase antibodies. The modified tTG was evaluated using ELISA and SPR and the optimum modification employed in electrochemical immunosensors. The developed sensors were applied to the detection of anti-tTG antibodies in real patient samples. The introduction of disulphides on the antigenic protein enabled a simple and convenient one-step surface modification procedure involving only spontaneous gold-thiol covalent binding.

3.3 Experimental

3.3.1 Chemicals and materials

Potassium ferrocyanide (III) and potassium ferrocyanide (II), strontium nitrate, cystamine dihydrochloride, N-(3-dimethylaminopropyl) - N - ethylcarbodiimide (EDC), N-hydroxysuccinimide (NHS), sodium cyanoborohydride ($NaCNBH_3$), HEPES (4-(2-hydroxyethyl) piperazine-1-ethanesulfonic acid) buffer, phosphate-buffered saline (PBS) with 0.05 % v/v Tween 20 (PBS-Tween), carbonate bicarbonate capsules for preparation of carbonate buffer (0.05 M, pH 9.6), ready to use 3,3,5,5- tetramethylbenzidine (TMB) liquid substrate and dithiopropionic acid succinimidyl ester (DTSP) were purchased from Sigma-Aldrich (Spain). Ethanol, acetone, dimethyl sulphoxide (DMSO), hydrochloric acid, sodium di-hydrogen phosphate (NaH2PO4) and di-sodium hydrogen phosphate (Na_2HPO_4) were obtained from

Panreac Quimica (Barcelona, Spain). Sulfuric acid (H_2SO_4), sodium acetate, acetic acid, potassium hydroxide, sodium chloride, potassium chloride, ethylene glycol, sodium periodate and sodium hydroxide were purchased from Scharlau (Barcelona, Spain). 2-(2-(2-(11-mercaptoundecyloxy) ethoxy) ethoxy) ethanol (PEG-SH) was obtained from SensoPath Technologies (Bozeman, USA). Anti-tissue transglutaminase rabbit produced polyclonal antibody was purchased from Zedira (Darmstadt, Germany). Anti-human IgA and anti-human IgG labeled with HRP antibodies used for electrochemical measurements were provided in the commercial Eu-tTG ELISA kits; tissue transglutaminase (tTG) was supplied from EUROSPITAL (Trieste, Italy). Each kit contained five human serum calibrators with titers expressed in arbitrary units (AU) per milliliter (0, 10, 20, 50 and 100 AU/mL). Real patient samples were provided by King's College London (UK). Centrifugal filter membranes 0.5 mL (MWCO 30 kDa) were purchased from Whatman GmbH (Dassel, Germany). Nunc MaxiSorp flat-bottom 96-well plates were purchased from VWR International Eurolab (Barcelona, Spain). Aqueous solutions were prepared using de-ionized water from a Milli-Q RG system, Millipore (Madrid, Spain) and all reagents were used as received.

3.3.2 Chemical modifications of tissue transglutaminase antigen

Disulphide groups were covalently introduced into the structure of tissue transglutaminase protein via its amines, carboxylic acids and carbohydrates according to the protocols previously reported [24]. The modification procedures are depicted in Scheme 3.1.

Chemical introduction of disulphides using -NH_2 residues. Introduction of disulphides was carried out by reacting lysine residues of the antigen with a disulphide-containing active ester to form a covalent bond between disulphide groups and antigen. Therefore, 0.25 mg of tTG (3.1×10^{-9} mol) diluted in 0.5 ml of 0.01 M carbonate buffer pH 9.5 were mixed with 0.035 mg of dithiopropionic acid succinimidyl ester (DTPS) (0.9×10^{-7} mol) prepared in 0.05 ml of DMSO. The mixture reacted for 5 h at room temperature under stirring conditions in the dark. The excess of DTSP was eliminated by ultrafiltration using 30 kDa Molecular Weight Cut Off (MWCO) membranes and the modified antigen was recollected in PBS buffer pH 7.4.

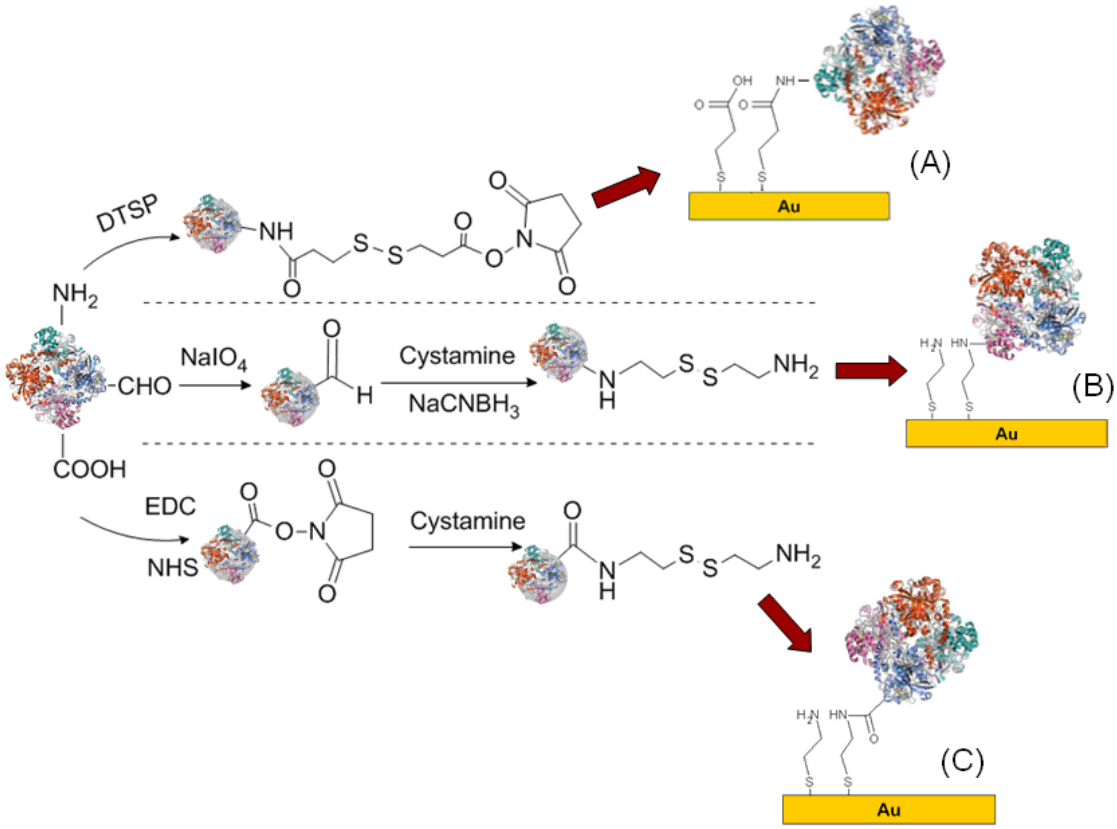

Scheme 3.1. Reaction schemes for the disulphide modification of the antigen protein through the different moieties (A) amine, (B) carbohydrates and (C) carboxyl groups.

Chemical introduction of disulphides using carbohydrates. Initially, 0.25 mg of tTG (3.1 x 10^{-9} mol) were diluted in 100 µl of 0.01M acetate buffer pH 5.0, and then a 5 mM solution of sodium periodate was added to the antigen solution. The mixture was allowed to react under stirring conditions for 1 h at room temperature in dark conditions. The oxidized antigen solution was slowly added to 450 µl of a 0.1 M cystamine solution diluted in 0.05 M carbonate buffer pH 9.5 and left to react for 3 h at room temperature to allow the formation of Schiff bases. Subsequently, unstable imines were reduced to amine bonds by adding 10 mM cyanoborohydride into the solution for 1 h. Finally, the antigen solution was purified from the excess of cystamine by filtration using 30 kDa MWCO membranes and the modified antigen was recollected in PBS buffer pH 7.4.

Chemical introduction of disulphides using –COOH residues. Firstly, 0.25 mg of tTG (3.1 x 10^{-9} mol), 3.9 mg of sulfo-NHS (1.8 x 10^{-5} mol) and 3.45 mg of EDC (1.8 x 10^{-5} mol) were mixed and incubated for 10 min under stirring conditions at room temperature in 100 µl of 10 mM

acetate buffer pH 4.5. Subsequently, the mixture was added to 450 µl of 50 mM HEPES buffer pH 8.5 containing 10 mg of cystamine (4.5×10^{-5} mol). The reaction took place for 2 h at room temperature under stirring conditions. Excess reagents and by-products were removed by filtration (30 kDa MWCO membranes) and the antigen was collected in PBS buffer pH 7.4.

3.3.3 Evaluation of modified tTG antigenicity

Enzyme Linked Immunosorbent Assay. The performance of the modified tTG was evaluated colorimetrically by an indirect capture ELISA. The absorbance was measured using a SPECTRAmax PC plate reader (bioNova científica, Spain). The immobilization of the disulphides-containing antigen was carried out using a 5 µg/ml solution of antigen dissolved in 0.05 M carbonate buffer pH 9.6, which was added (50 µl/well) on a NUNC MaxiSorp 98 well plates for 60 min at 37 °C. After blocking the well surface with 200 µl of 0.01M PBS-Tween for 60 min at 37 °C, various concentrations of rabbit anti-tTG antibodies (0.16 – 10 µg/ml) prepared in PBS-Tween were added into the corresponding wells and incubated for 60 min at 37 °C. Then, 50 µl of anti-rabbit IgG labelled with HRP enzyme (90 ng/mL) also prepared in PBS-Tween were added into the well plate and allowed to react for 60 min at 37 °C. Finally, the presence of the HRP enzyme was detected using TMB ready-to-use liquid substrate and stopping the reaction using 1 M H_2SO_4 after 20 min. The absorbance was measured at 450 nm.

Surface plasmon resonance analysis. Biacore gold chips (SIA Au kit), were first cleaned using a Piranha's solution (1:3 v/v H_2O_2 and H_2SO_4) *(Warning: Piranha's solution is highly corrosive and violently reacts with organic materials; this solution is potentially explosive and must be used with extreme caution)* for 1 min over the surface and then rinsed several times with ethanol and repeated twice for each gold chip. Real time analysis was performed using a surface plasmon resonance (SPR) Biacore 3000® (GE Healthcare, US); All SPR experiments were done using 0.01 M PBS-Tween, filtered and degassed, as running buffer and unless stated in all the dilutions used. Gold chips were first conditioned using a 20 µL/min flow of running buffer until a stable signal was achieved. Protein binding was performed at a flow rate of 5 µL/min, one channel at a time, injecting 150 µL of 0.1 mg/mL of the modified antigen. Subsequently in order to block non-specific interactions 100µL of 1 mM PEG-SH solution was flowed over all the channels, and surface functionalised with PEG-SH alone was used as a control. Antibody binding was performed at a flow rate of 20 µL/min recording for 6 minutes association and dissociation steps, injecting buffered solution in the presence and absence of target antibody. Regeneration of the surface was performed by injecting 20 µL of a solution of 50 % ethyleneglycol pH 10 between each analyte injection.

3.3.4 Electrode modification

Gold disk electrodes CHI 101 (CH Instruments Inc, US) were first polished with aqueous alumina slurries of 25 and 1 µm (Buehler, US) and then rinsed with Milli-Q water, sonicated for 1 minute and dried with nitrogen. The electrodes were treated with a mixture of H_20_2 (30%) and KOH (0.1 M) for 10 minutes, followed by an electrochemical cleaning in 0.1 M potassium hydroxide, performed using linear sweep voltammetry between -0.2 and -1.8 V [39] using a conventional three electrode cell, standard silver/silver chloride (sat. KCl) CHI111 (CH Instruments, US) as reference, and a platinum gauze was used as the counter electrode. Electrodes were immersed in a solution of 0.1 mg/mL of the modified antigen dissolved in PBS-Tween 0.01 M pH 7.4 for 1 hour, rinsed with water and dried with nitrogen. To block non-specific adsorption, the electrodes were immersed in an ethanolic solution of 1 mM PEG-SH for 30 minutes and then rinsed with ethanol.

3.3.5 Electrochemical analysis

Amperometric measurements were carried out at -0.20 V vs Ag/AgCl in a 5 mL electrochemical cell containing TMB substrate. All the electrochemical measurements were performed at room temperature. The electrodes were incubated for 15 minutes in different antibody concentrations, reference serum solutions or patient's serum followed by another 15 minutes of the corresponding anti-rabbit or anti-human HRP-labelled antibody. The immobilization and detection schematic is outlined in Scheme 3.2.

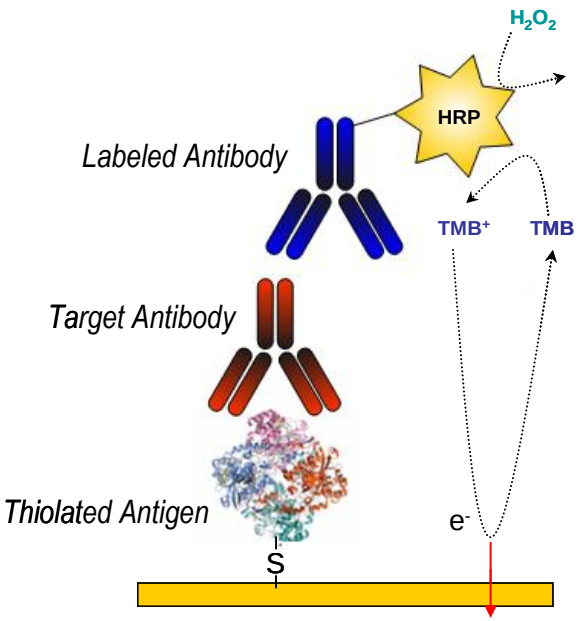

Scheme 3.2. Architecture of the immunoassay including electrochemical detection

3.3.6 ELISA analysis of the reference serum solutions

The commercial ELISA kit Eu-tTG from Eurospital was used to perform the calibration curve for anti-tTG IgG and IgA using the reference serum solutions. tTG was already precoated in the well plates. Different concentrations of the reference serum solutions (anti-tTG IgA and IgG calibrators) were added into their corresponding wells (50 µl/well) and incubated for 45 min at room temperature. The plates were washed three times with the washing solution provided in the kit and then, 50 µl/well of the ready-to-use enzyme-antibody conjugate (anti-human IgA or anti-human IgG depending on the case), also provided in the kit, were added and allowed to react for 30 min at room temperature. Finally, after washing the plate, the presence of HRP label was detected using TMB substrate. The reaction was stopped after 15 min by adding 50 µl/well of 0.5 M solution of H_2SO_4 and the absorbance was measured at 450 nm.

3.4 Results and discussion

3.4.1 Analysis of modified tTG antigenicity

The antigenicity of the modified protein was first studied using an Enzyme-Linked Immunosorbent Assay (ELISA) to investigate if the modifications introduced had resulted in a loss of antigenicity of the tissue transglutaminase due to an induced change in structure or the epitope sites.

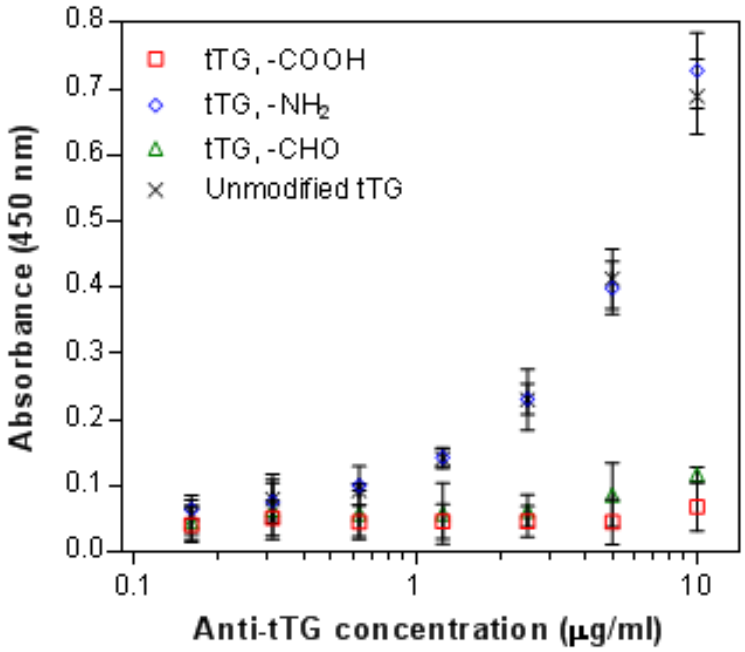

Figure 3.1. ELISA analysis of the antigenicity of the modified tissue transglutaminase

As can clearly be seen in Figure 3.1, retention of antigenicity was only observed for amine-mediated modification, with this modification showing the same antigenicity as the unmodified tTG, with both obtaining a detection limit (LOD) of 0.50 μg/mL. The LOD was estimated as the concentration determined from the signal of the zero concentration plus three times its standard deviation.

The immobilisation of the disulphides-containing tTG on gold surfaces was then characterized using SPR. The theoretical amount of modified antigen chemisorbed was quantified by measuring the immobilisation levels and assuming that for planar surfaces an SPR signal of 3000 RU equals 1 ng/mm^2 [40, 41]. The surface concentrations obtained were of 3.0, 1.9 and 3.2 pmol/cm^2 for the antigen modified via amines, carbohydrates and carboxylic moieties respectively (a molecular weight of 80000 Da was considered for tTG).The results showed a similar successful degree of immobilisation onto the gold surface for the different modified antigens, with the level of immobilisation of PEG-SH as barrier for non-specific adsorption being on average 2.8 x 10^{-10} moles/cm^2, values typical for protein immobilisation and thiol monolayer formation [23, 42, 43].

The antigenic performance of the modified proteins was then tested using different concentrations of polyclonal IgG anti-tissue transglutaminase (Figure 3.2). The response of the interaction was calculated by measuring the signal at the end of the dissociation phase. Bulk responses were subtracted for all the graphs and signals are an average of two complete experiments. In all cases control experiments with only PEG-SH did not show any relevant non-specific binding (data not shown). The results confirmed the findings obtained by ELISA, with only tTG modified through its amine moiety showing a trend in its antigenic response, obtaining a limit of detection obtained was 6.11 μg/mL with a sensitivity of 0.54 RU/μg/mL^{-1}. Regeneration of the surfaces was achieved by injecting a 1 minute pulse of a solution of 50 % ethyleneglycol pH 10.0 between each analyte injection. Regeneration efficiencies were higher than the 90 % for all experiments.

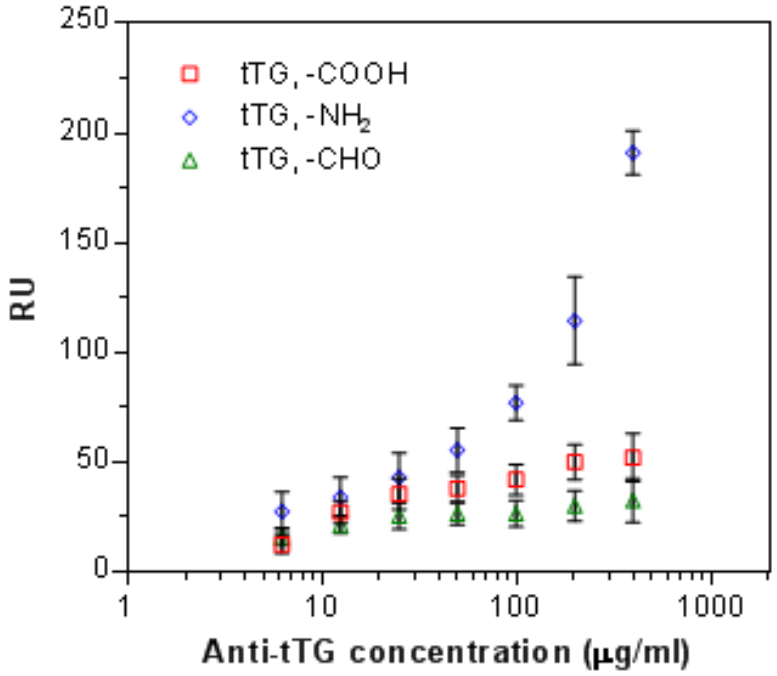

Figure 3.2. Surface Plasmon Resonance analysis of the antigenicity of the chemisorbed modified tissue transglutaminase.

3.4.2 Electrochemical Detection

Using electrochemical detection, antibody binding was again only observed with the tissue transglutaminase modified through its amine moieties (Figure 3.3), achieving a limit of detection of 0.26 µg/mL and a sensitivity of 10 nA/µg·mL^{-1} with a linear dynamic range from 0.26 to 6.9 µg/mL. The R^2 was of 0.994 and the average relative standard deviation (RSD) of 9.5 % (n = 6).

To demonstrate the robustness of the functionalized electrodes with the developed surface chemistry, accelerated stability studies were performed. Electrodes were functionalized with disulphides-modified tTG via its primary amines and stored at 37 ^{o}C and 4 ^{o}C for accelerated and real-time stability testing, respectively. The sensors were stored in the presence of the commercial StabilCoat Plus® stabilizer (SurModics, Inc., Eden Prairie, USA), which was deposited onto the protein-coated electrodes and allowed to dry in a vacuum desiccator for 1 h prior to storage of the electrodes. On a weekly basis, the arrays were assessed using the reference serum solution of 50 AU/mL form the commercial ELISA kit over a period of 8 weeks. The response was recorded amperometrically and compared with the

signal of fresh prepared electrodes. Pre-coated electrodes did not show loss of activity over the period of study at any of the storage temperatures assayed with a relative signal response in week 8 of 99.4 ± 2 % and 101.3 ± 6 % for the electrode arrays stored at 4 ºC and 37 ºC, respectively.

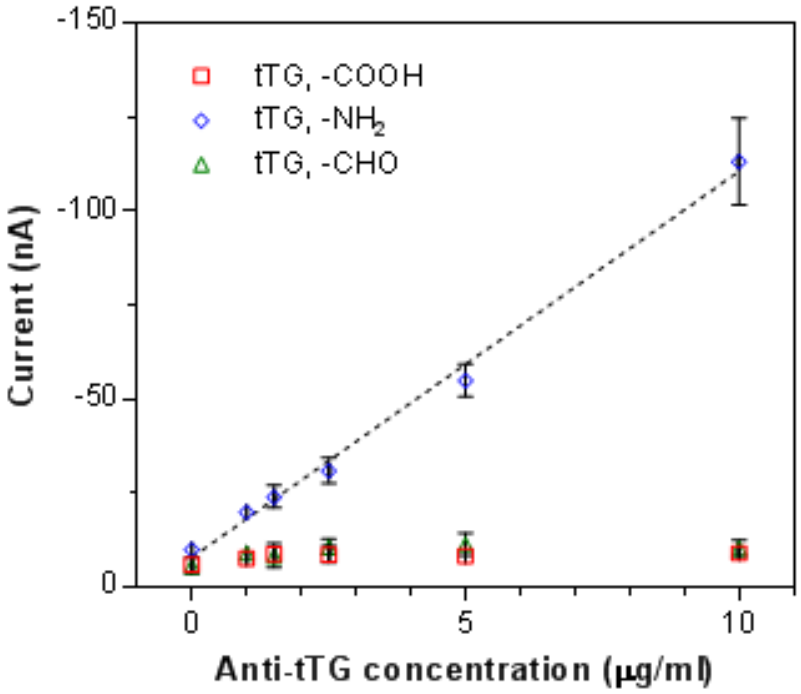

Figure 3.3. Electrochemical detection of polyclonal antibodies on tissue transglutaminase-modified electrodes.

Clinical reference serum solutions from commercial ELISA kits were used in order to evaluate the performance of the functionalised immunosensor. The detection of IgG and IgA anti-tissue transglutaminase in the presence of the complex serum matrix was explored (Figure 3.4). The disulphides-modified tTG via its primary amines exhibited a linear response for the concentration range assayed, reaching an LOD of 6.2 AU/ml and linear dynamic range from 6.2 to 72.3 AU/ml for IgG anti-tTG antibodies. In the case of anti-tTG IgA the LOD was of 10.8 AU/ml with a dynamic range from 10.8 to 71.8 AU/ml. This result clearly demonstrates that the immobilised tTG modified via its amine groups maintained its antigenicity and can be used to discriminate and quantify IgA and IgG anti-tTG antibodies at clinically relevant concentrations.

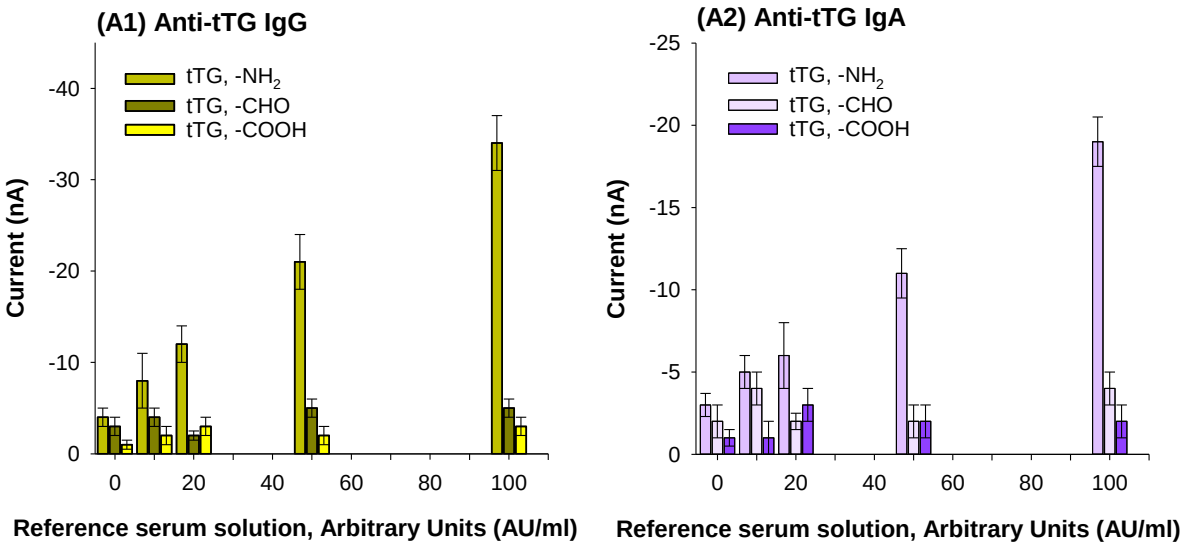

Figure 3.4. Electrochemical analysis of anti-tissue transglutaminase antibodies isotype IgG (A1) and IgA (A2) in reference serum solution.

Finally, the electrochemical detection of real coeliac disease patient's serum was compared with the equivalent ELISA assay from the commercial kit for the IgA isotype due to its clinical relevance (Figure 3.5). The amperometric signals obtained for each of five patient samples were interpolated using a calibration curve generated using reference serum solutions, to obtain equivalent arbitrary units and compared to those found when analysing the same samples using the Eurospital commercial ELISA kit. According to manufacturer's instructions, normal anti-tTG IgA values are <9 AU/ml, borderline values are between 9 and 16 AU/ml and positive values >16 AU/ml. As observed the developed amperometric sensor was able to identify all coeliac disease patients with an excellent correlation with the ELISA-based detection, indicating the potential applicability of the immunosensor for clinical use. Moreover, the amperometric sensor exhibited a significantly reduced assay time of 30 min compared with the time required for the ELISA kit (90 min).

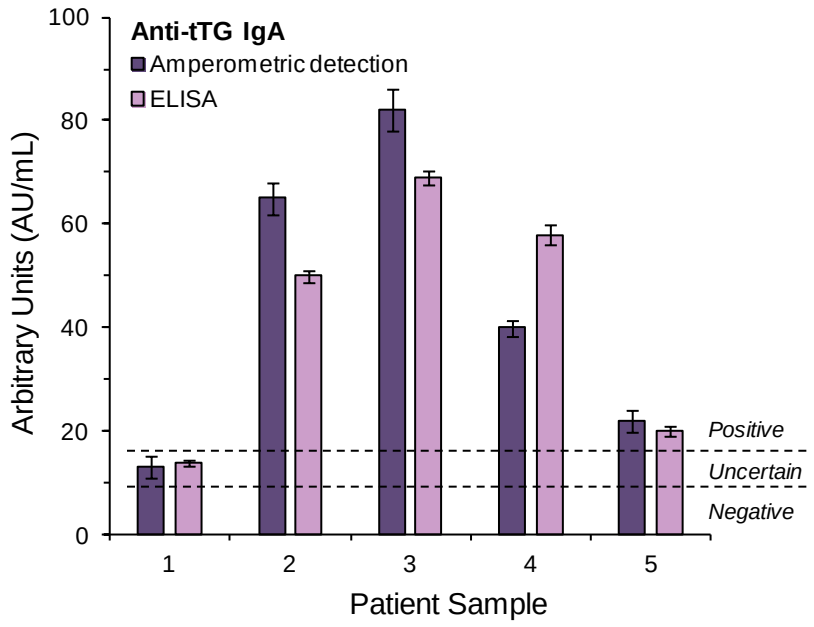

Figure 3.5. Comparison of electrochemical vs. ELISA-based detection of anti-tTG IgA from real coeliac disease patient's serum using the disulphide-containing tTG modified through its amine groups. Clinically relevant diagnostic cut-off levels are shown.

3.5 Conclusions

The introduction of disulphides into an antigienic protein through different moieties and their immobilisation on gold surfaces was achieved for the detection of coeliac disease related anti-tTG autoantibody detection. Using rabbit polyclonal antibodies and ELISA detection with simple physical adsorption of the modified antigens, the antigenicity of tissue transglutaminase was observed to have been lost when disulphide groups were introduced through either the carbohydrate or carboxyl moieties, with only the amine-based modification retaining antigenic properties. The developed electrochemical immunosensors were applied to the detection of IgA anti-tissue transglutaminase in real patient samples and the results compared to that obtained using commercial ELISA kits, with an excellent degree of correlation observed, with the entire assay being completed in just 30 minutes.

3.6 References

1. Willmott C, Arrowsmith JE, Gregory K, Lewandrowski K, Lee-Lewandrowski E, Lewandrowski K, Lewandrowski K, Cott EM Van (2010) Point-of-care testing. Surgery 28:159–160. doi: 10.1016/j.mpsur.2010.01.019

2. Rotariu L, Lagarde F, Jaffrezic-Renault N, Bala C (2016) Electrochemical biosensors for fast detection of food contaminants – trends and perspective. TrAC Trends Anal Chem 79:80–87. doi: 10.1016/j.trac.2015.12.017
3. Chikkaveeraiah B V., Bhirde AA, Morgan NY, Eden HS, Chen X (2012) Electrochemical immunosensors for detection of cancer protein biomarkers. ACS Nano 6:6546–6561. doi: 10.1021/nn3023969
4. Jia X, Liu Z, Liu N, Ma Z (2014) A label-free immunosensor based on graphene nanocomposites for simultaneous multiplexed electrochemical determination of tumor markers. Biosens Bioelectron 53:160–166. doi: 10.1016/j.bios.2013.09.050
5. Li Y, Fang L, Cheng P, Deng J, Jiang L, Huang H, Zheng J (2013) An electrochemical immunosensor for sensitive detection of Escherichia coli O157:H7 using C60 based biocompatible platform and enzyme functionalized Pt nanochains tracing tag. Biosens Bioelectron 49:485–491. doi: 10.1016/j.bios.2013.06.008
6. Reverté L, Prieto-Simón B, Campàs M (2016) New advances in electrochemical biosensors for the detection of toxins: Nanomaterials, magnetic beads and microfluidics systems. A review. Anal Chim Acta 908:8–21. doi: 10.1016/j.aca.2015.11.050
7. Mastichiadis C, Niotis AE, Petrou PS, Kakabakos SE, Misiakos K (2008) Capillary-based immunoassays, immunosensors and DNA sensors – steps towards integration and multi-analysis. TrAC Trends Anal Chem 27:771–784. doi: 10.1016/j.trac.2008.08.003
8. Akhavan O, Ghaderi E, Rahighi R, Abdolahad M (2014) Spongy graphene electrode in electrochemical detection of leukemia at single-cell levels. Carbon N Y 79:654–663. doi: 10.1016/j.carbon.2014.08.058
9. Rosales-Rivera LC, Acero-Sánchez JL, Lozano-Sánchez P, Katakis I, O'Sullivan CK (2012) Amperometric immunosensor for the determination of IgA deficiency in human serum samples. Biosens Bioelectron 33:134–138.
10. Dulay S, Lozano-Sánchez P, Iwuoha E, Katakis I, O'Sullivan CK (2011) Electrochemical detection of celiac disease-related anti-tissue transglutaminase antibodies using thiol based surface chemistry. Biosens Bioelectron 26:3852–3856. doi: 10.1016/j.bios.2011.02.045
11. Fragoso A, Latta D, Laboria N, von Germar F, Hansen-Hagge TE, Kemmner W, Gärtner C, Klemm R, Drese KS, O'Sullivan CK (2011) Integrated microfluidic platform for the electrochemical detection of breast cancer markers in patient serum samples. Lab Chip 11:625–31. doi: 10.1039/c0lc00398k
12. Kim J, Hong SC, Hong JC, Chang CL, Park TJ, Kim H-J, Lee J (2015) Clinical immunosensing of tuberculosis CFP-10 antigen in urine using interferometric optical fiber array. Sensors Actuators B Chem 216:184–191. doi: 10.1016/j.snb.2015.04.046
13. Hasanzadeh M, Shadjou N, Soleymani J, Omidinia E, de la Guardia M (2013) Optical immunosensing of effective cardiac biomarkers on acute myocardial infarction. TrAC Trends Anal Chem 51:158–168. doi: 10.1016/j.trac.2013.06.010
14. Wiseman ME, Frank CW (2012) Antibody Adsorption and Orientation on Hydrophobic Surfaces.
15. Barton AC, Collyer SD, Davis F, Garifallou G-Z, Tsekenis G, Tully E, O'Kennedy R, Gibson T, Millner PA, Higson SPJ (2009) Labeless AC impedimetric antibody-based sensors with pgml−1 sensitivities for point-of-care biomedical applications. Biosens Bioelectron 24:1090–1095. doi: 10.1016/j.bios.2008.06.001

16. Shalev M, Miriam A (2011) Sol-Gel Entrapped Levonorgestrel Antibodies: Activity and Structural Changes as a Function of Different Polymer Formats. Materials (Basel) 4:469–486. doi: 10.3390/ma4030469
17. Albarghouthi M, Fara DA, Saleem M, El-Thaher T, Matalka K, Badwan A (2000) Immobilization of antibodies on alginate-chitosan beads. Int J Pharm 206:23–34. doi: 10.1016/S0378-5173(00)00470-1
18. Singhal R, Takashima W, Kaneto K, Samanta SB, Annapoorni S, Malhotra BD (2002) Langmuir-Blodgett films of poly(3-dodecyl thiophene) for application to glucose biosensor. Sensors Actuators, B Chem 86:42–48. doi: 10.1016/S0925-4005(02)00145-4
19. Asiaei S, Nieva P, Vijayan MM (2014) Fast kinetics of thiolic self-assembled monolayer adsorption on gold: modeling and confirmation by protein binding. J Phys Chem B 118:13697–703. doi: 10.1021/jp509986s
20. Yoon M, Hwang HJ, Kim JH (2011) Immobilization of antibodies on the self-assembled monolayer by antigen-binding site protection and immobilization kinetic control. J Biomed Sci Eng 4:242–247. doi: 10.4236/jbise.2011.44033
21. Yoshimoto K, Nishio M, Sugasawa H, Nagasaki Y (2010) Direct Observation of Adsorption-Induced Inactivation of Antibody Fragments Surrounded by Mixed-PEG Layer on a Gold Surface. J Am Chem Soc 132:7982–7989. doi: 10.1021/ja910372e
22. Love JC, Estroff LA, Kriebel JK, Nuzzo RG, Whitesides GM (2005) Self-Assembled Monolayers of Thiolates on Metals as a Form of Nanotechnology. Chem Rev 105:1103–1170. doi: 10.1021/cr0300789
23. Nassef HM, Civit L, Fragoso A, O'Sullivan CK (2009) Amperometric immunosensor for detection of celiac disease toxic gliadin based on fab fragments. Anal Chem 81:5299–5307. doi: 10.1021/ac9005342
24. Acero Sánchez JL, Fragoso A, Joda H, Suárez G, McNeil CJ, O'Sullivan CK (2016) Site-directed introduction of disulphide groups on antibodies for highly sensitive immunosensors. Anal Bioanal Chem 408:5337–46. doi: 10.1007/s00216-016-9630-9
25. Spampinato V, Parracino MA, La Spina R, Rossi F, Ceccone G (2016) Surface Analysis of Gold Nanoparticles Functionalized with Thiol-Modified Glucose SAMs for Biosensor Applications. Front Chem 4:8. doi: 10.3389/fchem.2016.00008
26. Sharma H, Mutharasan R (2013) Half Antibody Fragments Improve Biosensor Sensitivity without Loss of Selectivity. Anal Chem 85:2472–2477. doi: 10.1021/ac3035426
27. Dieterich W, Ehnis T, Bauer M, Donner P, Volta U, Riecken EO, Schuppan D (1997) Identification of tissue transglutaminase as the autoantigen of celiac disease. Nat Med 3:797–801. doi: 10.1038/nm0797-797
28. Stern M, Ciclitira PJ, van Eckert R, Feighery C, Janssen FW, Méndez E, Mothes T, Troncone R, Wieser H (2001) Analysis and clinical effects of gluten in coeliac disease. Eur J Gastroenterol Hepatol 13:741–7.
29. Mäki M, Collin P (1997) Coeliac disease. Lancet 349:1755–9. doi: 10.1016/S0140-6736(96)70237-4
30. Janatuinen EK, Kemppainen TA, Julkunen RJK, Kosma V-M, Mäki M, Heikkinen M, Uusitupa MIJ (2002) No harm from five year ingestion of oats in coeliac disease. Gut 50:332–5.
31. Briani C, Samaroo D, Alaedini A (2008) Celiac disease: From gluten to autoimmunity. Autoimmun Rev 7:644–650. doi: 10.1016/j.autrev.2008.05.006

32. Hill ID (2005) What are the sensitivity and specificity of serologic tests for celiac disease? Do sensitivity and specificity vary in different populations? Gastroenterology 128:S25–S32. doi: 10.1053/j.gastro.2005.02.012
33. Lagerqvist C, Dahlbom I, Hansson T, Jidell E, Juto P, Olcén P, Stenlund H, Hernell O, Ivarsson A (2008) Antigliadin immunoglobulin A best in finding celiac disease in children younger than 18 months of age. J Pediatr Gastroenterol Nutr 47:428–35. doi: 10.1097/MPG.0b013e31817d80f4
34. Kröger K, Bauer J, Fleckenstein B, Rademann J, Jung G, Gauglitz G (2002) Epitope-mapping of transglutaminase with parallel label-free optical detection. Biosens Bioelectron 11–12:937–944.
35. Habtamu HB, Sentic M, Silvestrini M, De Leo L, Not T, Arbault S, Manojlovic D, Sojic N, Ugo P (2015) A Sensitive Electrochemiluminescence Immunosensor for Celiac Disease Diagnosis Based on Nanoelectrode Ensembles. Anal Chem 87:12080–12087. doi: 10.1021/acs.analchem.5b02801
36. Giannetto M, Mattarozzi M, Umiltà E, Manfredi A, Quaglia S, Careri M (2014) An amperometric immunosensor for diagnosis of celiac disease based on covalent immobilization of open conformation tissue transglutaminase for determination of anti-tTG antibodies in human serum. Biosens Bioelectron 62:325–330. doi: 10.1016/j.bios.2014.07.006
37. Neves MMPS, González-García MB, Delerue-Matos C, Costa-García A (2013) Multiplexed electrochemical immunosensor for detection of celiac disease serological markers. Sensors Actuators B Chem 187:33–39. doi: 10.1016/j.snb.2012.09.019
38. Neves MMPS, González-García MB, Nouws HPA, Costa-García A (2012) Celiac disease detection using a transglutaminase electrochemical immunosensor fabricated on nanohybrid screen-printed carbon electrodes. Biosens Bioelectron 31:95–100. doi: 10.1016/j.bios.2011.09.044
39. Heiskanen AR, Spégel CF, Kostesha N, Ruzgas T, Emnéus J (2008) Monitoring of Saccharomyces cerevisiae Cell Proliferation on Thiol-Modified Planar Gold Microelectrodes Using Impedance Spectroscopy. Langmuir 24:9066–9073. doi: 10.1021/la800580f
40. Gizeli E, Lowe CR (2002) Biomolecular Sensors. Taylor & Francis, London
41. Schasfoort RBM, Tudos AJ (2008) Handbook of Surface Plasmon Resonance. doi: 10.1039/9781847558220
42. Fragoso A, Laboria N, Latta D, O'Sullivan CK (2008) Electron permeable self-assembled monolayers of dithiolated aromatic scaffolds on gold for biosensor applications. Anal Chem 80:2556–2563.
43. Widrig CA, Chung C, Porter MD (1991) The electrochemical desorption of n-alkanethiol monolayers from polycrystalline Au and Ag electrodes. J Electroanal Chem Interfacial Electrochem 310:335–359. doi: 10.1016/0022-0728(91)85271-P

4 Multiplex PCB-based electrochemical detection of cancer biomarkers using MLPA-barcode approach

Multiplex PCB-based electrochemical detection of cancer biomarkers using MLPA-barcode approach

J. Ll. Acero Sánchez[1], O. Y. F. Henry[1], H. Joda[1] , B. Werne Solnestam[2], L. Kvastad[2], E. Johansson[2], P. Akan[2], J. Lundeberg[2], N. Lladach[3], D. Ramakrishnan[4], I. Riley[4] and C. K. O'Sullivan[1,5]

[1] Universitat Rovira i Virgili, Departament de Enginyeria Química Av. Països Catalans 26, 43007 Tarragona, Spain.
[2] KTH Royal Institute of Technology, Science for Life Laboratory (SciLifeLab Stockholm), School of Biotechnology, Division of Gene Technology, SE-171 65 Solna, Sweden.
[3] MRC Holland, Willem Schoutenstraat 6, 1057 DN Amsterdam, The Netherlands
[4] Labman Automation Ltd., Seamer Hill, Seamer, Stokesley, North Yorkshire, TS9 5NQ, United Kingdom.
[5] Institució Catalana de Recerca i Estudis Avançats, Passeig Lluís Companys 23, 08010 Barcelona, Spain.

4.1 Abstract

Asymmetric multiplex ligation-dependent probe amplification (MLPA) was developed for the amplification of seven breast cancer related mRNA markers and the MLPA products were electrochemically detected via hybridization. Seven breast cancer genetic markers were amplified by means of the MLPA reaction, which allows for multiplex amplification of multiple targets with a single primer pair. Novel synthetic MLPA probes were designed to include a unique barcode sequence in each amplified gene. Capture probes complementary to each of the barcode sequences were immobilized on each electrode of a low-cost electrode microarray manufactured on standard printed circuit board (PCB) substrates. The functionalised electrodes were exposed to the single-stranded MLPA products and following hybridization, a horseradish peroxidase (HRP)-labelled DNA secondary probe complementary to the amplified strand completed the genocomplex, which was electrochemically detected following substrate addition. The electrode arrays fabricated using PCB technology exhibited an excellent electrochemical performance, equivalent to planar photolithographically-fabricated gold electrodes, but at a vastly reduced cost (>50 times lower per array). The optimised system was demonstrated to be highly specific with negligible cross-reactivity allowing the simultaneous detection of the seven mRNA markers, with limits of detections as low as 25 pM. This approach provides a novel strategy for the genetic profiling of tumour cells via integrated "amplification-to-detection".

4.2 Introduction

It has been shown that circulating tumour cells (CTCs) have prognostic value in metastatic breast cancer patients and a plethora of methods and technologies have been developed to isolate, enumerate and analyse CTCs, which are defined as cancer cells that have detached from the primary tumour site and entered the peripheral blood circulation. Isolation and enumeration of CTCs may be highly important not only for early detection of metastatic disease early but also for monitoring disease progression. Furthermore, molecular characterization of the CTCs is of great importance. Genetic profiling using a limited set of genetic markers has potential as a rapid and cost-effective molecular diagnostic tool for analysing CTCs [1].

Multiplex ligation-dependent probe amplification (MLPA) has garnered huge importance in molecular diagnostics due to its' accuracy, robustness, low cost, relative simplicity and high multiplexability for up to 40-50 different target sequences in one reaction [2,3]. MLPA exploits specifically designed MLPA probes (55-80 mer) consisting of two or three oligonucleotides (right and left hybridization oligonucleotides, and in some cases also a spanning oligonucleotide), containing target-specific sequences and universal PCR primer sequences. In the presence of a complementary target sequence, the MLPA probes hybridize next to each other and are subsequently ligated, followed by classic exponential amplification using a single primer pair. Amplified products vary in length, typically between 130 and 480 bases, depending on the probe length and are analysed using capillary electrophoresis [2]. In the absence of a complementary target sequence, ligation will not occur and amplification of the complete complex of the two MLPA probes does not take place. MLPA is dependent on length-based discrimination of the products, which requires the use of capillary electrophoresis, and also limits the number of probes within a single reaction to 40-50 probe pairs. To analyse a higher numbers of targets, array based MLPA assays has been reported where selective DNA tag sequences were incorporated into the MLPA probes [4, 6], with detection being based on the hybridization of the tag sequence to a surface-immobilized DNA probe, with fluorescence read out.

In recent years, electrochemical detection has been shown to have great potential as an alternative to fluorescence for genetic analysis, as it is characterised by high sensitivity, ease of use, low cost, rapid response, low power requirements and compatibility with integration in microsystems [7, 8].

The use of Printed Circuit Board (PCB) technology in the biosensor field has recently emerged as an alternative to standard photolithographic techniques for electrode array microfabrication [9-11], as PCB technology offers low cost mass production, not requiring clean room facilities. Clinical Micro Sensors Inc. (now GenMark Diagnostics, Inc.), reported on the first use of PCB platform in molecular diagnostics [12, 13], where they reported electrochemical sequence specific detection of DNA via sandwich hybridization with a reporter probe containing ferrocene moieties. Gassmann and his colleagues [14] developed a PCB based DNA chip for amplification and electrochemical detection, while Tseng and his group [15] recently described a PCB based electrochemical biosensor array for the quantitative detection of PCR amplicons using methylene blue as the redox indicator.

In this paper, we report the electrochemical detection of seven genes relevant to the molecular characterization of breast cancer cells amplified using MLPA incorporating unique barcode sequences using a novel low-density electrode array fabricated using standard printed circuit board (PCB). The CDH1 gene encoding for epithelial Cadherin 1 is a tumour suppressor gene, which expression has been implicated in cancer progression and metastasis. The CDH2 gene encodes for the protein Cadherin 2 and appears to be a potential breast cancer metastases marker. The CD24 and CD44 genes, the ratio “CD44 positive-to-CD24 negative” are of particular clinical relevance in breast cancer and are used to classify breast cancer cells with stem-like characteristics. The protein CD24 is involved in cell adhesion and found at the surface of most B Lymphocytes and differentiating neuroblasts, whilst CD44 is involved in cell-cell interactions, cell adhesions and expressed in a large number of mammalian cell types. The ERBB2 gene encodes for the protein HER2 (Human Epidermal Growth Factor Receptor 2), of which over-expression plays a major role in the development and progression of certain breast cancer types. E3 ubiquitin-protein ligase HUWE1 is an enzyme that is encoded by the HUWE1 gene, which has been identified as being overexpressed in breast, lung and colorectal cancers. Finally, the KRT19 gene encodes for the proteins Keratin, type I cytoskeletal 19 known to support epithelial cell integrity and that can be used as a reference marker due to its' high sensitivity in the diagnosis of disseminated breast cancer tumour cells.

The microarray consists of 64 individually addressable gold working electrodes sharing common reference and counter electrodes. Cancer genetic biomarkers were amplified by asymmetric MLPA and the ssDNA amplicons hybridized to capture probes complementary to each of the incorporated barcode sequences. The surface bound DNA duplexes were then hybridized with a secondary DNA probe labelled with HRP molecule and finally a precipitating

TMB substrate for membranes was added and detected using fast electrochemical pulse amperometry. Assay conditions such as hybridization time and temperature were optimised and the specificity and sensitivity evaluated.

4.3 Material and methods

4.3.1 Materials

Chemicals were purchased from Sigma Aldrich (Spain) unless otherwise stated. Ultrapure water was obtained from a Millipore purification system (Millipore, Spain).

4.3.2 Instrumentation

Electrochemical characterization of the electrode array was performed using a PGSTAT12 potentiostat (Metrohm AG, The Netherlands) using an external Ag/AgCl wire reference electrode and a platinum counter electrode. The PGSTAT12 was equipped with four MUX modules (Metrohm AG, The Netherlands) of sixteen channels each. The MUX module allows sequential interrogation of up to 64 working electrodes that share the same reference and counter electrode.

All electrochemical DNA detection assays were performed using a dedicated 64-channel measuring system. This system allows simultaneous amperometric measurements of all electrodes using the on-chip reference and counter electrodes. The study of the effect of mixing on the hybridization efficiency was carried out using a Cavro^{TM} syringe pump obtained from Tecan Systems (San Jose, CA, USA).

4.3.3 Electrode chip design

The electrode chip was designed “in-house” using AutoCAD software (Autodesk Inc, USA) and manufactured at Fineline GmbH (Hilden, Germany) using printed circuit board (PCB) technology. Its' design was based on a previous sensor chip prototype designed and manufactured “in-house” using the same technology [11]. The electrode array is a one-layer PCB of 1 mm thick fabricated using the classical FR-4 glass epoxy resin (30 μm Cu thickness) as rigid substrate and with a surface finish of 3 μm soft gold deposited on a nickel layer of approximately 4 μm. Soft gold surface finish refers to the electrolytic deposition of gold onto nickel-protected copper tracks from a gold deposition bath of 99.99% purity as per manufacturer's instructions. This PCB-based chip has a square shape with a side-length of 24.6 mm and consists of 64 individually addressable circular gold working electrodes of 300 μm diameter, sharing a common gold counter and common gold reference electrode, also circular

and 250 µm of diameter. All electrodes are linked to connection pads, which are located at the edges of the PCB, through tracks of approximately 100 µm wide separated by a gap of 175 µm. The electrode arrays were insulated with green solder mask with openings to define the geometrical area of the connection pads, working, counter and reference electrodes, and to avoid exposure of the electrode tracks to fluids (Figure 4.1, A and B).

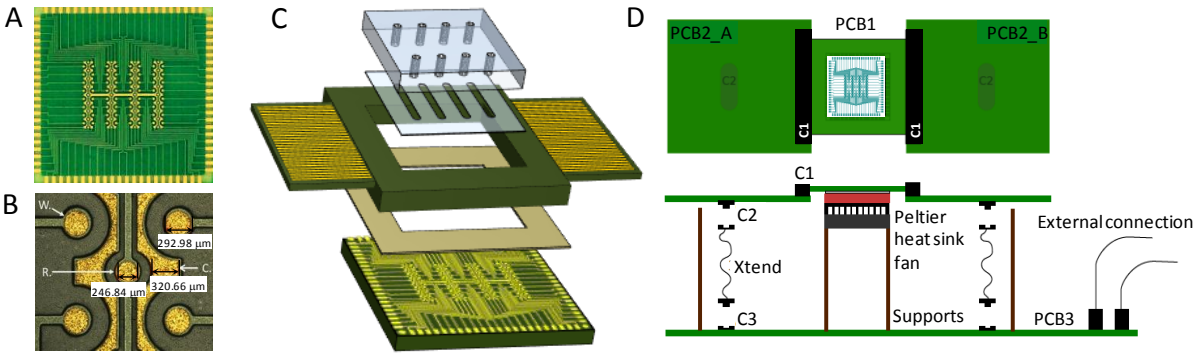

Figure 4.1. Electrochemical detection platform. A) 64-electrode array realised on PCB; B) Magnified image of the PCB chip showing the working (W), counter (C) and reference (R) electrodes; C) Schematic representation of the sensor (1. PCB chip, 2. Anisotropic conductive adhesive tape, 3. PCB carrier, 4. Microfluidic channels of double-sided adhesive tape and 5. Laser machined PMMA gasket); D) Detection unit fully assembled.

4.3.4 Electrochemical detection unit set-up

In order to allow the connectivity between the electrode chip and the potentiostat, as well as the injection of samples to the array, a laboratory test set-up was designed, fabricated and assembled (Figure 4.1, C and D). The unit consists of the PCB sensor, four interface PCBs, and a series of connectors and cables coupled to the potentiostat. The PCB chip is first mounted onto a PCB carrier with the help of an anisotropic conductive double-sided adhesive gasket (3M, USA). This PCB carrier slots through edge connectors into two interface PCBs, which can be connected to either the commercial PGSTAT12 potentiostat or the dedicated measuring prototype system. To allow the addition of samples to the sensor, simple microfluidic flow cells were fabricated using a Fenix CO_2 laser (Synrad Inc., USA) to cut and drill 2 mm thick poly(methylmethacrylate) (PMMA) sheets and define the microfluidic channels in 100 µm thick medical grade double-sided adhesive gasket (Adhesives Research Ltd., Ireland).

4.3.5 Oligonucleotide sequences

DNA probes designed *in-silico* and synthetic single stranded DNA (ssDNA) were purchased as lyophilized pellets from Biomers.net or MWG Operon GmbH (Germany) and reconstituted in Rnase and Dnase-free water. The details of the sequences used can be found in the Supporting information (SI).

4.3.6 Barcode design

In-house barcode generation software to generate unique barcodes composed of only purines or pyrimidines [16] was exploited. Only unique barcodes with no significant hybridization with each other or any adapters used in the experiments were considered. The uniqueness of barcodes was determined based on how many base changes, insertions or deletions (edit distance) were required to convert one barcode to another. A relatively high edit distance (6) to ensure unique mapping after sequencing was chosen.

Random DNA sequences of 23 bases in length and composed of only purines or pyrimidines were generated. Not more than three mono- di- or tri-mer repeats were included. Only those with 45% to 65% GC content were taken further. Sequences with low complexities (e.g. containing repeats) were removed using the Lempel-Ziv (LZ) compression algorithm [17]. Sequences with low complexity were compressed better due to their poor information content, whereas those with higher complexity were compressed less, leading to higher compression scores. Only sequences with compression score greater than 11 were selected. This was done empirically based on the number of sequences eliminated. Only sequences that were at least 6 Levenshtein edit distance to each other were considered, i.e. even if five errors per barcode were introduced during experiment or sequences, all the barcodes were uniquely mapped. Levenshtein distance is the minimum number of changes (insertions, deletions, substitutions) to convert one string to another [18]. We paired barcodes to gene-specific primers if no significant hybridization formed between them (deltaG >= -5 kcal/mol at 50.0 C). Sequences that hybridize to each other were also discarded (maximum Tm = 50.0) [165].

4.3.7 Asymmetric multiplexed ligand dependant probe amplification (MLPA)

MLPA primers and probes were designed and quality tested by MRC-Holland according to their standardized protocols. A universal primer pair (primer X and Y) was used to amplify all ligated probes by PCR, (Primer pair obtained from MWG, Supporting Information). A 2.5 µl of a positive quality control sample containing a mixture of 10 nM of each cancer biomarker

template was used. An initial incubation of 5 min at 98°C was followed by the addition of 1.5 µl of a mix containing 0.75 µl MLPA Buffer (MRC-Holland, Amsterdam, the Netherlands) and 0.75 µl of a solution containing 3 fmol of each target-specific oligonucleotide. The mixture was incubated at 95°C for 60 s to denature the probes, after which hybridization took place at 60°C for 1 h. Subsequently, ligation of MLPA probes was performed by adding 8 µl of a mix containing 1.5 µl ligase buffer A (MRC-Holland, Amsterdam, the Netherlands), 1.5 µl Ligase Buffer B (MRC-Holland, Amsterdam, the Netherlands), 1 µl Ligase-65 (MRC-Holland) and 4 µl of water. Ligation was performed for 4 minutes at 54°C followed by an incubation of 5 min at 98 ^{o}C.

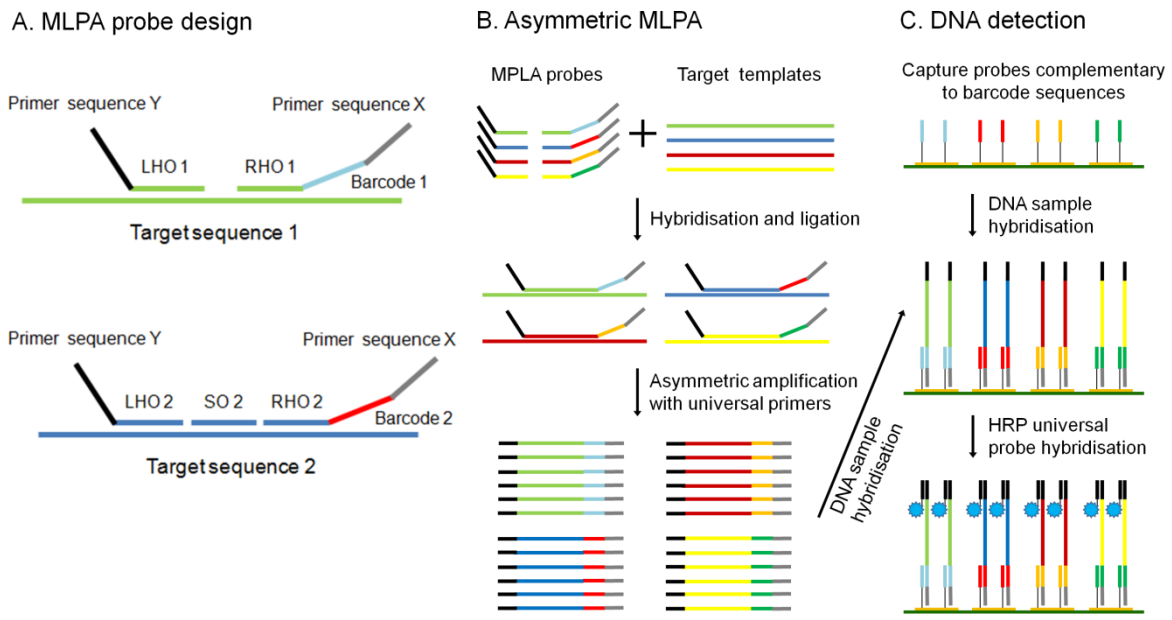

Figure 4.2. A) Design of the MLPA probes. The MLPA probe mix consists of either two or three oligonucleotides: a left hybridization oligonucleotide (LHO) consisting of a target-specific sequence and a universal primer sequence Y, a right hybridization oligonucleotide (RHO) consisting of a target-specific sequence, a unique barcode and a universal primer sequence X. Some of the probes also had a sequence-specific spanning oligonucleotide (SO) to increase specificity. B) Schematic representation of the asymmetric MLPA process showing the hydridization and ligation of the MLPA probes to the single strand MLPA samples and the asymmetric amplification with universal primers. C: Schematic layout of the electrochemical detection using unique barcodes and a universal reporter probe labelled with HRP enzyme.

Finally, single stranded DNA amplicons were generated by asymmetric multiplex amplification, which was performed by addition of 8 µl of a mix containing 1.2 units SALSA Polymerase (MRC-Holland, Amsterdam, the Netherlands), 4 nmol dNTPs, 20 pmol of Cy3-labeled forward primer Y, 3 pmol of unmodified reverse primer X and 4 µl of Q-solution

(Qiagen, Hilden, Germany). Asymmetric amplification consisted of 35 PCR cycles (30 s 95°C, 30 s 60°C, and 60 s 72°C). After the final cycle of the PCR, the samples were held at 72°C for 10 min (Figure 4.2, A and B).

4.3.8 Electrode chip functionalization and assay

Electrode arrays were successively sonicated for 5 minutes in deionised water, acetone and isopropanol and blow dried in a stream of compressed air before being plasma treated for 20 minutes (5 SSCM O_2/ 5 SSCM Ar) using a Orion-8-HV sputter (AJA Internacional Inc., USA). Cleaned arrays were subsequently immersed in a 1 mM ethanolic solution of carboxylate-terminated aromatic dithiol (Sensopath Ltd., USA) overnight. Following extensive washing with ethanol, the arrays were immersed for 30 minutes in a solution of 200 mM EDC and 50 mM NHS prepared in deionised water, rinsed with water and dried in a stream of compressed air. DNA probes were dissolved to a concentration of 10 µM in 50 mM sodium phosphate (pH 8.5) printing buffer and spotted onto individual electrodes by contact printing using an XActII microarrayer (LabNext Inc., USA). The modified arrays were incubated overnight in a wet chamber containing a solution of saturated NaCl to achieve approximately 75% relative humidity. Following rinsing with deionised water, the arrays were blocked with ethanolamine (50 mM, 0.1M Tris buffer pH 9), rinsed with deionised water and stored at 4^{o}C until use. Negative controls consisted of unspotted sensors blocked with ethanolamine.

Approximately 10 µL of the diluted ssDNA MLPA products were injected into the microfluidic set-up and incubated for 60 minutes at 37 ^{o}C. Channels were subsequently flushed with 100 µL of Tris buffer pH 8.0 containing 1 M of NaCl (hybridization buffer) before injecting 20 µL of HRP-labelled secondary probe prepared at a concentration of 10 nM in hybridization buffer and left to incubate for 30 minutes at 37 ^{o}C, before flushing the microfluidics with 100 µL of hybridization buffer (Figure 4.2.C). The presence of the HRP label was measured by fast amperometry following injection of 20 µL of TMB Enhanced HRP membrane substrate (Diarect AG, Germany) and measuring the reduction current derived from the reduction of the HRP-oxidized TMB at -0.2 V (vs. internal reference).

Data were processed using a Visual Basic macro running under MS Excel to treat the current traces recorded at the 64 electrodes. Initially, the current response at 500 ms was used as hybridization signal. Limits of detection were taken as the concentration value corresponding to the averaged current response of the negative control sensors over the entire concentration range plus three times the average standard deviation.

4.4 Results and discussion

4.4.1 Electrochemical characterization of the PCB-electrode array

The cost associated with the fabrication of sputtered planar electrode arrays typically escalate due to the many lithographic steps that need to be realised in a clean room environment. In this process, expensive glass or silicon wafers are first coated with a photosensitive lift-off resin, photopatterned by exposure to UV through a photomask followed by the development of the pattern, metal coated and finally dipped in a suitable lift-off solvent to reveal the metal pattern. In a final step, the electrode tracks are insulated by spin-coating another resin that is further photopatterned and developed to create openings at the electrode active sites and their connections. The resulting wafer is finally carefully diced to release individual sensor chip. This type of process is widely accepted and results in well-defined electrodes with sub-micrometers resolution. However, the associated cost is high and incompatible with inexpensive clinical diagnostics, as well. Thus, for biosensors to truly impact on the medical device industry and move from research laboratories settings to the point-of-care and deliver valuable information on a patient's conditions, the fabrication costs have to be considerably decreased without jeopardising the quality of the data generated. Metal micro-patterning based on current printed circuit board fabrication techniques, is an interesting approach for the low-cost mass fabrication of electrochemical sensor arrays. A copper-clad FR4 substrate can be photopatterned and etched, and structures with dimensions as low as 50 μm can be routinely achieved. The copper layer can subsequently be coated with thin layers of gold, silver or nickel either via electrolytic or electroless metal deposition techniques. Using PCB technology, electronic components can be directly integrated on the same device, the thermal conductivity can be adjusted, the electrical conductivity is excellent (<1 ohm cm^{-2}) and flexible substrates such as Kapton can also be used, demonstrating the versatility and maturity of the technology.

However, the quality of the biosensor metal surface is of crucial importance, as the controlled immobilization of specific biological or synthetic receptors at their surface is required. Cleanliness, metal contamination and surface roughness are factors that will affect the orientation and density of the immobilized receptors, as well as possibly leading to elevated electrochemical background noise. To address those pitfalls, the PCB arrays were manufactured with a surface finish of high purity 3 μm soft-gold electroplated on a 4 μm thick nickel layer, which in turn, was electrodeposited on a 30 μm thick single copper clad FR4 substrate. The nickel layer acts as a physical barrier limiting the solid state diffusion of copper

into the soft-gold layer and thus preventing the further copper oxidation at the electrode surface. In an initial attempt, an electroless nickel immersion gold (ENIG) process [19] was used to coat the copper layer with gold. This approach resulted in highly contaminated and electrochemically unstable electrodes (data not shown), whilst the soft-gold PCB electrodes exhibited electrochemical behaviour comparable to those of polished polycrystalline electrodes. As seen in Figure 4.3.A, the voltammogram of a single 300 µm diameter electrode presents a well defined gold oxide region centred at 1.1 V and a sharp reduction peak centred at 0.733 V as can be expected from a pure gold layer, showing no contamination of the gold surface by the underlying copper and nickel layers. Furthermore, three oxidation waves were measured at 1.035 V, 1.115 V and 1.216 V. These features indicate the polycrystalline nature of the gold surface and can be attributed to the low-index crystallographic planes Au(111), Au(100) and (110) for which the stability of an adsorbate is known to differ depending on the surface crystallographic orientation of the gold substrate in the order Au(1 1 1) < Au(1 0 0) < Au(1 1 0) [20, 21].

The real-surface area, as described by Trassati et al. was calculated from the charge required to reduce the oxide layer and estimated to 5.16 10^{-3} cm^2, i.e. roughness factor of 7.3 [22]. In a final test, we immersed the electrodes in a 5 mM ethanolic solution of 3-mercaptopropionic acid (3-MPA) to assess the ability of the electrolytic gold surface to support the formation of high quality self-assembled monolayers. As can be seen in Figure 4.3.B, the SAM coating insulated the electrode surface. The bare electrode exhibited well defined oxidation and reduction peaks in the presence of 5 mM $K_2Fe(CN)_6$ centred at 0.218 V and 0.138 V of 1.489 µA and -1.413 µA in intensity, respectively. Following immobilization of the alkanethiol SAM these peaks were shifted and suppressed indicating the efficient blocking of the electrode by the 3-MPA. The intensity of the oxidation wave positioned at 0.294 V decreased slightly to 1.117 µA. However, the reduction wave was considerably more affected being shifted to 0.007 V and broadened to a current maximum of -0.853 µA. The SAM was finally electrochemically desorbed in degassed NaOH to estimate the electrode surface coverage. Following three cycles of desorption, the reduction peaks seen at -0.869 V, -1.068 V and -1.103 V had effectively disappeared, indicating the efficient removal of the SAM from the electrode surface (Figure 4.3.C). A total reduction charge of 50.32 nC was measured, which translated into a surface coverage of 1.091 10^{-10} mol cm^{-2}, in agreement with results previously published on the deposition of 3-MPA SAM on polycrystalline gold electrodes [23]. Electrochemical impedance spectroscopy was used to further confirm the quality of the SAM (Figure 4.3.D). Upon functionalisation of the electrode, the resistance to charge transfer (R_{ct})

increased significantly from 3209.18 for the bare electrode to 81073.7 ohm, and the surface coverage calculated as $(1 - \tilde{o}) = R_{ct0}/R_{ct}$ was estimated to be 96 % of the electrode surface.

The quality of the electrodes obtained by electrolytic soft-gold plating was therefore found equivalent to that of planar photolithographically fabricated gold electrodes. The results of the preliminary electrochemical characterization demonstrated the absence of contaminants, such as nickel, at the electrode surface as well as the ability of the fold PCBs to support well-organized SAMs of MPA. The cost of the electrode array was vastly reduced, with a cost of ca. 2€ per array as compared to >100€ per array as compared to photolithographically fabricated electrodes.

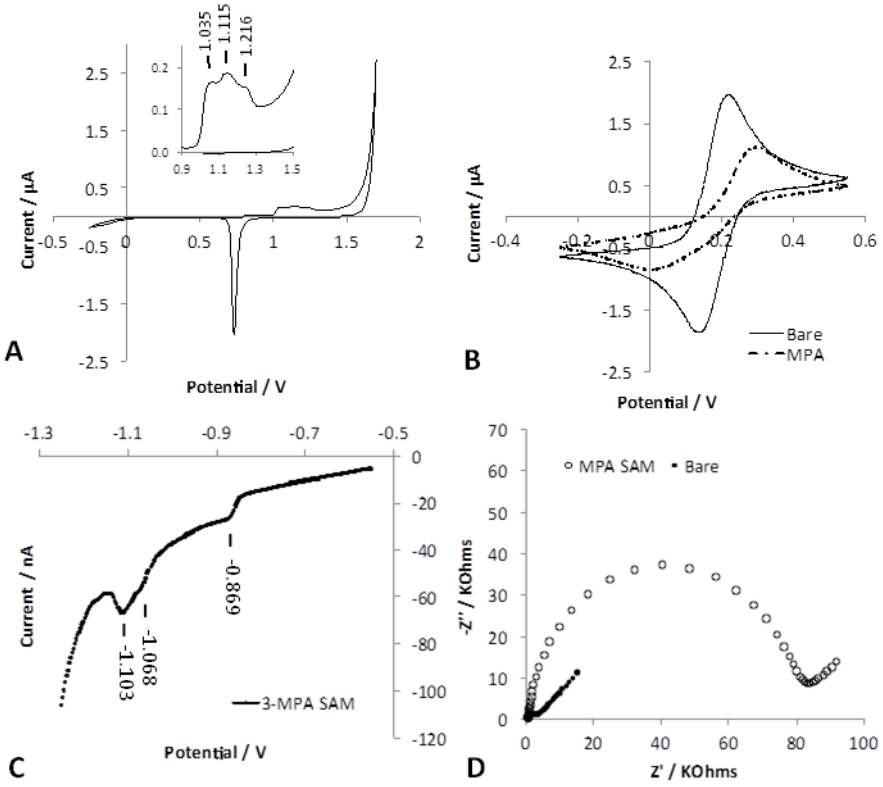

Figure 4.3. A) Cyclic voltammetry in 0.5M sulfuric acid of a single electrode after O_2/Ar plasma treatment indicating the polycrystallinity nature of the 3 µm thick gold deposited; B) Cyclic voltammetry in 5 mM potassium ferricyanide prepared in 10 mM phosphate buffer (100 mV s^{-1}) for a bare and an MPA modified 300 µm in diameter electrode made on PCB; C) Reductive desorption of the MPA monolayer in 0.1M NaOH; D) Electrochemical impedance spectroscopy in 5 mM potassium ferricyanide (10^6 to 1 Hz, 5 mV sinusoidal excitation, at 0 V bias potential vs. OCP) for a bare and an MPA modified electrode.

4.4.2 Genosensor preparation and assay optimization

The sandwich assay format exploited offers very high sensitivity, as previously demonstrated [24]. The target DNA present in a sample hybridizes to a short complementary

DNA probe immobilized on the electrode surface and complementary to a short sequence of the targeted DNA sequence. In a second step, a HRP labelled secondary probe is introduced and hybridized selectively to a second region of the targeted DNA. Finally, the substrate TMB is used to reveal the presence of HRP, which is proportional to the concentration of target DNA captured at the electrode surface (Figure 4.2.C). The system however suffered from relatively high RSD (relative standard deviation) values and high background signals.

The high RSD was reduced by automating several preparative steps, improving the sensor-to-sensor as well as chip-to-chip reproducibility (n=160, 14% RSD and n=5, 11% RSD respectively, 10 nM CD24). Physical cleaning methods, such as O_2/Ar plasma cleaning, were preferred over harsh chemical solutions such as piranha etching. It was also found that if the O_2 present in the plasma could effectively remove any organic materials left over from the microarray patterning process, the Ar plasma in turn helped generating a fresh gold surface at an etch rate of approximately 2 nm min^{-1} [25]. The treated arrays were immediately functionalised with -COOH terminated bipodal PEG alkanethiol [26] and kept under vacuum until further use. The immobilized SAM served the dual function of protecting the array from environmental contamination as well as enabling the coupling of $–NH_2$ terminated DNA probes via EDC/NHS carbodiimide chemistry deposited onto individual electrodes using a microarray contact spotter.

The high background signal was found to originate from the active transport of the oxidized TMB (TMB_{ox}) during its' injection into the microfluidic cell (Figure 4.4.A). Theoretical calculations and molecular modelling ruled out the possibility of passive diffusion of TMB_{ox} to generate such a high background current in the experimental timeframe, as 295 and 374 seconds were required for the TMB_{ox} to migrate to the next electrodes 1.155 and 1.465 mm away, respectively (Supporting Information). However, due to TMB:HRP reaction kinetics and the fluid dynamics, the TMB_{ox} generated at one electrode can be actively transported to the next electrode even minutes after the TMB injection, resulting in high background current (Figure 4.4.C). To limit the transport of TMB_{ox} to adjacent electrodes, different means of either slowing down the reaction kinetics or forcing the precipitation of TMB_{ox} were investigated. Precipitating TMB formulations, which typically contain additives such as alginic acid, methyl vinyl ether/maleic anhydride copolymer, dextran sulfate and/or carrageenan, can readily precipitate TMB_{ox} and are commonly used in immunohistochemistry and Western blotting. The use of precipitating TMB as an efficient electrochemical substrate has already been reported [27], and the precipitated TMB was found to conserve its' electroactivity, albeit producing

lower currents. More importantly, it formed a stable electroactive precipitate at the electrode surface that could not be dissolved in aqueous buffer. Consequently, following the hybridization and HRP-labelling steps, the arrays were incubated for 5 minutes in precipitating TMB and flushed with 100 μL of Tris buffer before carrying out the electrochemical measurement (Figure 4.4.A).

Figure 4.4.C presents a comparison of the genosensor array measured under various conditions for a CDH1 sensor exposed to a concentration of 1 nM CDH1 (synthetic amplicon). Currents measured in conventional TMB substrate (ELISA) averaged 175.9 ± 11.8 nA and a low signal-to-background ratio (S/B) of 3.9. Performing the same assay but measuring in p-TMB considerably decreased the background signal, as well as the specific signal, although the S/B ratio was considerably improved to 10.2. Flushing the electrode array with Tris buffer was found to rinse any p-TMB poorly adsorbed at the electrode surface (Figure 4.4.A), further reducing the background current to 2.7 ± 0.3 nA whilst not affecting the intensity of the specific signal. Under those conditions the S/B was improved by a factor of 7.5. Finally, by comparing the raw data for a control electrode and a CDH1 positive electrode exposed to p-TMB and measured in Tris buffer, as presented in Figure 4.4.B, the final current value could be measured after 100 ms which corresponds to the time required by a control electrode to reach a steady-state response. Holding the electrode at 0 V for 10 ms followed by a potential step at -0.2 V for 490 ms results in the development of a small non-faradaic current, seen as a rapid return to baseline at the control electrode. The combination of precipitated TMB and rapid redox-cycling by the HRP at the electrode surface leads to the development of a large faradaic current that rapidly decays and stabilizes. The measurement was therefore taken at 100 ms to limit background signals and conserve a high specific signal, with a S/B of 26.9.

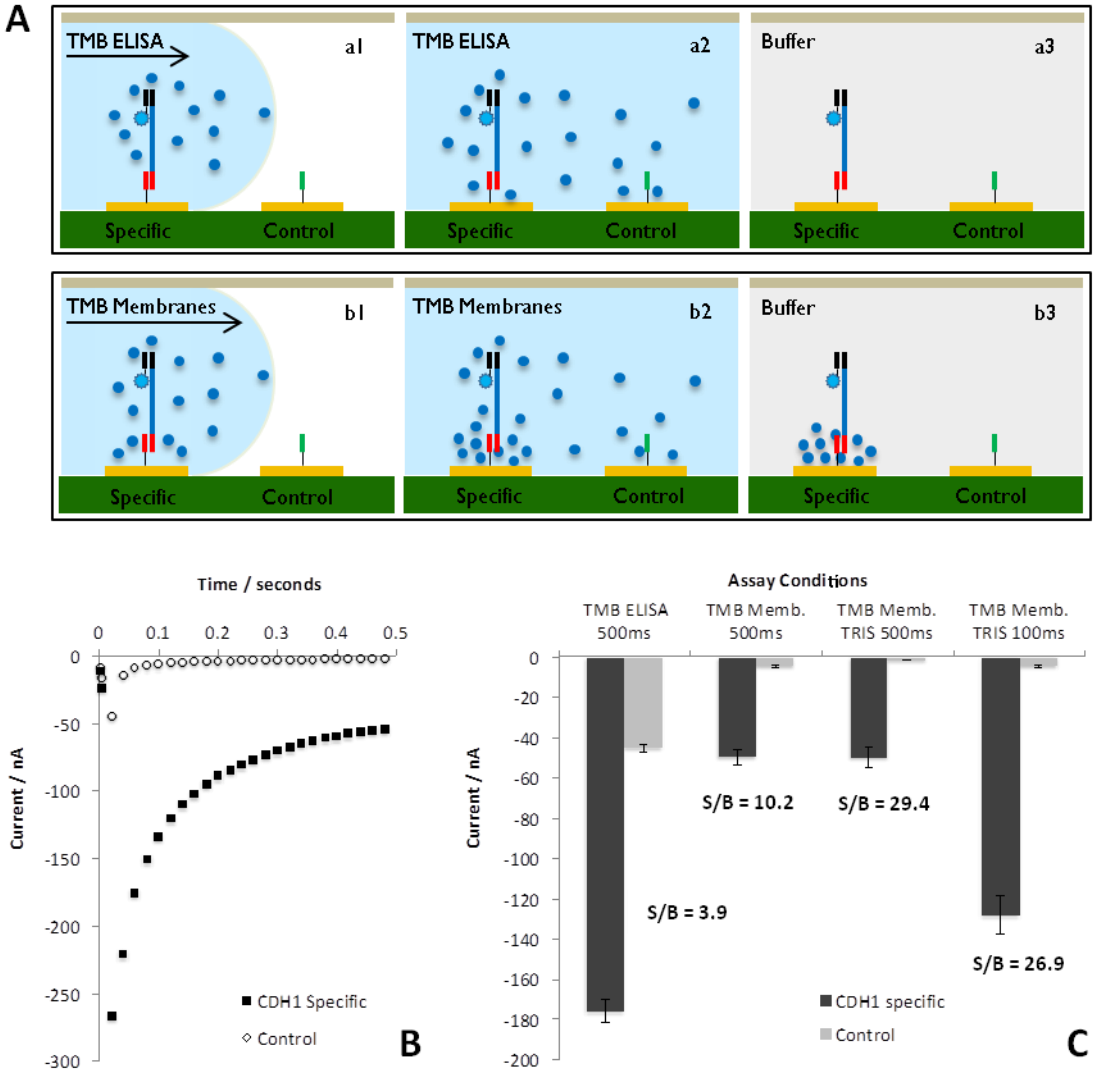

Figure 4.4. Schematic representation of the assay designed to suppress background signal. Illustrations a1 and a2, and b1 and b2 show the injection in the flowcell of TMB-ELISA and TMB membrane respectively. TMB ELISA leads to large background signal due to diffusion. Using precipitating TMB, a stable TMB coating forms onto the electrode. A buffer flush removes adsorbed TMB and decrease background signals. Representations a3 and b3 depicts the state of each system after flushing with buffer; B) Raw data measured in TMB-ELISA for a control and a CDH1 specific sensor exposed to 1 nM of CDH1 synthetic amplicon and subsequently HRP-labelled; C) Comparison of the signal measured under different conditions (TMB ELISA vs. precipitating TMB, at 500 ms and 100 ms).

Several aspects also have a remarkable influence on the output of solid phase hybridization assays. In order to further improve the assay performance, the effect x of factors such as temperature, time and mixing have were also evaluated. Carboxylate-modified PCB electrodes were functionalised with two genetic markers, CD24 and ERBB2, as previously described and each assessed with 1 nM synthetic ERBB2 target at various hybridization

temperatures (room temperature (RT), 37 and 50 ^{o}C) and times (2, 10, 30 and 60 min). The temperature was monitored via the use of a purpose-built temperature-controlled device that consisted of a heating element that was mounted beneath the electrode chip. This device allowed execution of constant-temperature experiments. Once set at the desired temperature, approximately 60 seconds were required to re-establish the experimental temperature upon injection of room temperature reagents. As presented in Figure 4.5.A, performing hybridization at 37 ^{o}C considerably enhances hybridization efficiency, and for a hybridization of 30 minutes at 37 ^{o}C, the current values measured were approximately 3.1 times higher than those obtained with hybridization at room temperature. At 37 ^{o}C, the current readings for 30 and 60 min were very similar, indicating saturation of the probe-functionalised surface by target DNA. Performing the experiments at 50 ^{o}C considerably reduced the sensitivity of the assay, as this temperature adds considerable stringency to the assay, which is translated into smaller signals. Increased hybridization temperatures and times did not have a significant impact on the background signals measured on both the control and the non-specific CD24 probe modified electrodes.

Hybridization depends on the diffusion of a DNA target from the bulk solution to a surface-bound DNA probe so an efficient DNA diffusion is required. To enhance sample diffusion at the electrode surface, the effect of mixing during both the target and the DNA-HRP hybridization steps was evaluated. In another array prepared as described above, a concentration of 1 nM of synthetic ERBB2 marker was injected into the microfluidic cell and allowed to react for 60 min at RT with and without mixing. The mixing was achieved by repeatedly passing the sample back and forth over the sensor surface using syringe pumps at withdrawing/dispensing flow rates of 0.8 µL/s. Following washing, a 10 nM solution of DNA-HRP was injected into the cell and left to react for 30 min at RT under static or mixing conditions. As outlined in Figure 4.5.B, higher current levels were obtained when mixing was implemented.

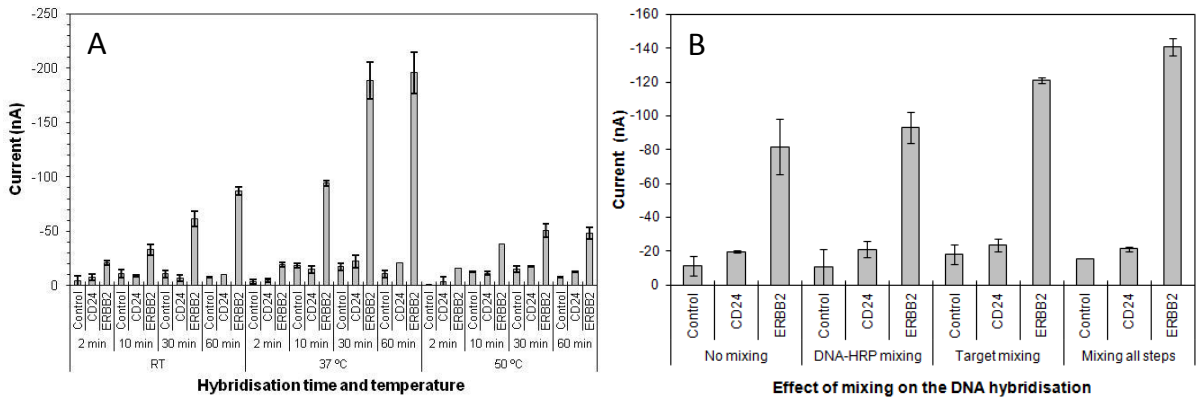

Figure 4.5. Effect of time, temperature (A) and mixing (B) on the DNA hybridization efficiency of the synthetic ERBB2 amplicon.

4.4.3 Assay performances and multiplexed detection of MLPA products

4.4.3.1 Assay performances using synthetic oligonucleotides

The sequence and composition of receptor DNA probes have a great impact on the specificity and sensitivity of the assay. Based on the optimised electrochemical assay, each probe was assessed individually for hybridization efficiency and possible cross-reactivity. The electrodes were exposed to known concentrations of their respective synthetic amplicons, prepared in hybridization buffer solution. Sensitivities vary for each of the genosensor, from 59.0 $nA \cdot nM^{-1}$ for HUWE1 to 171.5 $nA \cdot nM^{-1}$ for ERBB2. The limits of detection taken as the marker concentration equivalent to the current response recorded at a control sensor plus three times the standard deviation (n=8) were 53 pM, 29 pM, 258 pM, 161 pM, 36 pM, 25 pM and 122 pM for ERBB2, KRT19, CD24, CD44, CDH1, CDH2 and HUWE1, respectively (Supporting Information).

To evaluate the specificity of the assay, a cross-reactivity study was carried out. The electrode arrays were functionalised with probes for the detection of each of the seven genetic markers, as already described. Subsequently, a concentration of 1 nM of each synthetic marker was injected individually to the sensor to test its' interaction with all the probes. As can be observed in the Figure 4.6.A, very low cross-reactivity was measured. The signals recorded for unrelated probes remain close to that recorded for the negative control sensors (i.e. coated with the carboxylate-terminated aromatic dithiol). All assay steps were realised at a constant temperature of 37 ^{o}C. Electrochemical measurements were carried out using the developed measuring system, which allows the simultaneous reading of the 64

working electrodes in less than 5 seconds. The variations in sensor sensitivity are attributed to the marker probe design. Whilst the designs were optimised *in silico* by adjusting the GC contents, melting temperature and reducing cross-reactivity between probes, the different sequences will lead to heterogeneous hybridization efficiencies. Both the low cross-reactivity and low detection limits observed, demonstrate the suitability of the barcode-based detection approach and its' ability to accurately assess the levels of DNA amplicons in unknown samples, making the developed assay suitable for detection of MLPA amplicons.

4.4.3.2 Analysis of MLPA product

To confirm the suitability of the barcode approach for the detection of MLPA amplicons, a positive control sample containing all seven gene markers was prepared. The generation of ssDNA was carried out by multiplexed asymmetric amplification, which preferably amplifies one strand of the DNA target, by limiting the concentration of one of the primers. A PCB sensor array was prepared for the simultaneous detection of the seven genetic markers. The ssMLPA sample was diluted three times in the hybridization buffer and injected onto the sensor chip via the microfluidics. In another microfluidic channel, a solution containing a mixture of all synthetic markers at a 1 nM concentration was injected as a calibrator for quantification. All gene markers were successfully detected in the MLPA sample with current signals ranging from 151 to 214 nA while maintaining low current levels in the control electrodes (12 nA) (Figure 4.6.B). Using the current values measured in the reference channel, the concentration of each cancer marker present in the sample was estimated by interpolation. The concentrations were of 1.8, 2.5, 2.6, 2.9, 2.9, 3.4 and 2.1 nM for CD24, CD44, CDH1, CDH2, ERBB2, HUWE1 and KRT19, respectively.

This result shows the potential applicability of the MLPA-barcode-detection approach for genetic profiling. The system exhibited great possibilities for miniaturization and integration into a stand-alone module for the amplification and detection of DNA. Indeed, the barcode approach could be used to generate generic electrode array platforms for detection of different sets of MLPA products on different arrays, but using the same barcode sequences, highlighting the huge potential application of the developed approach.

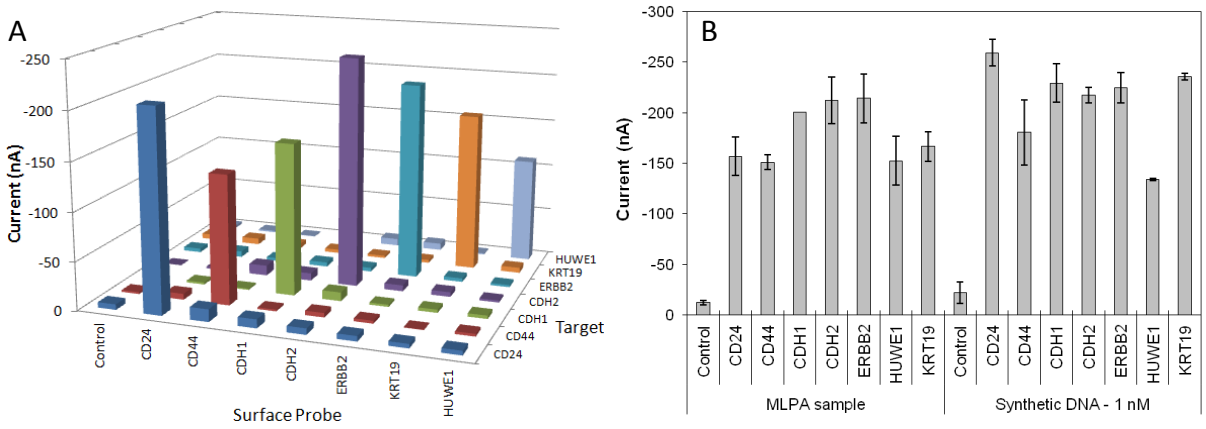

Figure 4.6. A) Electrochemical cross-reactivity study carried out for a breast cancer marker set (CD24, CD44, CDH1, CDH2, ERBB2, KRT19 and HUWE1). The PCB sensor was functionalized with each one of the thiolated DNA capture probes of the set, and then assessed for the detection of a concentration of 5 nM of each synthetic amplicons; B) Electrochemical detection of single stranded MLPA generated by asymmetric PCR. In the calibration channel, a mixture of each synthetic marker was injected at a concentration of 1 nM.

4.5 Conclusions

A method for the multiplex amplification and detection of seven genetic markers present in circulating breast cancer cells was reported. mRNA detection was based on DNA amplification exploiting asymmetric MLPA, which facilitates simultaneous amplification and ssDNA generation of multiple genes. The MLPA probes were specifically designed to incorporate a unique barcode sequence in each amplified gene, which was subsequently used for hybridisation to a surface-immobilised probe. A low-cost, low-density electrode array fabricated using standard PCB technology, was designed and fabricated, exhibiting excellent electrochemical properties as well as array-to-array and sensor-to-sensor reproducibility. The electrochemical measurement was optimised to considerably improve the signal-to-background ratio as well as enhancing hybridization via mixing, achieving limits of detection as low as 25 pM. High specificity was demonstrated, thus facilitating the simultaneous detection of seven gene markers. This approach provides a novel strategy for the multiplexed genetic profiling of tumour cells and the use of barcodes provides a generic platform for detection of other MLPA amplicon sets e.g. lung cancer / prostate cancer, incorporating the same barcodes and thus using the same surface-tethered probes on an electrode array.

4.6 Acknowledgements

The research leading to these results has received the financial support from the European Community's Seventh Framework Programme (FP7), ICT-257743 and partly describes work undertaken in the context of the MIRACLE project “Magnetic Isolation and moleculaR Analysis of single CircuLating and disseminated tumour cElls on chip".

4.7 Supporting information

4.7.1 Oligonucleotide sequences used

MLPA primer sequences

	Sequence (5’ – 3’)
Forward PCR primer	Cy3-gggttccctaagggttgga
Reverse PCR primer	ggacgcgccagcaagatccaatctaga

MLPA probes and barcodes

MARKER	TARGET SEQUENCE DETECTED (5’-3’)	Barcode (5’-3’) attached to 3`of RHO
CD24	LHO: caagtaactcctcccagagtacttccaact (30)	
	SO: ctgggttggccccaaatccaacta (24)	
	RHO: atgccaccaccaaggcggctggtggtgccctgca (34)	tctacaggctcgtatatgta (20)
CD44	LHO: tgccgctgagcctggcgcagatcgattt (28)	
	SO: gaatataacctgccgctttgcaggtgtat (29)	
	RHO: tccacgtggagaaaaatggtcgctacagcatctc (34)	catcgcacgaatataataca (20)
HUWE1	LHO: ccaccaagctgaagggcaaaatgcagagcaggtttgac (38)	
	RHO: atggctgagaatgtggtaattgtggcatctcag (33)	attacgacgaactcaatgaa (20)
CDH1	LHO: ccttggaggaattcttgctttgctaattctgat (33)	
	RHO: tctgctgctcttgctgtttcttcggaggagagcg (34)	ataggctggttcgtaatcgg (20)
ERBB2	LHO: cgttctgaggattgtcagagcctg (24)	
	RHO: acgcgcactgtctgtgccggtggctgtg (28)	ctaagtagccgaattcctag (20)
KRT19	LHO: tgggccctcccgcgactacagccactactacac (33)	
	SO: gaccatccaggacctgcgggacaagattcttgg (33)	
	RHO: tgccaccattgagaactccaggattgtcctgcagatcgacaa (42)	aaccttagagcggattaggg (20)
CDH2	LHO: caatcctccagagtttactgccatgacgtt (30)	
	RHO: ttatggtgaagttcctgagaacagggtagacatcatagta gctaat (47)	ttaccgttgaaatcgatcga (20)

Electrochemical sensor array surface probes (5' – 3').

CD24	NH_2-T15-tacatatacgagcctgtaga
CD44	NH_2-T15-gtattatattcgtgcgatg
CDH1	NH_2-T15-ccgattacgaaccagcctat
CDH2	NH_2-T15-tcgatcgatttcaacggtaa
KRT19	NH_2-T15-ccctaatccgctctaaggtt
ERBB2	NH_2-T15-ctaggaattcggctacttag
HUWE1	NH_2-T15-ttcattgagttcgtcgtaat

Synthetic amplicons (5' – 3').

CD24

g**ggttccctaagggttgga**caagtaactcctcccagagtacttccaactaatccaactaatgccaccaccaaggcggctggtggtgccctgcatctacaggctcgtatatgtatctagattggatcttgctggcgcgtcc

CD44

g**ggttccctaagggttgga**tgccgctgagcctggcgcagatcgatttttgaggtgtattccacgtggagaaaaaggtcgctacagcatctccatcgcacgaatataatacatctagattggat cttgctggcgcgtcc

CDH1

g**ggttccctaagggttgga**ccttggaggaattcttgctttgctaattctgattctgctgctcttgctgtttcttcggaggagagcgataggctggttcgtaatcggtctagattggatcttgctggcgcgtcc

CDH2

g**ggttccctaagggttgga**caatcctccagagtttactgccatgacgttatggtgaagttcctgagaacagggtagacatcatagtagctaatttaccgttgaaatcgatcgatctagattggatcttgctggcgcgtcc

KRT19

g**ggttccctaagggttgga**tgggccctcccgcgactacagccactactacacgccaccattgagaactccaggattgtcctgcagatcgacaaaaaccttagagcggattagggtctagattggatcttgctggcgcgtcc

ERBB2

g**ggttccctaagggttgga**cgttctgaggattgtcagagcctgacgcgcactgtctgtgccggtggctgtgctaagtagccgaattcctagtctagattggatcttgctggcgcgtcc

HUWE1

g**ggttccctaagggttgga**ccaccaagctgaagggcaaaatgcagagcaggtttgacatggctgagaatgtggtaattgtggcatctcagattacgacgaactcaatgaatctagattggatcttgctggcgcgtcc

HRP labelled universal reporter oligonucleotide probe (URP) – Complementary to all targets:

HRP- tccaacccttagggaacc

Please note that sequences highlighted with underline bind to corresponding immobilised probe and sequences highlighted in bold bind to URP.

4.7.2 Analysis for diffusion over a distance of the electroactive oxidised TMB.

Following the equation establishing the relationship for diffusion from a point source based on Fick's first law:

$X^2 = qiDt$,

Where X^2 is the mean-square displacement, qi a numeral constant depending on dimensionality, D the diffusion coefficient and time t.

Taking the following value:

$D_{TMB} = 3.1\ 10^{-6}\ cm^2\ s^{-1}$

qi = 6 to account for the diffusion of TMB in 3 dimensional space

t = 120 seconds, i.e. the maximum time in TMB before starting the measurement

We come to the conclusion that X is equal to 0.47 mm over a period of 120 seconds.

The electrode-to-electrode separation being 1.155 and 1.465 mm in X and Y (Figure 4.7 (SI), it is therefore impossible that sufficient amounts of HRP-oxidised TMB reach the neighbouring electrodes in the experiment timeframe.

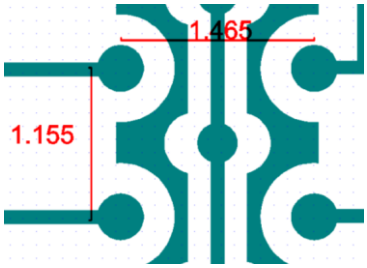

Figure 4.7 (SI). CAD of the 64-electrode array (dimensions in mm)

4.7.3 Calibration curves for the synthetic markers for breast cancer.

The calibration curves for each of the seven amplicons are presented in Figure 4.8 (SI). The electrodes were exposed to known concentrations of their respective synthetic amplicons, prepared in hybridization buffer solution.

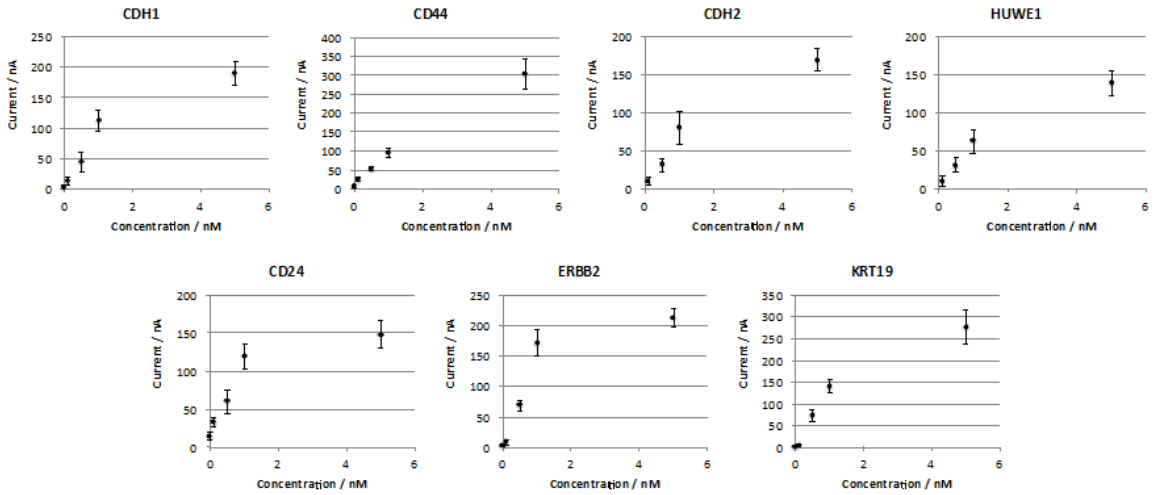

Figure 4.8 (SI). Calibration curve for each of the seven amplicons selected for the preparation of the low-density electrochemical sensor arrays (n=8).

The assay performance was evaluated by determining both the sensitivity and LOD, which were estimated within the linear range 0 – 1 nM (for all curves R^2>0.980) (Table 4.1 (SI)).

Table 4.1 (SI). LOD and sensitivity

Amplicon	CD24	CD44	CDH1	CDH2	ERBB2	HUWE1	KRT19
Sensitivity / nA nM^{-1}	100.7	83.6	107.9	77.2	171.5	59.0	143.9
LOD / pM	258	161	36	25	53	122	29

4.8 References

1. Kvastad L, Werne Solnestam B, Johansson E, Nygren AO, Laddach N, Sahlén P, Vickovic S, Bendigtsen SC, Aaserud M, Floer L, Borgen E, Schwind C, Himmelreich R, Latta D, Lundeberg J (2015) Single cell analysis of cancer cells using an improved RT-MLPA method has potential for cancer diagnosis and monitoring. Sci Rep 5:16519. doi: 10.1038/srep16519
2. Schouten JP, Schouten JP, McElgunn CJ, McElgunn CJ, Waaijer R, Waaijer R, Zwijnenburg D, Zwijnenburg D, Diepvens F, Diepvens F, Pals G, Pals G (2002) Relative quantification of 40 nucleic acid sequences by multiplex ligation-dependent probe amplification. Nucleic Acids Res 30:e57. doi: 10.1093/nar/gnf056
3. Sellner LN, Taylor GR (2004) MLPA and MAPH: New Techniques for Detection of Gene Deletions. Hum Mutat 23:413–419. doi: 10.1002/humu.20035
4. Rooms L, Vandeweyer G, Reyniers E, Van Mol K, De Canck I, Van Der Aa N, Rossau R, Kooy RF (2011) Array-based MLPA to detect recurrent copy number variations in patients with idiopathic mental retardation. Am J Med Genet Part A. doi: 10.1002/ajmg.a.33810

5. Zeng F, Ren ZR, Huang SZ, Kalf M, Mommersteeg M, Smit M, White S, Jin CL, Xu M, Zhou DW, Yan J Bin, Chen MJ, Van Beuningen R, Huang SZ, Dunnen J Den, Zeng YT, Wu Y (2008) Array-MLPA: Comprehensive detection of deletions and duplications and its application to DMD patients. Hum Mutat. doi: 10.1002/humu.20613
6. Yan J-B, Xu M, Xiong C, Zhou D-W, Ren Z-R, Huang Y, Mommersteeg M, van Beuningen R, Wang Y-T, Liao S-X, Zeng F, Wu Y, Zeng Y-T (2011) Rapid screening for chromosomal aneuploidies using array-MLPA. BMC Med Genet. doi: 10.1186/1471-2350-12-68
7. Wang J (2002) Electrochemical nucleic acid biosensors. Anal Chim Acta 469:63–71.
8. Ghindilis AL, Smith MW, Schwarzkopf KR, Roth KM, Peyvan K, Munro SB, Lodes MJ, Stöver AG, Bernards K, Dill K, McShea A (2007) CombiMatrix oligonucleotide arrays: Genotyping and gene expression assays employing electrochemical detection. Biosens Bioelectron 22:1853–1860.
9. Bhavsar K, Fairchild A, Alonas E, Bishop DK, La Belle JT, Sweeney J, Alford TL, Joshi L (2009) A cytokine immunosensor for Multiple Sclerosis detection based upon label-free electrochemical impedance spectroscopy using electroplated printed circuit board electrodes. Biosens Bioelectron 25:506–509. doi: 10.1016/j.bios.2009.07.017
10. Li X, Zang J, Liu Y, Lu Z, Li Q, Li CM (2013) Simultaneous detection of lactate and glucose by integrated printed circuit board based array sensing chip. Anal Chim Acta 771:102–107. doi: 10.1016/j.aca.2013.02.011
11. Salvo P, Henry OYF, Dhaenens K, Acero Sanchez JL, Gielen a, Werne Solnestam B, Lundeberg J, O'Sullivan CK, Vanfleteren J (2014) Fabrication and functionalization of PCB gold electrodes suitable for DNA-based electrochemical sensing. Biomed Mater Eng 24:1705–1714. doi: 10.3233/bme-140982
12. Farkas D (1999) Bioelectric Detection of DNA and the Automation of Molecular Diagnostics. J Assoc Lab Autom 4:20–24. doi: 10.1016/S1535-5535(04)00029-2
13. Umek RM, Lin SW, Vielmetter J, Terbrueggen RH, Irvine B, Yu CJ, Kayyem JF, Yowanto H, Blackburn GF, Farkas DH, Chen Y-P (2001) Electronic Detection of Nucleic Acids: A Versatile Platform for Molecular Diagnostics. J Mol Diagnostics 3:74–84.
14. Gassmann S, Gotze H, Hinze M, Mix M, Flechsig GU, Pagel L (2012) PCB based DNA detection chip. IECON Proc (Industrial Electron Conf 3982–3986. doi: 10.1109/IECON.2012.6389254
15. Tseng H, Adamik V, Parsons J, Lan S, Malfesi S, Lum J, Shannon L, Gray B (2014) Sensors and Actuators B: Chemical Development of an electrochemical biosensor array for quantitative polymerase chain reaction utilizing three-metal printed circuit board technology. Sensors Actuators B Chem 204:459–466. doi: 10.1016/j.snb.2014.07.123
16. Costea PI, Lundeberg J, Akan P (2013) TagGD: Fast and Accurate Software for DNA Tag Generation and Demultiplexing. PLoS One 8:1–5. doi: 10.1371/journal.pone.0057521
17. Ziv J, Lempel a. (1977) A universal algorithm for sequential data compression. IEEE Trans Inf Theory. doi: 10.1109/TIT.1977.1055714
18. Levenshtein VI (1966) Binary Codes Capable of Correcting Deletions, Insertions and Reversals. Sov Phys Dokl 10:707.
19. Milad G, Mayes R (1998) Electroless nickel/immersion gold finishes for application to surface mount technology: A regenerative approach. Met Finish 96:42–46.
20. Arihara K, Ariga T, Takashima N, Arihara K, Okajima T, Kitamura F, Tokuda K, Ohsaka T (2003) Multiple voltammetric waves for reductive desorption of cysteine and 4-mercaptobenzoic acid monolayers self-assembled on gold substrates. Phys Chem Chem Phys 5:3758.
21. Strutwolf J, O'Sullivan CK (2007) Microstractures by selective desorption of self-assembled monolayer from polycrystalline gold electrodes. Electroanalysis 19:1467–1475.
22. Trasatti S, Petrii OA (1991) REAL SURFACE-AREA MEASUREMENTS IN ELECTROCHEMISTRY. Pure Appl Chem 63:711–734.
23. Henry OYF, Maliszewska A, O'Sullivan CK (2009) DNA surface nanopatterning by selective

reductive desorption from polycrystalline gold electrode. Electrochem commun 11:664–667.

24. Henry OYF, Sanchez JLA, O'Sullivan CK (2010) Bipodal PEGylated alkanethiol for the enhanced electrochemical detection of genetic markers involved in breast cancer. Biosens Bioelectron 26:1500–1506. doi: 10.1016/j.bios.2010.07.095
25. Lewicka Z a., Yu WW, Colvin VL (2011) An alternative approach to fabricate metal nanoring structures based on nanosphere lithography. In: Dobisz EA, Eldada LA (eds) SPIE. pp 810213-810213–7
26. Fragoso A, Laboria N, Latta D, O'Sullivan CK (2008) Electron permeable self-assembled monolayers of dithiolated aromatic scaffolds on gold for biosensor applications. Anal Chem 80:2556–2563.
27. del Río JS, Yehia Adly N, Acero-Sánchez JL, Henry OYF, O'Sullivan CK (2014) Electrochemical detection of francisella tularensis genomic DNA using solid-phase recombinase polymerase amplification. Biosens Bioelectron 54:674–678.

5 Electrochemical genetic profiling of single cancer cells

Electrochemical genetic profiling of single cancer cells

Josep Ll. Acero Sánchez[1], Hamdi Joda[2] , Olivier Y. F. Henry[3] , Beata W. Solnestam[4], Linda Kvastad[4], Pelin S. Akan[4], Joakim Lundeberg[4], Nadja Laddach[5], Dheeraj Ramakrishnan[6], Ian Riley[6], Carmen Schwind[7], Daniel Latta[7] and Ciara K. O'Sullivan[1,8]

[1] Universitat Rovira i Virgili, Departament de Enginyeria Química Av. Països Catalans 26, 43007 Tarragona, Spain.
[2] University of Miami, Miller School of Medicine, Department of Biochemistry and Molecular Biology, 1011 NW 15th Street, Miami, Florida 33136, USA.
[3] The Wyss Institute for Biologically Inspired Engineering at Harvard University, 3 Blackfan Circle, Floor 5, Boston, MA02115, USA.
[4] KTH Royal Institute of Technology, Science for Life Laboratory (SciLifeLab Stockholm), School of Biotechnology, Division of Gene Technology, SE-171 65 Solna, Sweden.
[5] MRC Holland, Willem Schoutenstraat 6, 1057 DN Amsterdam, The Netherlands
[6] Labman Automation Ltd., Seamer Hill, Seamer, Stokesley, North Yorkshire, TS9 5NQ, United Kingdom.
[7] Fraunhofer (ICT-IMM), Carl-Zeiss-Str. 18-20, 55129 Mainz, Germany.
[8] Institució Catalana de Recerca i Estudis Avançats, Passeig Lluís Companys 23, 08010 Barcelona, Spain.

5.1 Abstract

Recent understandings in the development and spread of cancer have lead to the realisation of novel single cell analysis platforms focused on circulating tumour cells (CTCs). A simple, rapid and inexpensive analytical platform capable of providing genetic information of these rare cells is highly desirable to support clinicians and researchers alike to either support the selection or adjustment of therapy or provide fundamental insights into cell function and cancer progression mechanisms. We report on the genetic profiling of single cancer cells, exploiting a combination of multiplex ligation-dependent probe amplification (MLPA) and electrochemical detection. Cells were isolated using laser capture, lysed and the mRNA extracted and transcribed into DNA. Seven specific markers were amplified by MLPA, which allows for the simultaneous amplification of multiple targets with a single primer pair, using MLPA probes containing unique barcode sequences. Capture probes complementary to each of these barcode sequences were immobilized on a PCB manufactured electrode array and exposed to single-stranded MLPA products, and subsequently to a single stranded DNA

reporter probe bearing a HRP molecule, followed by substrate addition and fast electrochemical pulse amperometric detection. We present a simple, rapid, flexible, inexpensive approach for the simultaneous quantification of multiple breast cancer related mRNA markers, with single tumour cell sensitivity.

5.2 Introduction

Metastasis is the major cause of cancer-related deaths [1]. In a metastatic process, tumour cells are released from the primary tumour site into the bloodstream and colonize distant sites of the body. In recent years, circulating tumour cells (CTCs) have emerged as a marker with important diagnostic, prognostic and predictive values for early and metastatic cancers. The counting of these cells has already been used as a prognosis marker [2-4], however their rare and complex nature requires a deeper analysis of each cell [5-7]. Gene expression analysis of single CTCs may help to reveal the biological processes and molecular mechanism of tumourigenesis and metastasis and thus there is a need for an easy-to-use, cost-effective analytical platform for genetic profiling of individual cells. Moreover, analysis of mRNA expression profiles holds great promise for the future paradigm of personalized medicine, facilitating optimization of treatment strategies as well as monitoring response therapy [8], thus reducing mortality, health care cost and side-effects associated with cancer treatments.

Genetic profiling is normally achieved via the analysis of a limited set of genetic markers, known to be up or down regulated in cancer cells [9, 10]. Once isolated, the cells are lysed, mRNA extracted, transcribed and amplified. Several multiplexed gene amplification approaches exist [11], however multiplexed ligation-dependant probe amplification system (MLPA) provides an elegant solution enabling the simultaneous amplification of up to 100 markers using a single primer set [12, 13]. MLPA consists of two or three marker-specific probes flanked with forward (Fwd) and reverse (Rev) primers, respectively, that are designed to hybridise next to each other along the targeted marker. Following hybridization, a ligation step fuses the probes into a single DNA probe sequence with Fwd and Rev primers present at both ends. This ligated sequence, complementary to the initial target, is then exponentially amplified using conventional polymerase chain reaction (PCR). However, if the marker-specific pair of probes do not assemble along the targeted DNA, ligation cannot occur and hence amplification does not follow. In addition, the MLPA probes can be designed to include short sequences, i.e. barcodes, to act as recognition site for subsequent microarray analysis [14-16], based on the hybridisation of the barcode sequence to the capture DNA probe, providing an accurate and quantitative detection of each target gene.

Electrochemical DNA biosensors arrays are currently widely used for multiplex gene analysis, offering an alternative to classic DNA microarrays mostly based on fluorescence. Electrochemical sensing offer several advantages such as high sensitivity, low cost, multiplexed analysis, ease of miniaturisation and integration in microsystems [17-20]. Although the associated electronics are relatively inexpensive, the disposable electrode arrays are comparatively costly as high end electrodes arrays are ideally photolithographically microfabricated using sputtering in a clean room environment [21]. Alternative metal patterning techniques such as standard printed circuit board (PCB) technology offers a low cost mass production and a number of versatile fabrication options. In recent years, there have been some reports of electrochemical arrays manufactured with this technology [15, 22-24].

Working towards the development of a fully automated amplification-detection microsystem for the genetic profiling of breast cancer CTCs, we developed a MLPA system incorporating unique barcode sequences and a functionalised low-density electrode array capable of detecting seven genetic biomarkers with single tumour cell sensitivity. The mRNA was extracted from single cancer cells from the MCF7 cell line, transcribed into DNA and subsequently, the markers of interest were simultaneously amplified and then detected via hybridization with a probe surface tethered on individual electrodes of an array, followed by amperometric detection. The system was also capable to differentiate between a cancer patient and a healthy control when assessed with real CTCs. The electrode array consisted of 64 gold working electrodes sharing common reference and counter electrodes fabricated using standard PCB technology. Some assay conditions and manufacturing considerations such as spotting buffer for probe immobilisation, probe immobilisation time and stability of both functionalised sensors and DNA reporter probe were assessed.

5.3 Materials and methods

5.3.1 Materials

Dithiolaromatic triethyleneglycol was obtained from SensoPath Technologies Inc. (Bozeman, USA); 3,3’,5,5’-Tetramethylbenzidine (TMB) enhanced one component HRP Membrane was purchased from Diarect AG (Germany); maleimide activated plates from Thermo Scientific (Spain) and 2mm thick polymethylmethacrylate (PMMA) was purchased from Indústria de la Goma (Spain) and double-sided medical grade adhesive foil provided by Adhesive Research (Ireland).

5.3.2 Instrumentation

SpectraMax 340PC384 microplate reader from Molecular Devices (Madrid, Spain). DNA probes were immobilized by contact printing using a XactII microarrayer (LabNext Inc., USA). A devoted amperometric measuring system consisting of 64 channels was used for the electrochemical analysis, which enables simultaneous readings of electrodes (Labman Automation, UK).

5.3.3 Electrode chip design

The printed circuit board (PCB) electrode array was manufactured at Fineline GmbH (Hilden, Germany) [15, 24], using FR-4 glass epoxy resin with a Cu thickness of 30 μm as substrate with a surface finish of 3 μm soft gold electrolytically deposited on a nickel layer of 4 μm. The PCB-based chip has dimensions of 54.1 x 61.0 mm^2, incorporating 64 individual working electrodes organised in four channels of sixteen electrodes (Figure 5.1A). The gold working electrodes have a circular shape of 300 μm in diameter and share a common gold counter and common gold reference electrode, 250 μm in diameter. The array consists of a two-layer PCB of 1 mm thickness, the top layer bearing all electrodes and connection pads and the bottom layer containing the tracks that connect half of the electrodes with the pads from the top layer using conductive vias of 500 μm, through the PCB. All electrodes are linked to the connection pads through tracks of approximately 100 μm width separated by a gap of 175 μm, insulated with solder mask. Microfluidic cells were fabricated using a Fenix CO_2 laser (Synrad Inc., USA) to cut and drill 2 mm thick poly(methylmethacrylate) (PMMA) sheets, with microfluidic channels housed within 100 μm thick medical grade double-sided adhesive gasket (Figure 5.1B). The electrochemical detection unit consists of the PCB sensor and an interface PCB, which allows connectivity with the dedicated electronic read-out prototype instrument (Figure 5.1C).

5.3.4 Oligonucleotide sequences

Synthetic oligonucleotides were designed *in-silico* and purchased from Biomers.net (Germany) as lyophilized pellets and reconstituted in HyClone® nuclease-free deionised ultrapure water obtained from Thermo Scientific (Spain). DNA probes were modified at the 5'-end with a thiol moiety and included both C_6 and C_{18} triethylene glycol spacers for extension of the probe from the electrode surface. All amplicons contain both a barcode sequence complementary to the capture probe and a specific sequence complementary to the universal reporter oligonucleotide probe (URP). The URP was modified at the 5'-end with a C_6 spacer and a horseradish-peroxidase enzyme. The details of the sequences used can be found in the Supporting Information.

5.3.5 Reverse Transcriptase Multiplexed Ligation-dependent Probe Amplification (RT-MLPA) on single MCF7 cells

A MCF-7 breast cancer cell line was cultivated at 37°C in a 5% CO_2 environment and cells were harvested during log-phase growth (60-70% confluency). Single MCF7 cells were captured using the CellCut tool for laser capture microdissection (LCM) from Molecular Machines and Industry (MMI) coupled to an IX81F-3 microscope with an IX2-UCB external power supply (Olympus, Shinjuku, Japan) [14]. MLPA probes incorporated a unique genetic barcode specific to each mRNA marker for its subsequent electrochemical detection via hybridization assays (Figure 5.2 A and B). A universal primer pair was used to amplify all ligated probes using PCR.

Single cells were dissolved in lysis buffer (0.2% v/v Tween-20, 0.2% v/v NP-40, 19 mM Tris-HCl pH 7.5 and 1 ng/µl of the single stranded viral vector M13mp18, heated for 2 min at 80°C and then placed on ice. Reagents for reverse transcription and preamplification were added yielding a final concentration of 50 mM Tris-HCl (pH 8.3), 75 mM KCl, 3 mM $MgCl_2$, 10 mM DTT (dithiothreitol), 1 pmol of each forward and reverse primer, 0.1 mM dNTPs, 5% w/v DMSO, 8 µg BSA, 40 units Reverse Transcriptase, 0.4 units of SALSA polymerase and 0.048 units of Pfu DNA Polymerase. Reverse transcription was performed for 10 min at 42°C, immediately followed by 25 cycles of PCR (30 s 95°C, 5 min 54°C, and 60 s 72°C) and 2.5 µl of the pre-amplification mix was used for MLPA. An incubation of 5 min at 98°C to inactivate the polymerase was followed by the addition of 1.5 µl of a mix containing 0.75 µl MLPA Buffer and 0.75 µl of a solution containing 3 fmol of each target-specific oligonucleotide was added. The mixture was incubated at 95°C for 60 s to denature the probes, after which hybridization took place at 60°C for 1h. Combined ligation and multiplex amplification was performed using reagents from MRC-Holland, (The Netherlands), by adding 16 µl of a mix containing 1.5 µl ligase buffer A, 1.5 µl Ligase Buffer B, 4 nmol dNTPs, 5 pmol each of Cy3-labeled primer Y and biotinylated primer X, 1 µl Ligase-65, 1.2 units SALSA Polymerase, and 4 µl Q-solution (Qiagen, Hilden, Germany). Ligation was performed for 4 minutes at 54°C followed by 5 minutes at 98°C for enzyme inactivation followed by 35 cycles of PCR (30 s 95°C, 30 s 60°C, and 60 s 72°C), and the samples were then held at 72°C for 10 min. The details of the primers and MLPA probes can be found in the Supporting Information.

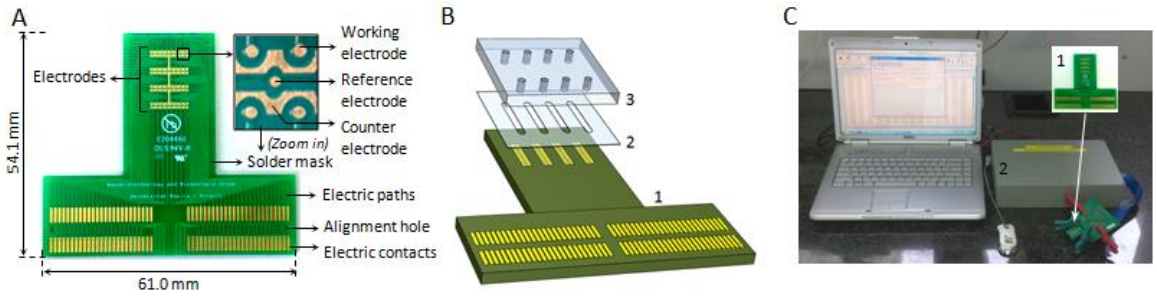

Figure 5.1. Electrochemical detection unit. A. 64-electrode array manufactured on PCB with close up image of the PCB array displaying the working, counter and reference electrodes; B. schematic representation of the assembly of the sensor and flow cell (1. PCB chip, 2. Microfluidic channels of double-sided adhesive tape and 3. Laser machined PMMA gasket); C. Experimental detection set-up showing the connection of the DNA sensor (1), the purpose-made 64-channel potentiostat (2) and the control computer.

Single stranded DNA was generated from MLPA products using streptavidin-coated Dynabeads M-270 (Life Technologies, USA). 20 µl of magnetic beads were washed with 40 µl 1x Binding & Washing (B&W) buffer containing 5 mM Tris-HCl, 0.5 mM EDTA and 1 M NaCl. A sample volume of 10 µl was incubated with gentle rotation for 10 minutes in 1x B&W buffer (total volume 40 µl). The magnetic beads were then washed with 50µl 1x SSC buffer and the DNA was denatured in 22 µl 0.1 M NaOH for 10 min, and the supernatant containing the forward strand of the MLPA probes transferred to a new tube. The solution was neutralized with 18 µl 0.1 M HCl, and the samples mixed with 40 µl of a 2x buffer containing 10x SSC buffer and 0.4% w/v SDS (sodium dodecyl sulfate) buffer.

The MLPA amplified and single stranded DNA fragments were analyzed electrochemically and by electrophoresis on the 2100 Bioanalyzer automated system (Agilent Technologies Inc., Santa Clara, CA, USA).

5.3.6 RT-MLPA on a patient sample.

Blood (4.0 ml) from a metastatic breast carcinoma patient was obtained from the Norwegian Radium Hospital (Oslo, Norway). The immu-nomagnetic enrichment of tumour cells was carried out using AdnaSelect (BreastCancerSelect, QIAGEN Hannover) according to manufactures' instructions. Cells were subsequently lysed and subjected to RT-MLPA as previously described in this article. In parallel, blood sample from a healthy donor was subjected to the same treatment and used as negative control.

5.3.7 Electrode chip functionalisation by contact pin-spotting

Electrode arrays were rinsed in deionised water and ethanol and blow dried with nitrogen before being treated with a solution containing KOH (50 mM) and H_2O_2 (25 %) for 10 min [25]. Subsequently, the arrays were thoroughly washed in deionized water and ethanol and incubated for 20 min in an UV/O_3 chamber provided with an ozone producing Mercury Grid Lamp [26]. Finally, the electrodes were rinsed in water, dried under nitrogen and used immediately for subsequent DNA functionalisation by contact pin-spotting.

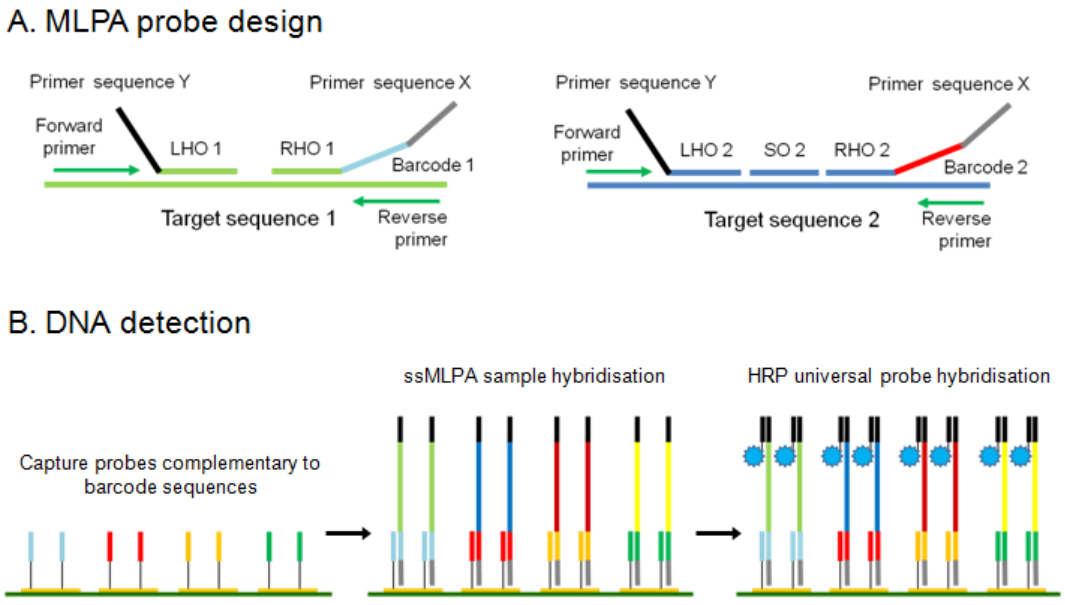

Figure 5.2. A. RT-MLPA probes design. The RT-MLPA probe mix consists of either two or three oligonucleotides: a left hybridization oligonucleotide (LHO) and a right hybridization oligonucleotide (RHO), both composed of a target-specific sequence and a universal primer sequence, and a sequence-specific spanning oligonucleotide (SO), necessary in some of the probes. The DNA sample is denatured and incubated with the synthetic RT-MLPA probes, further ligated, amplified by PCR and the resulting dsMLPA sample converted to single strand. Finally, the ssMLPA is analysed on the electrochemical sensor; B. Schematic representation of the sandwich assay-based electrochemical detection of single stranded MLPA using unique barcodes and a universal reporter probe labeled with HRP enzyme (represented as a blue star).

Thiolated DNA probes complementary to the barcode sequences were prepared at a concentration of 10 µM in several printing buffers containing 100 µM of dithiolated aromatic triethylene glycol (DT-TEG) as co-immobiliser, to prevent the nonspecific absorption from proteins found in PCR products as well as the enzyme label of the reporter probe [27]. To minimise the spot-to-spot variation during the array preparation, the DNA/DT-TEG solution was spotted on the clean gold electrode array surface by contact printing using a XActII

automated microarrayer with a 0.14 mm diameter single capillary pin (LabNext Inc., USA). The relative humidity was set to 70 % and the print cycle consisted of the pin wash ethanolic solution followed by vacuum drying, DNA sample pick up, pre-spotting on a dummy array and final spotting on the specific array. The tip pin wash step consisted of two cycles of 2 s exposure to a 70 % ethanol solution followed by a 2s vacuum drying process, and was applied between each sample spotted to avoid cross-contamination. Following spotting, the arrays were incubated in a humidity chamber containing deionised water. Finally, the electrodes were washed in stirred Milli-Q water for 10 min and the DNA arrays were dried in a stream of nitrogen and stored in Petri dishes at 4 ^{o}C. Negative controls of electrodes spotted with a 100 μM solution of DT-TEG were included in the electrode array.

5.3.8 Electrochemical measurement

The detection assay was based on an enzymatic sandwich assay in which capture probes complementary to each of the barcode sequences were immobilized and exposed to single-stranded DNA samples. The surface bound DNA duplexes were detected with the URP and quantified using fast electrochemical pulse amperometry. Upon electrode array functionalisation, the polymeric microfluidic system was assembled and mounted on the PCB array surface to form four individual microchannels for sample injection. Initially, the array was conditioned with 100 μL of 0.05M Tris buffered saline (TBS) pH 8.0 containing 1 M of NaCl (hybridization buffer) and then, 20 μL of synthetic DNA markers or 10 μL of ssDNA MLPA was injected into the system and incubated for 60 minutes at 37 ^{o}C. Subsequently, 100 μL of hybridization buffer were injected in the channels followed by an injection of 20 μL of 10 nM URP and an incubation of 30 minutes at 37 ^{o}C, before flushing the microfluidics with 100 μL of hybridization buffer. Finally, 20 μL of 3, 3', 5, 5'-Tetramethylbenzidine (TMB) enhanced HRP Membrane were injected and the hybridization event was quantified by measuring the reduction current of the HRP-oxidized TMB by pulse amperometry (0 V for 10ms followed by −0.2 V for 500 ms).

5.4 Results and discussion

5.4.1 Optimisation of spotting buffer and immobilisation time

To increase the reproducibility and reliability of the DNA sensors, the electrode arrays were functionalized by automated contact printing using a single pin. During both the spotting and post-spotting step, factors such as the spotting buffer, immobilization time, humidity and temperature play an important role since they affect the spot morphology and DNA coverage

[28, 29]. The pin was submerged in a thiolated DNA solution in a 384-well plate and loaded by the action of the capillary force and then contacted with the PCB electrode surface and the DNA probe was deposited due to the surface tension between the spotting buffer and substrate [30]. Several printing buffers were assayed and evaluated according to their hybridization efficiency. The electrode arrays were modified by co-immobilization of a 10 µM solution a thiolated DNA probe and 200 µM of the PEGylated alkanethiol, prepared in different spotting buffers, followed by 3 h incubation in a humidity chamber. The arrays were then assessed with 10 nM solution of the complementary URP-HRP for 30 min (Figure 5.3. A).

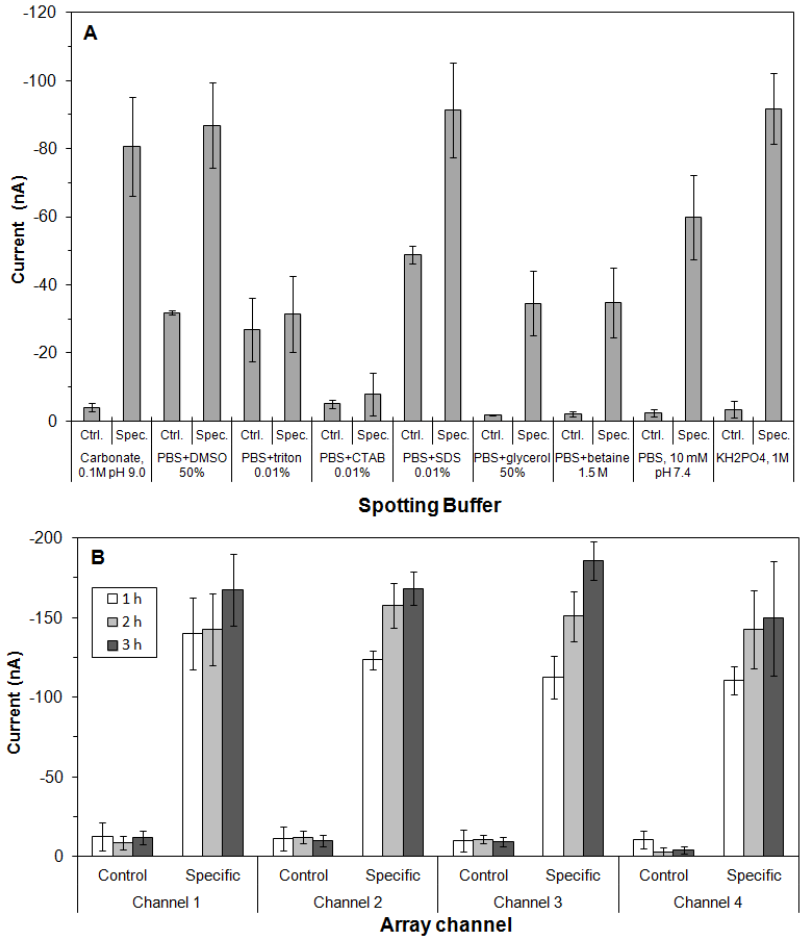

Figure 5.3. Electrochemical response of both specific (Spec.) and control (Ctrl.) electrodes for (A) various spotting buffers for the PCB microarray functionalisation using the LabNext XactII arrayer (10 nM solution of URP was used as target); and (B) three immobilization times (1, 2 and 3 hours) of the thiolated CD24 capture probe (5 nM solution of complementary CD24 was used as target). Each bar corresponds to the average current of 8 electrodes.

The buffers assayed were based on 0.01 M phosphate buffered saline (PBS) pH 7.4 solutions containing different additives: 50 % (v/v) dimethyl sulfoxide (DMSO), 1.5 M betaine, 50 % (v/v)

glycerol, 0.01% (v/v) sodium dodecyl sulfate (SDS), 0.01% (v/v) cetyl trimethyl ammonium bromide (CTAB), and 0.01% (v/v) octylphenol poly(ethyleneglycolether)n (Triton X-100). Carbonate buffer 0.1 M, pH 9.0 and monopotassium phosphate (KH_2PO_4) 1 M solution were also assessed. Three types of detergent additives were used, non-ionic (Triton X-100), cationic (CTAB) and anionic (SDS) and whilst the use of these detergents has been reported to improve the spot morphology [31-33], very poor hybridization efficiency was observed when detergent additives were used. The use of betaine, DMSO and glycerol reduce the spot evaporation rate [34, 35], and unfold any formed DNA structures [29], resulting in more homogeneous spots. This was observed in the case of betaine and glycerol, which exhibited a good signal-to-background (S/B) ratio of 17.0 and 19.9, respectively. However, the specific signal intensity for these additives was more than 2.5 times lower compared to the maximum signal, which can be attributed to the slower rehydration rate observed, with more than 3 h required to achieve complete immobilization. The best results in terms of high specific and low control signals and reproducibility were obtained for those spotting solutions without additives, i.e. KH_2PO_4, carbonate and PBS with S/B ratios of 27.0, 26.6 and 20.2 and relative standard deviations (RSD) of 11.3 %, 20.8 % and 18.0 %, respectively. The low RSD exhibited for the KH_2PO_4 solution also indicates a better reproducibility between replicate spots. The results obtained are consistent with previously reported works [36, 37].

The DNA surface coverage is of critical importance for the optimum performance of subsequent target hybridization [38, 39]. The effect of probe immobilization time on the hybridization performance was also evaluated as a means to control the probe density on the electrode surface. The PCB chips were functionalized with thiolated CD24 probe and PEGylated alkanethiol prepared in a 1 M KH_2PO_4 solution as already described, followed by an incubation of 1, 2 and 3 h at room temperature in a humidity chamber. Subsequently, the sandwich DNA assay was completed by injecting 5 nM solution of the complementary CD24 marker and subsequent injection of the complementary URP. The hybridization signals for each immobilization time were measured amperometrically (Figure 5.3B). High binding levels were obtained for all probe incubation times assayed with average current signals of -168, -149 and -122 nA for an immobilization period of 3, 2 and 1 h, respectively. Results suggested a rapid DNA coverage during the first hour, after which it tended to level off with a 28 % improvement on the hybridization intensity after 3 h, agreeing with previous reports [37, 40].

5.4.2 Stability of DNA-functionalized sensors and URP

For the true application of biosensors, they must assure stability under storage conditions. Accelerated aging studies expose the samples to stress to simulate real time aging for long

term storage periods [41]. To demonstrate the robustness of the developed sensor and predict the product's shelf life, accelerated stability studies were performed on the DNA pre-coated PCBs. Electrodes were functionalized with a thiolated ERBB2 probe and stored at 37 ºC and 4 ºC for accelerated and real-time stability testing, respectively. The sensors were stored in the absence or the presence of the commercial stabilizer StabilCoat® (SurModics, Inc., Eden Prairie, USA), which was deposited onto the DNA-coated electrodes and allowed to dry in a vacuum desiccator for 1 h prior to storage of the PCB chips.

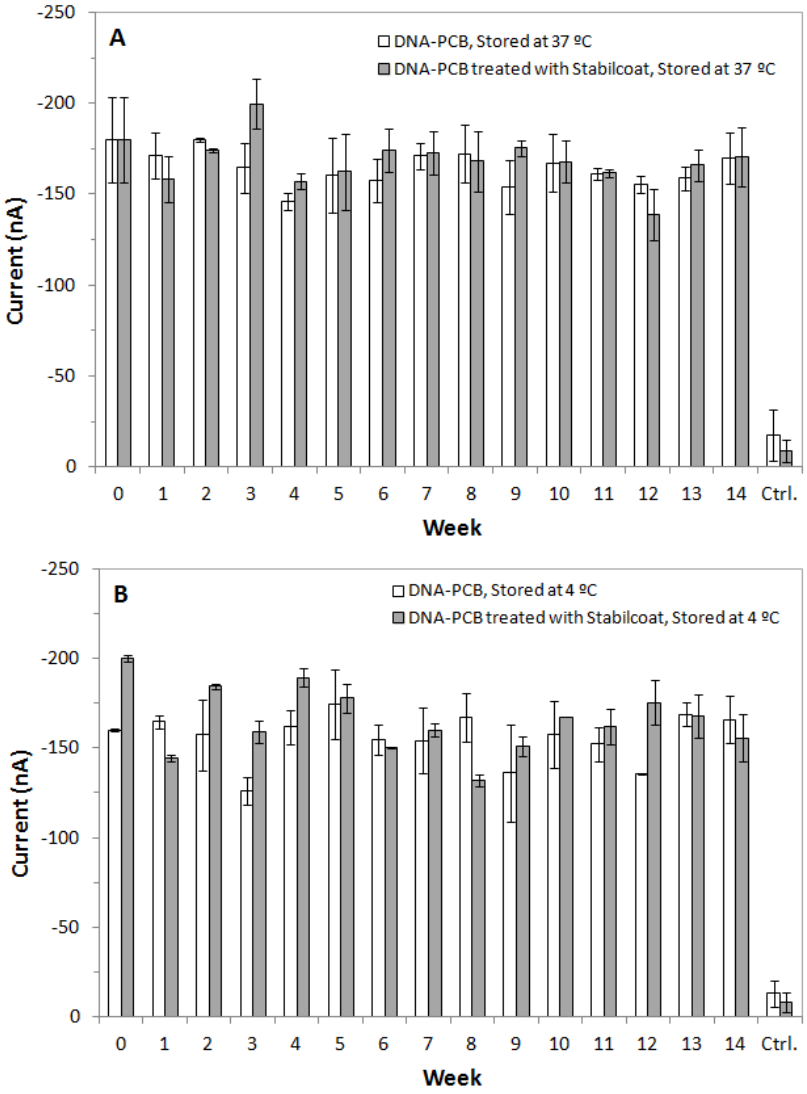

Figure 5.4. Electrochemical signals corresponding to a stability study of DNA functionalised electrode arrays stored under accelerated aging conditions at 37 ºC (A) and at 4 ºC (B). In both cases, the DNA-modified PCB chips were treated with and without the commercial Stabilcoat stabilizer. The chips were assessed with a 5 nM solution of ERBB2 synthetic amplicon. Each electrode bar corresponds to the average current of 3 electrodes, whereas the currents measured in the control electrodes (Ctrl.) correspond to an average of 15 measurements performed during the study.

On a weekly basis, the arrays were assessed using 5 nM of the complementary ERBB2 target over a period of 14 weeks. Pre-coated PCBs showed no loss of activity over the period of study at any of the storage temperatures assayed with average currents of 164.6 ± 9.6 nA and 157.7 ± 13.5 nA, observed for the electrode arrays stored at 37 ^{o}C and 4 ^{o}C, respectively (Figure 5.4A and B). The use of the stabilising agent improved the S/B ratio since the current for the control electrodes decreased between 38 and 50 %, which also demonstrated its suitability as a blocking agent. The shelf life of the DNA-coated PCBs was estimated by the Q Rule method, which states that a product degradation rate changes exponentially with the temperature, and is proportional to $(Q_{10})^n$, where n is the temperature change (^{o}C) divided by 10. The value of Q_{10} is typically set at either 2, 3, or 4 because these correspond to reasonable activation energies [42]. Therefore, assuming that the functionalized sensors are only stable for the period of the study, that is 14 weeks (98 days), an n value of 3.3 ((37 – 4 ^{o}C) / 10 ^{o}C) and a conservative Q_{10} value of 2, the predicted stability of the product at 4 ^{o}C is of at least 2.6 years. However, a much longer stability can be expected as no loss in signal was observed after 14 weeks.

Additionally, a stability study of the HRP-modified URP was carried out. Several reporter probe aliquots of 10 nM were prepared in 0.05 M TBS pH 8.0 containing 1 M NaCl, as well as in StabilGuard Choice®, Stabilzyme HRP® and Protein-free stabilizer® (Surmodics, USA). Each sample solution was stored at 4 ºC. The URP probe was dissolved in TBS containing 1 M NaCl, aliquoted and lyophilised. Dried aliquots were stored at 4 ºC and reconstituted with deionised water to prepare a 10 nM solution. To determine the stability of the probe, a single stranded DNA probe complementary to the HRP-labelled universal reporter probe (200 nM in PBS pH 7.4) was immobilized on maleimide activated plates overnight at room temperature followed by the addition of 6-mercaptohexanol (100 μM in PBS pH 7.4) for 60 min at room temperature. The URP probe of each storage condition was then added allowed to hybridize for 30 min at 37 ^{o}C. Finally, TMB liquid substrate was added and the absorbance measured. A control well functionalized with 6-mercaptohexanol was prepared to assess non-specific adsorption. After 10 weeks, the URP hybridization signals measured in TBS, Stabilzyme HRP® and Protein-free stabilizer® were observed to have decreased 73, 81 and 83 %, respectively as compared to their initial signal, indicating a loss of the activity of the URP probe, and these solutions were thus excluded from further study. As shown in Figure 5.5, the URP-HRP probe preserved its activity when stored at 4 ^{o}C dissolved in StabilGuard Choice® stabilizer or in its lyophilized form.

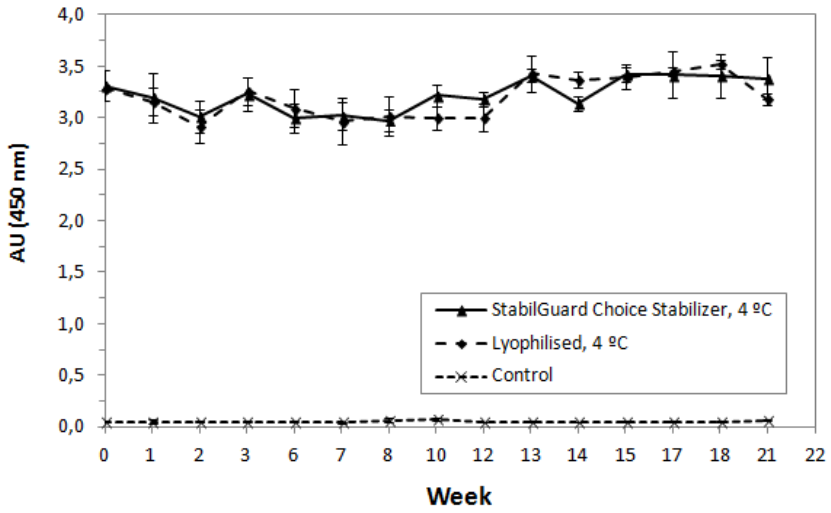

Figure 5.5. Absorbance signals for the HRP-labelled DNA (10 nM solution) binding levels for different storage conditions: i) prepared in StabilGuard® Choice commercial stabilizer and stored 4 ºC and ii) lyophilized, stored at 4 ºC and reconstituted in TBS containing 1 M NaCl (n =3).

5.4.3 Electrochemical analysis of MLPA amplicons from single MCF7 cells

Three single cancer cells from a MCF7 cell line were isolated by laser capture microdissection, lysed, the mRNA extracted, transcribed into DNA and subsequently, seven genetic biomarkers of interest were simultaneously amplified using the MLPA-barcode technique. A panel of seven markers was selected according to their high prognostic value for breast cancer tumours: CD24, CD44, CDH1, CDH2, ERBB2, HUWE1 and KRT19 [4, 43-46]. The amplified samples were 1:3 diluted in hybridization buffer prior to their injection to the assembled PCB-microfluidic chips. The electrodes of each microfluidic channel were functionalized with the capture probes specific for each of the seven markers. The MLPA products were analyzed in parallel using gel electrophoresis. Figure 5.6 presents comparative plots of the analytical results obtained for each cell. Current values superior to three times that of the control sensors (black line) were deemed a positive signal. Results from both techniques are in agreement on all three samples. The electrochemical analysis identified a gene expression pattern similar to that measured electrophoretically on cell A, where three of the seven markers are clearly expressed, i.e. CD24, KRT19 and HUWE1. The results measured for cell B and C also concord. Although the presence of HUWE1 was measured electrochemically in cell B, the signal is equal to that of the established threshold and therefore considered negative. Similarly, the electrochemical results for cell C are similar to those obtained by electrophoresis. Moreover, the results indicate the genetic heterogeneity among cells from the same cell line, in agreement with previous reports [47].

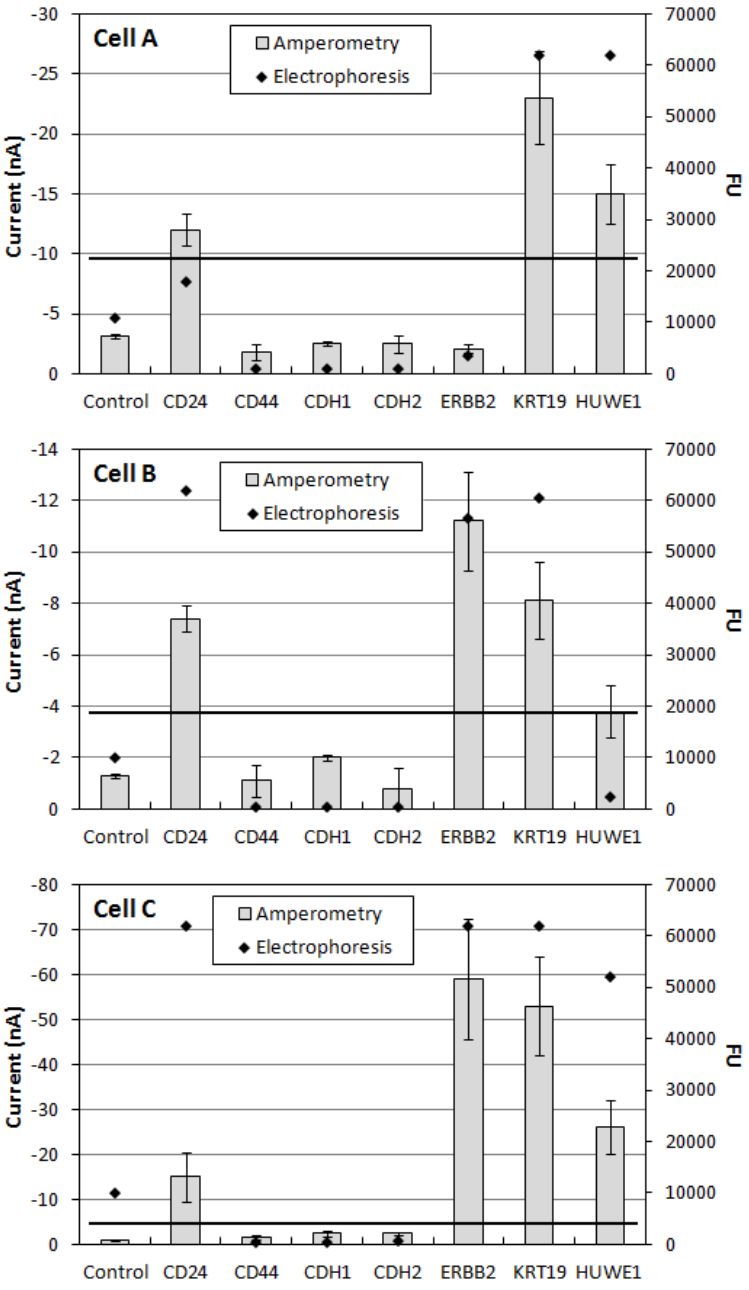

Figure 5.6. Comparison of the electrochemical and the electrophoretic genetic analysis of three single MCF7 cell.

5.4.4 Electrochemical analysis of MLPA amplicons from a patient sample

Tumour cells from a metastatic breast cancer patient were isolated by immunomagnetic enrichment, subsequently lysed and subjected to the amplification of genetic biomarkers using the RT-MLPA-barcode protocol as previously described. Alternatively, a blood sample from a healthy donor was exposed to the same protocol and used as negative control. The MLPA products were injected to the PCB arrays and analysed by electrochemical pulse amperometry

as described. Results revealed the presence of CDH1, ERBB2, KRT19 and HUWE1 in the patient sample whereas no markers were detected in the control sample, which demonstrate the ability of the MLPA-barcode-detection approach for real sample analysis.

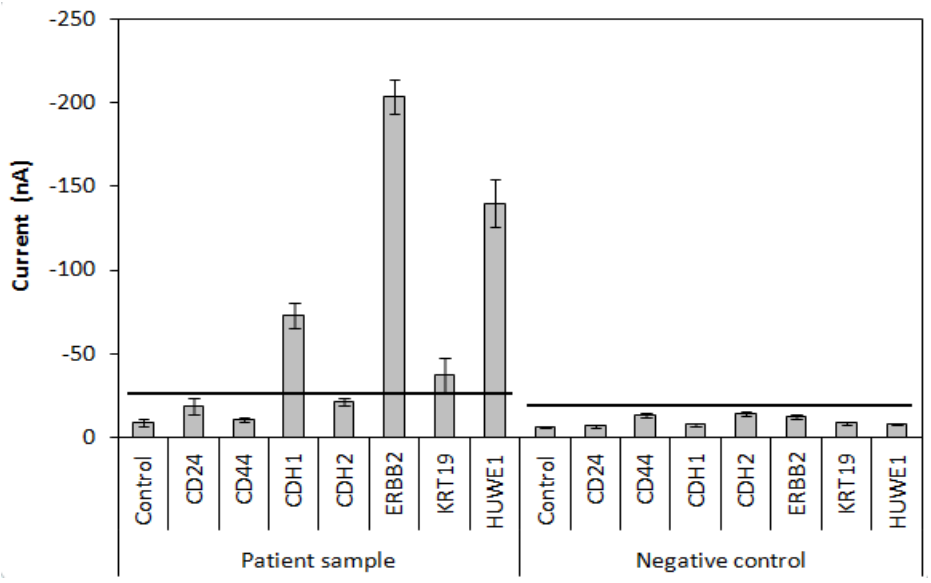

Figure 5.7. Electrochemical analysis of MLPA amplicons from a cancer patient sample and a healthy donor (negative control).

5.5 Conclusions

A strategy for the amplification and detection of multiple mRNA markers from CTCs with single cell sensitivity was reported. The amplification of the genetic material from an individual tumour cell was based on an MLPA-barcode approach, which allows for the simultaneous amplification of multiple biomarkers. The same approach was also successfully applied on real samples, showing the ability to discriminate between a cancer patient and healty donor. MLPA probes were designed to incorporate specifically designed barcodes for use as recognition sites for hybridization with the capture probes immobilized on the surface of each electrode of the PCB array. The choice of the optimal spotting buffer was critical, having a significant effect on DNA surface coverage, hybridization efficiency and a consequential impact on the sensitivity of the sensor. Stability studies performed for both the DNA functionalized PCB sensors and the electrochemical reporter probe demonstrated their stability for long-term storage periods. This result shows the potential applicability of the MLPA-barcode-detection approach for genetic profiling with immense potential where amplification is combined with solid-phase

hybridization, demonstrating a generic approach that can be applied to the detection of any set of biomarkers.

5.6 Acknowledgment

The research leading to these results has received the financial support from the European Community's Seventh Framework Programme (FP7) and partly describes work undertaken in the context of the MIRACLE project “Magnetic Isolation and moleculaR Analysis of single CircuLating and disseminated tumour cElls on chip".

5.7 Supporting information

Sequences of the oligonucleotides used in both the Reverse Transcriptase Multiplexed Ligation-dependent Probe Amplification (RT-MLPA) and the electrochemical detection.

5.7.1 Oligonucleotide sequences used

Reverse transcription (RT) primers

Gene	*Forward primer (5’-3’)*	*Reverse primer (5’-3’)*
CD24	caacaactggaacttcaagtaa	gaagagactggctgttgac
CD44	ctggggactctgcctc	tcagcggcctccgtc
HUWE1	tgaggagcagccacaga	ccacccaaaggtcgct
CDH1	attcctgccattctggggattc	ctgggggcagtaagggctcttt
ERBB2	ccctgttctccgatgtgtaa	gctcatggcagcagtcagt
KRT19	ctggtaccagaagcaggg	gaagtcatctgcagccagac
CDH2	catcacagtgacagatgtcaatg	tgatccttatcggtcacagttag

MLPA primer sequences

	Sequence (5’ – 3’)
Forward PCR primer	Cy3-gggttccctaagggttgga
Reverse PCR primer	Biotin-ggacgcgccagcaagatccaatctaga

MLPA probes and barcodes

MARKER	TARGET SEQUENCE DETECTED (5'-3')	Barcode (5'-3') attached to 3`of RHO
CD24	LHO: caagtaactcctcccagagtacttccaact (30)	
	SO: ctgggttggccccaaatccaacta (24)	
	RHO: atgccaccaccaaggcggctggtggtgccctgca (34)	tctacaggctcgtatatgta (20)
CD44	LHO: tgccgctgagcctggcgcagatcgattt (28)	
	SO: gaatataacctgccgctttgcaggtgtat (29)	
	RHO: tccacgtggagaaaaatggtcgctacagcatctc (34)	catcgcacgaatataataca (20)
HUWE1	LHO: ccaccaagctgaagggcaaaatgcagagcaggtttgac (38)	
	RHO: atggctgagaatgtggtaattgtggcatctcag (33)	attacgacgaactcaatgaa (20)
CDH1	LHO: ccttggaggaattcttgctttgctaattctgat (33)	
	RHO: tctgctgctcttgctgtttcttcggaggagagcg (34)	ataggctggttcgtaatcgg (20)
ERBB2	LHO: cgttctgaggattgtcagagcctg (24)	
	RHO: acgcgcactgtctgtgccggtggctgtg (28)	ctaagtagccgaattcctag (20)
KRT19	LHO: tgggccctcccgcgactacagccactactacac (33)	
	SO: gaccatccaggacctgcgggacaagattcttgg (33)	
	RHO: tgccaccattgagaactccaggattgtcctgcagatcgacaa (42)	aaccttagagcggattaggg (20)
CDH2	LHO: caatcctccagagtttactgccatgacgtt (30)	
	RHO: ttatggtgaagttcctgagaacagggtagacatcatagta gctaat (47)	ttaccgttgaaatcgatcga (20)

Electrochemical sensor array surface probes (5' – 3').

CD24	SH-T15-tacatatacgagcctgtaga
CD44	SH-T15-gtattatattcgtgcgatg
CDH1	SH-T15-ccgattacgaaccagcctat
CDH2	SH-T15-tcgatcgatttcaacggtaa
KRT19	SH-T15-ccctaatccgctctaaggtt
ERBB2	SH-T15-ctaggaattcggctacttag
HUWE1	SH-T15-ttcattgagttcgtcgtaat

Synthetic amplicons (5' – 3').

CD24

g**ggttccctaagggttgga**caagtaactcctcccagagtacttccaactaatccaactaatgccaccaccaaggcggctggtggt gccctgcatctacaggctcgtatatgtatctagattggatcttgctggcgcgtcc

ERBB2

g**ggttccctaagggttgga**cgttctgaggattgtcagagcctgacgcgcactgtctgtgccggtggctgtgctaagtagccgaatt cctagtctagattggatcttgctggcgcgtcc

HRP labelled universal reporter oligonucleotide probe (URP) – Complementary to all targets:

HRP- tccaacccttagggaacc

Please note that sequences highlighted with underline bind to corresponding immobilised probe and sequences highlighted in bold bind to URP.

5.8 References

1. Stewart BW, Wild C (2014) World cancer report 2014. Geneva WHO 632.
2. Banys M, Müller V, Melcher C, Aktas B, Kasimir-Bauer S, Hagenbeck C, Hartkopf A, Fehm T (2013) Circulating tumor cells in breast cancer. Clin Chim Acta 423:39–45. doi: 10.1016/j.cca.2013.03.029
3. Alunni-Fabbroni M, Sandri MT (2010) Circulating tumour cells in clinical practice: Methods of detection and possible characterization. Methods 50:289–297. doi: 10.1016/j.ymeth.2010.01.027
4. Lacroix M (2006) Significance, detection and markers of disseminated breast cancer cells. Endocr Relat Cancer 13:1033–1067. doi: 10.1677/ERC-06-0001
5. Blainey PC, Quake SR (2014) Dissecting genomic diversity, one cell at a time. Nat Methods 11:19–21.
6. Bendall SC, Nolan GP (2012) From single cells to deep phenotypes in cancer. Nat Biotechnol 30:639–47. doi: 10.1038/nbt.2283
7. Chen X-X, Bai F (2015) Single-cell analyses of circulating tumor cells. Cancer Biol Med 12:184–92. doi: 10.7497/j.issn.2095-3941.2015.0056
8. Onstenk W, Gratama JW, Foekens JA, Sleijfer S (2013) Towards a personalized breast cancer treatment approach guided by circulating tumor cell (CTC) characteristics. Cancer Treat Rev 39:691–700. doi: 10.1016/j.ctrv.2013.04.001
9. Liu R, Wang X, Chen GY, Dalerba P, Gurney A, Hoey T, Sherlock G, Lewicki J, Shedden K, Clarke MF (2007) The prognostic role of a gene signature from tumorigenic breast-cancer cells. N Engl J Med 356:217–226.
10. Strati A, Markou A, Parisi C, Politaki E, Mavroudis D, Georgoulias V, Lianidou E (2011) Gene expression profile of circulating tumor cells in breast cancer by RT-qPCR. BMC Cancer 11:422. doi: 10.1186/1471-2407-11-422
11. Fakruddin M, Mannan KS Bin, Chowdhury A, Mazumdar RM, Hossain MN, Islam S, Chowdhury MA (2013) Nucleic acid amplification: Alternative methods of polymerase chain reaction. J Pharm Bioallied Sci 5:245–52. doi: 10.4103/0975-7406.120066
12. Schouten JP, Schouten JP, McElgunn CJ, McElgunn CJ, Waaijer R, Waaijer R, Zwijnenburg D, Zwijnenburg D, Diepvens F, Diepvens F, Pals G, Pals G (2002) Relative quantification of 40 nucleic acid sequences by multiplex ligation-dependent probe amplification. Nucleic Acids Res 30:e57. doi: 10.1093/nar/gnf056
13. Sellner LN, Taylor GR (2004) MLPA and MAPH: New Techniques for Detection of Gene Deletions. Hum Mutat 23:413–419. doi: 10.1002/humu.20035
14. Kvastad L, Werne Solnestam B, Johansson E, Nygren AO, Laddach N, Sahlén P, Vickovic S, Bendigtsen SC, Aaserud M, Floer L, Borgen E, Schwind C, Himmelreich R, Latta D, Lundeberg J (2015) Single cell analysis of cancer cells using an improved RT-MLPA method has potential for cancer diagnosis and monitoring. Sci Rep 5:16519. doi: 10.1038/srep16519
15. Acero Sánchez JL, Henry OYF, Joda H, Werne Solnestam B, Kvastad L, Johansson E, Akan P, Lundeberg J, Lladach N, Ramakrishnan D, Riley I, O'Sullivan CK (2016) Multiplex PCB-based electrochemical detection of cancer biomarkers using MLPA-barcode approach. Biosens Bioelectron. doi: 10.1016/j.bios.2016.04.018
16. Costea PI, Lundeberg J, Akan P (2013) TagGD: Fast and Accurate Software for DNA Tag Generation and Demultiplexing. PLoS One 8:1–5. doi: 10.1371/journal.pone.0057521

17. Liao W-C, Chuang M-C, Ho JA (2013) Electrochemical sensor for multiplex screening of genetically modified DNA: Identification of biotech crops by logic-based biomolecular analysis. Biosens Bioelectron 50:414–420. doi: 10.1016/j.bios.2013.06.044
18. Manzanares-Palenzuela CL, de-los-Santos-Álvarez N, Lobo-Castañón MJ, López-Ruiz B (2015) Multiplex electrochemical DNA platform for femtomolar-level quantification of genetically modified soybean. Biosens Bioelectron 68:259–265. doi: 10.1016/j.bios.2015.01.007
19. Liu G, Lao R, Xu L, Xu Q, Li L, Zhang M, Song S, Fan C (2013) Single-nucleotide polymorphism genotyping using a novel multiplexed electrochemical biosensor with nonfoulingsurface. Biosens Bioelectron 42:516–521. doi: 10.1016/j.bios.2012.11.005
20. Ghindilis AL, Smith MW, Schwarzkopf KR, Roth KM, Peyvan K, Munro SB, Lodes MJ, Stöver AG, Bernards K, Dill K, McShea A (2007) CombiMatrix oligonucleotide arrays: Genotyping and gene expression assays employing electrochemical detection. Biosens Bioelectron 22:1853–1860.
21. Wang J (2002) Portable electrochemical systems. TrAC - Trends Anal Chem 21:226–232.
22. Gassmann S, Gotze H, Hinze M, Mix M, Flechsig GU, Pagel L (2012) PCB based DNA detection chip. IECON Proc (Industrial Electron Conf 3982–3986. doi: 10.1109/IECON.2012.6389254
23. Tseng H, Adamik V, Parsons J, Lan S, Malfesi S, Lum J, Shannon L, Gray B (2014) Sensors and Actuators B : Chemical Development of an electrochemical biosensor array for quantitative polymerase chain reaction utilizing three-metal printed circuit board technology. Sensors Actuators B Chem 204:459–466. doi: 10.1016/j.snb.2014.07.123
24. Salvo P, Henry OYF, Dhaenens K, Acero Sanchez JL, Gielen a, Werne Solnestam B, Lundeberg J, O'Sullivan CK, Vanfleteren J (2014) Fabrication and functionalization of PCB gold electrodes suitable for DNA-based electrochemical sensing. Biomed Mater Eng 24:1705–1714. doi: 10.3233/bme-140982
25. Fischer LM, Tenje M, Heiskanen AR, Masuda N, Castillo J, Bentien A, Émneus J, Jakobsen MH, Boisen A (2009) Gold cleaning methods for electrochemical detection applications. Microelectron Eng 86:1282–1285. doi: 10.1016/j.mee.2008.11.045
26. Moon DW, Kurokawa A, Ichimura S, Lee HW, Jeon IC (1999) Ultraviolet-ozone jet cleaning process of organic surface contamination layers. J Vac Sci Technol A Vacuum, Surfaces, Film 17:150. doi: 10.1116/1.581565
27. Henry OYF, Sanchez JLA, O'Sullivan CK (2010) Bipodal PEGylated alkanethiol for the enhanced electrochemical detection of genetic markers involved in breast cancer. Biosens Bioelectron 26:1500–1506. doi: 10.1016/j.bios.2010.07.095
28. Thomassen M, Skov V, Eiriksdottir F, Tan Q, Jochumsen K, Fritzner N, Brusgaard K, Dahlgaard J, Kruse TA (2006) Spotting and validation of a genome wide oligonucleotide chip with duplicate measurement of each gene. Biochem Biophys Res Commun 344:1111–20. doi: 10.1016/j.bbrc.2006.03.227
29. Dufva M (2005) Fabrication of high quality microarrays. Biomol Eng 22:173–184. doi: 10.1016/j.bioeng.2005.09.003
30. Hegde P, Qi R, Abernathy K, Gay C, Dharap S, Gaspard R, Hughes JE, Snesrud E, Lee N, Quackenbush J (2000) A concise guide to cDNA microarray analysis. Biotechniques 29:548–50, 552–4, 556 passim.
31. Rickman DS, Herbert CJ, Aggerbeck LP (2003) Optimizing spotting solutions for increased reproducibility of cDNA microarrays. Nucleic Acids Res 31:e109.
32. Auburn RP, Kreil DP, Meadows LA, Fischer B, Matilla SS, Russell S (2005) Robotic spotting of cDNA and oligonucleotide microarrays. Trends Biotechnol 23:374–9. doi: 10.1016/j.tibtech.2005.04.002
33. Falciani F (2007) Microarray Technology Through Applications. Garland Science
34. Lee J (2012) Evaluation of Microarray Sensitivity for DNA Profiling. J Korean Chem Soc 56:530–534.

35. Calevro F, Charles H, Reymond N, Dugas V, Cloarec J-P, Bernillon J, Rahbé Y, Febvay G, Fayard J-M (2004) Assessment of 35mer amino-modified oligonucleotide based microarray with bacterial samples. J Microbiol Methods 57:207–18. doi: 10.1016/j.mimet.2004.01.009
36. Herne TM, Tarlov MJ (1997) Characterization of DNA Probes Immobilized on Gold Surfaces. J Am Chem Soc 119:8916–8920. doi: 10.1021/ja9719586
37. Peterson AW, Heaton RJ, Georgiadis RM (2001) The effect of surface probe density on DNA hybridization. Nucleic Acids Res 29:5163–5168. doi: 10.1093/nar/29.24.5163
38. Steel AB, Herne TM, Tarlov MJ (1998) Electrochemical Quantitation of DNA Immobilized on Gold. Anal Chem 70:4670–4677. doi: 10.1021/ac980037q
39. Herne TM, Tarlov MJ (1997) Characterization of DNA Probes Immobilized on Gold Surfaces. J Am Chem Soc 119:8916–8920. doi: 10.1021/ja9719586
40. Steel AB, Levicky RL, Herne TM, Tarlov MJ (2000) Immobilization of nucleic acids at solid surfaces: Effect of oligonucleotide length on layer assembly. Biophys J 79:975–981.
41. Laboria N, Fragoso A, O'Sullivan CK (2011) Storage Properties of Peroxidase Labeled Antibodies for the Development of Multiplexed Packaged Immunosensors for Cancer Markers. Anal Lett 44:2019–2030. doi: 10.1080/00032719.2010.539732
42. Anderson G, Scott M (1991) Determination of Product Shelf-Life and Activation-Energy for 5 Drugs of Abuse. Clin Chem 37:398–402.
43. Athanassiadou P, Grapsa D, Gonidi M, Athanassiadou A-M, Tsipis A, Patsouris E (2009) CD24 expression has a prognostic impact in breast carcinoma. Pathol - Res Pract 205:524–533. doi: 10.1016/j.prp.2009.01.008
44. Mylona E, Giannopoulou I, Fasomytakis E, Nomikos A, Magkou C, Bakarakos P, Nakopoulou L (2008) The clinicopathologic and prognostic significance of CD44+/CD24−/low and CD44−/CD24+ tumor cells in invasive breast carcinomas. Hum Pathol 39:1096–1102. doi: 10.1016/j.humpath.2007.12.003
45. Ricciardi G, Adamo B, Barresi V, Ieni A, Franchina T, Caruso M, Zacchia A, Fazzari C, Tuccari G, Adamo V (2015) 1893 The role of Androgen Receptor, E-cadherin and Ki67 as novel prognostic markers in Triple Negative Breast Cancer (TNBC). Eur J Cancer 51:S297. doi: 10.1016/S0959-8049(16)30843-7
46. Wang X, Lu G, Li L, Yi J, Yan K, Wang Y, Zhu B, Kuang J, Lin M, Zhang S, Shao G (2014) HUWE1 interacts with BRCA1 and promotes its degradation in the ubiquitin–proteasome pathway. Biochem Biophys Res Commun. doi: 10.1016/j.bbrc.2014.01.075
47. Huang S (2009) Non-genetic heterogeneity of cells in development: more than just noise. Development 136:3853–3862. doi: 10.1242/dev.035139

6 Conclusions

6.1 General conclusions

This thesis describes the development of electrochemical immunosensors and genosensors for the detection of protein and DNA biomarkers respectively for the diagnosis of human diseases such as ischemic stroke, celiac disease and breast cancer. It was developed a one-step method for the covalent self-assembly of antibodies on gold surfaces based on the chemical introduction of disulphides groups into the antibody structure. An antibody raised against the stroke marker NSE was employed in the study and the disulphides were introduced through three different moieties of the protein, such as primary amines, carbohydrates and carboxylic groups. This strategy exploits the presence functional groups into the protein structure to introduce sulphur-containing molecules which form a covalent bond with the gold surface. The surface chemistry based on the site-directed modification via the carbohydrate chains exhibited the best biosensor performance probably due to a better orientation of the antibody at the surface, since the sugar moieties in IgGs are specifically located on the Fc region. The results obtained compared well with typical surface chemistries used in biosensing for the covalent attachment of the capture antibody, such as the traditional two-step mixed SAM and the commercial CM5 chips based on a carboxymethylated dextran matrix. The same methodology was also applied for the direct immobilisation of the tTG antigienic protein in gold surfaces, which is used for the detection of the celiac disease related anti-tTG antibody. In this case, the introduction of the disulphide groups through the amine moieties exhibited the best immunosensor performance. This immunosensor was also assessed successfully with real patient samples exhibiting very low background levels, which demonstrates the suitability of the developed surface chemistry for real sample analysis. Overall, the introduction of disulphides in proteins used as bioreceptor in immunosensors provides a simple and attractive approach for a one-step covalent immobilisation, omitting the need for surface pre-treatment.

Concerning the genosensors, it was developed a novel method for the multiplex barcode-MLPA-based amplification and detection of seven breast cancer related mRNA markers with single tumour cell sensitivity. The DNA amplification was performed using the barcode-MLPA approach, which enables the simultaneous amplification of multiple genes and their subsequent electrochemical detection via hybridisation of the barcode sequences to complementary surface immobilised probes. The use of barcodes enables the development of generic detection platforms, since the same barcode sequences can be used for the detection of other biomarker sets using the same surface probes. For the multiplex electrochemical detection, a low-cost electrode array was fabricated using PCB technology, which exhibited

excellent conditions for biomolecules immobilisation, signal transduction and reproducibility. The developed system provides an elegant strategy for the multiplex genetic profiling of tumour cells with great possibilities for miniaturisation and integration into a stand-alone module.

7 Appendices

7.1 Appendix 1. List of figures

7.2 Appendix 2. List of tables

7.3 Appendix 3. List of schemes

7.4 Appendix 3. List of abbreviations

Abbreviation	**Definition**
11-MUOH	11-mercapto-1-undecanol
16-MHA	16-mercapto-1-hexadecanoic acid
A	Adenine
Abs	Antibodies
AGA	Anti-gliadin antibody
AP	Alkaline phosphatase
ATP	Adenosine triphosphate
bp	Base pair
BSA	Bovine serum albumin
C	Cytosine
CD	Coeliac disease
C_{dl}	Double layer capacitance
cDNA	Complementary DNA strand
CEA	Carcino Embryonic Antigen
C_H	Constant domain of the heavy chain
C_L	Constant domain of the light chain
CNT	Carbon nanotube
CTAB	Cetyl trimethyl ammonium bromide
CTC	Circulating tumour cell
CVP	Chemical vapour deposition
DMSO	Dimethyl sulfoxide
DNA	Deoxyribonucleic acid
dNTPs	Deoxyribose nucleoside triphosphate, also known as nucleotide
DPV	Differential pulse voltammetry
dsDNA	Double stranded DNA
DTPS	Dithiopropionic acid succinimidyl ester
DTT	Dithiothreitol
DT-TEG	Dithiolated aromatic triethylene glycol
EC50	Concentration of target needed to obtain a 50 % of the maximum signal
EDC	1-Ethyl-3-(3-dimethylamino-propyl) carbodiimide
EDTA	Ethylenediaminetetraacetic acid
EIS	Electrochemical impedance strectroscopy
ELISA	Enzyme-linked immunosorbent assay
ELONA	Enzyme-linked oligonucleotide assay
EMA	Anti-endomysium antibodies
ENIG	Electroless nickel immersion gold

Fab	Fragment antigen binding
Fc	Fragment crystallizable
FR4	Flame retardant 4
FRA	Frequency response analyzer
Fwd	Forward
G	Guanine
GOx	Glucose oxidase
GPES	General purpose electrochemical system
HBS	HEPES buffered saline
HRP	Horseradish peroxidase
IC	Integrated-circuit
IgA	Immunoglobulin A
IgD	Immunoglobulin D
IgE	Immunoglobulin E
IgG	Immunoglobulin G
IgM	Immunoglobulin M
ISE	Ion selective electrode
IUPAC	International Union of Applied Chemistry
K_A	Association constant
K_D	Dissociation constant
LAMP	Loop mediated isothermal amplification
LCM	Laser capture microdissection
LCR	Ligase chain reaction
LHO	Left hybridization oligonucleotide
LOC	Lab on a chip
LOD	Limit of detection
MAb	Monoclonal antibody
MCF7	Michigan Cancer Foundation-7
mer	From Greek meros, "part". The length of an oligonucleotide
MIP	Molecularly-imprinted polymer
MLPA	Multiplex ligation-dependent probe amplification
MPA	Mercaptopropionic acid
mRNA	Messenger RNA
MWCO	molecular weight cut off
NASBA	Nucleic acid sequence based amplification
NHS	N-hydroxy succinimide
NSE	Neuron specific enolase
NTA	Nitrilotriacetic acid
NTC	Non-template control
PBS	Phosphate-buffered saline
PC	Personal computer

PCB	Printed circuit board
PCR	Polymerase chain reaction
PEG	Polyethilene glycol
Pfu	Pyrococcus furiosus
PMMA	Polymethylmethacrylate
PNA	Peptide nucleic acid
POC	Point of care
POCDs	Point-of-care devices
PSA	Prostate specifc antigen
PVD	Physical vapour deposition
R&D	Research and development
RCA	Rolling circle amplification
Rct	Charge transfer resistance
Rev	Reverse
RHO	Right hybridization oligonucleotide
Rmax	theoretical maximum antigen binding capacity
RNA	Ribonucleic acid
R_s	Solution resistance
RSD	Relative standard deviation
RT-MLPA	Reverse transcriptase MLPA
RT-PCR	Reverse transcriptase polymerase chain reaction
RU	Ressonance units
S/B	Signal-to-background ratio
SAM	Self-assembled monolayer
sat	saturated
SDA	Strand displacement amplification
SDS	Sodium dodecyl sulfate
SELEX	Systematic evolution by exponential enrichment
SNP	Single nucleotide polymorphisms
SO	Spanning oligonucleotide
SPR	Surface plasmon resonance
SSC	Saline-sodium citrate
SSCM	Standard cubic centimeters per minute
ssDNA	Single stranded DNA
T	Thymine
TBS	Tris-buffered saline
TMB	3,3’,5,5’-tetramethylbenzidine
TRIS	Tris(hydroxymethyl)aminomethane
tTG	Tissue transglutaminase
U	Uracyl
UM-PCR	Universal multiplex PCR

URP	Universal reporter oligonucleotide probe
UV	Ultraviolet
V_H	Variable domain of the heavy chain
V_L	Variable domain of the light chain